
AFRL-RZ-WP-TR-2009-2063

# EVALUATION AND TESTING OF THE SUITABILITY OF A COAL-BASED JET FUEL

**X. Zabarnick, D.K. Phelps, Z.J. West, L.S. Shafer, J.S. Ervin, M.J. DeWitt, K.E. Binns, T.F. Williams, G..L. Dieterle, L.M. Balster, and W.E. Harrison, III**

**University of Dayton Research Institute**

**JUNE 2008**
**Final Report**



**AIR FORCE RESEARCH LABORATORY**
**PROPULSION DIRECTORATE**
**WRIGHT-PATTERSON AIR FORCE BASE, OH 45433-7251**
**AIR FORCE MATERIEL COMMAND**
**UNITED STATES AIR FORCE**

# NOTICE AND SIGNATURE PAGE

Using Government drawings, specifications, or other data included in this document for any purpose other than Government procurement does not in any way obligate the U.S. Government. The fact that the Government formulated or supplied the drawings, specifications, or other data does not license the holder or any other person or corporation; or convey any rights or permission to manufacture, use, or sell any patented invention that may relate to them.

This report was cleared for public release by the USAF 88th Air Base Wing (88 ABW) Public Affairs Office (PAO) and is available to the general public, including foreign nationals. Copies may be obtained from the Defense Technical Information Center (DTIC) (http://www.dtic.mil).

AFRL-RZ-WP-TR-2009-2063 HAS BEEN REVIEWED AND IS APPROVED FOR PUBLICATION IN ACCORDANCE WITH ASSIGNED DISTRIBUTION STATEMENT.

* //Signature//

ROBERT MORRIS
Project Manager
Fuels and Energy Branch
Energy/Power/Thermal Division

//Signature//

JERMONT CHEN, Major, USAF
Chief, Fuels and Energy Branch
Energy/Power/Thermal Division
Propulsion Directorate

This report is published in the interest of scientific and technical information exchange and its publication does not constitute the Government's approval or disapproval of its ideas or findings.

*Disseminated copies will show "//Signature//" stamped or typed above the signature blocks.

# REPORT DOCUMENTATION PAGE

*Form Approved*
*OMB No. 0704-0188*



| 1. REPORT DATE *(DD-MM-YY)* | 2. REPORT TYPE | 3. DATES COVERED *(From - To)* |
|---|---|---|
| June 2008 | Final Report | 01 February 2005 – 31 December 2005 |

**4. TITLE AND SUBTITLE**

EVALUATION AND TESTING OF THE SUITABILITY OF A COAL-BASED JET FUEL

**5a. CONTRACT NUMBER**
F33615-03-2-2347

**5b. GRANT NUMBER**

**5c. PROGRAM ELEMENT NUMBER**
62203F

**6. AUTHOR(S)**
S. Zabarnick, Z.J. West, L.S. Shafer, J.S. Ervin, M.J. DeWitt, K.E. Binns, T.F. Williams, G.L. Dieterle, and L.M. Balster (University of Dayton Research Institute)
D.K. Phelps and W.E. Harrison, III (AFRL/RZPF)

**5d. PROJECT NUMBER**
3048

**5e. TASK NUMBER**
04

**5f. WORK UNIT NUMBER**
304804AK

**7. PERFORMING ORGANIZATION NAME(S) AND ADDRESS(ES)**

University of Dayton Research Institute
300 College Park
Dayton, OH 45469-0116

Fuels and Energy Branch (AFRL/RZPF)
Energy/Power/Thermal Division
Air Force Research Laboratory, Propulsion Directorate
Wright-Patterson Air Force Base, OH 45433-7251
Air Force Material Command, United State Air Force

**8. PERFORMING ORGANIZATION REPORT NUMBER**

**9. SPONSORING/MONITORING AGENCY NAME(S) AND ADDRESS(ES)**
Air Force Research Laboratory
Propulsion Directorate
Wright-Patterson Air Force Base, OH 45433-7251
Air Force Materiel Command
United States Air Force

**10. SPONSORING/MONITORING AGENCY ACRONYM(S)**
AFRL/RZPF

**11. SPONSORING/MONITORING AGENCY REPORT NUMBER(S)**
AFRL-RZ-WP-TR-2009-2063

**12. DISTRIBUTION/AVAILABILITY STATEMENT**
Approved for public release; distribution unlimited.

**13. SUPPLEMENTARY NOTES**
PAO Case Number: 88ABW 2008-0608, 29 February 2008. Report contains color.

**14. ABSTRACT**
A candidate coal-based fuel was evaluated both for use as substitute for conventional petroleum-derived JP-8 fuel and as a candidate for advanced application. Numerous properties and performance behavior were monitored through a combination of specification tests and research-type evaluations. This testing included a variety of physical and chemical property tests in the areas of high temperature thermal stability, low temperature flowability, and combustion emissions characteristics, as well as a thorough series of chemical analysis evaluations. The fuel was found to meet the vast bulk of the testing, but had some off-specification test results (for example, hydrogen content and API gravity) due to the unusual hydrocarbon constituents present in the fuel. In general, the fuel performed extremely well in thermal stability testing, but exhibited a higher viscosity than conventional fuels in low temperature evaluations. The significant oxidative and pyrolytic thermal stability benefits of the coal-based fuel could be used in the future to greatly improve the fuel heat sink and engine and aircraft technologies that are currently limited by thermal concerns.

**15. SUBJECT TERMS**
jet fuel, alternative fuel, coal-based fuel

| 16. SECURITY CLASSIFICATION OF: | | | 17. LIMITATION OF ABSTRACT: | 18. NUMBER OF PAGES | 19a. NAME OF RESPONSIBLE PERSON (Monitor) |
|---|---|---|---|---|---|
| a. REPORT | b. ABSTRACT | c. THIS PAGE | | | Robert W. Morris, Jr. |
| Unclassified | Unclassified | Unclassified | SAR | 76 | 19b. TELEPHONE NUMBER *(Include Area Code)* 937-255-3527 |

**Standard Form 298 (Rev. 8-98)**
Prescribed by ANSI Std. Z39-18

## TABLE OF CONTENTS

## LIST OF FIGURES

Figure Page

## LIST OF FIGURES (CONTINUED)

Figure Page

## LIST OF TABLES

Table Page

## PREFACE

This material is based on research sponsored by Air Force Research Laboratory under agreement number F33615-03-2-2347. Funding was provided by the Air Force Office of Scientific Research. The U.S. Government is authorized to reproduce and distribute reprints for Governmental purposes notwithstanding any copyright notation thereon. The views and conclusions contained herein are those of the authors and should not be interpreted as necessarily representing the official policies or endorsements, either expressed or implied, of Air Force Research Laboratory or the U.S. Government.

## 1. SUMMARY

This report summarizes studies of the suitability of a candidate coal-based aviation turbine fuel for general use as a substitute for conventional petroleum-based JP-8 fuel. In addition the candidate fuel was also evaluated for high temperature performance characteristics when used for advanced applications, e.g., as a fuel for hypersonic aircraft and missiles. The fuel was found to meet nearly all the JP-8 specification tests. It yielded results outside of the specification limits for the following tests: hydrogen content, API gravity, icing inhibitor concentration, and conductivity. The specification failures for hydrogen content, API gravity, along with a borderline heat of combustion reflect the unusual hydrocarbon makeup (i.e., high cycloparaffin content) of the fuel mixture. These properties may be acceptable, or even desirable (e.g., high density), for some applications. The failures for icing inhibitor concentration and conductivity specifications result from not treating the fuel with the standard JP-8 additive package (i.e., icing inhibitor, corrosion inhibitor, and static dissipating additives). Detailed chemical analysis of the fuel demonstrated that the fuel is almost completely composed of saturated cycloalkanes with very low levels (ca. 2%) of aromatic species. In contrast, petroleum-derived jet fuels consist of a mixture of normal alkanes, branched alkanes, cycloalkanes, and aromatics. In addition, the coal-based fuel contains much lower levels of polar species than petroleum-derived fuels. The differences in behavior observed between the coal-based and petroleum-based fuels over the range of test devices employed in this study can be explained by the compositional differences between these fuels.

The coal-based fuel was evaluated for its ability to resist surface and bulk deposit formation upon exposure to high temperature in the presence of oxygen (i.e., oxidative thermal stability). These properties are important as fuel is used to cool high temperature aircraft components and systems. The fuel demonstrated excellent thermal stability in the oxidative regime, producing negligible deposition over a range of tests with various residence times, temperatures, flow environments, and oxygen availabilities. The excellent oxidative thermal stability was attributed to the lack of heteroatomic species, which contribute to deposition in petroleum-derived fuels. Recirculation of the coal-based fuel was found to markedly increase deposit production, indicating that an antioxidant additive may be needed if the fuel is to be used in aircraft which employ fuel recirculation for component cooling. In addition to these oxidative reactions, at higher temperatures (>400°C) pyrolytic reactions cause fuel decomposition with resulting deposition. Fuels may be exposed to these higher temperatures when used for regenerative cooling in advanced hypersonic vehicles. The coal-based fuel demonstrated excellent pyrolytic thermal stability with reduced decomposition and deposition relative to petroleum-derived fuels. The improved pyrolytic stability was attributed to the high concentration of species which act as hydrogen donors in the coal-based fuel. A test rig pump failure during one of the oxidative tests illustrates that the coal-based fuel may require addition of a lubricity improving additive, but subsequent lubricity testing indicated that the fuel lubricity was satisfactory.

The coal-based fuel was also evaluated for its properties at sub-ambient temperatures. Low temperature performance is important because fuel is subjected to extremely low

temperatures at altitude (as low as ca. -50°C for JP-8 fuels) and needs to remain flowable throughout the fuel system and readily atomizable in the engine combustor at these reduced temperatures. Despite passing the viscosity specification for JP-8 fuel, the coal-based fuel was found to have liquid-phase viscosities at reduced temperatures that were significantly higher than typical petroleum-derived fuels. At even lower temperatures, where fuel components begin to solidify, visualization of the freezing of fuel in a flow demonstrated that the coal-based fuel produces significantly smaller crystals than the petroleum-derived fuels and did not form a rigid solid-liquid matrix which inhibits fuel flow. In addition at these very lower temperatures, the coal-based fuel has a lower viscosity than petroleum-derived fuels. This improved performance at very low temperatures results from the lack of normal alkanes in the coal-based fuel. In petroleum-derived fuels these species cause production of large crystals and a solid matrix which entraps liquid components and prevents fuel flow. Thus, at moderately low temperatures (-20 to -50°C), where a single liquid phase exists, petroleum-based fuels have more desirable low temperature properties, while at extremely low temperatures (<-50°C) where solidification begins, the coal-based fuel has more advantageous low temperature properties.

The combustion characteristics of the coal-based fuel were evaluated in a turboshaft gas turbine engine and in a research combustor. In the engine testing, the coal-based fuel demonstrated slightly increased particulate and unburned hydrocarbon gaseous emissions relative to petroleum-derived fuels. In the research combustor, moderately increased amounts of particulates were observed under fuel rich combustion conditions only. These observations are hypothesized to be due to the production of aromatic species from pyrolytic cycloparaffin dehydrogenation during the combustion process. As aromatic species were found to be major products in the pyrolytic stability studies, it is important to consider the effect of these pyrolytic reactions on combustion emissions if the fuel is to be heated to temperatures greater than ca. 400°C in the process of cooling aircraft or missile components and systems.

Brief studies of the elastomer swelling characteristics of the coal-based fuel show that the fuel swells nitrile o-rings to a similar extent as JP-8 fuel. This swelling occurs despite extremely low levels of species such as aromatics and polar compounds, which cause swelling in petroleum-derived fuels. The results suggest that cycloalkane species, the primary components of the coal-based fuel, may have excellent seal swell characteristics compared to acyclic hydrocarbons.

In addition to the petroleum-derived fuels and coal-based fuel, a synthetic fuel produced from natural gas via the Fischer-Tropsch process was also evaluated for comparison in this study. This synthetic JP-8, or "S-8," fuel consists almost entirely of normal and branched alkanes. The synthetic fuel demonstrated excellent oxidative thermal stability, equivalent to the coal-based fuel. This is due to the fact that both fuels contain negligible quantities of heteroatomic species. In addition, the synthetic fuel did not exhibit increased deposition upon recirculation in contrast to the coal-based fuel. In the pyrolytic temperature regime, the synthetic fuel demonstrated extremely poor thermal stability producing greater decomposition and deposition than either the coal-based or petroleum-

derived fuels. This poor pyrolytic thermal stability is attributed to the lack of components which can act as hydrogen donors in the synthetic fuel. These results indicate that the synthetic fuel may require addition of additives which can donate hydrogen atoms if the fuel is to be used in the pyrolytic temperature regime. With respect to low temperature characteristics, the synthetic fuel exhibited viscosity characteristics that were very similar to the petroleum-derived fuel, in contrast to the high viscosities displayed by the coal-based fuel. In low temperature flow visualization studies, the synthetic fuel demonstrated lower amounts of crystallization and solid matrix production than the petroleum-derived fuel, but more than the coal-based fuel. In both the engine tests and the research combustor, the synthetic fuel produced very substantial decreases in particulate and gaseous emissions relative to both the petroleum-derived and coal-based fuels. The synthetic fuel displayed very poor elastomer seal swell characteristics due to the lack of chemical species which interact with the seal polymer.

## 2. INTRODUCTION

The Fuels Branch of the Air Force Research Laboratory was tasked with testing, evaluating, and characterizing the suitability of a candidate coal-based aviation turbine fuel. This task was performed primarily by University of Dayton Research Institute researchers using on-site AFRL/PRTG facilities and the results are detailed in this report. This fuel, designated with accession number POSF-4765 by AFRL, was supplied by The Energy Institute of The Pennsylvania State University and PARC Technical Services of Harmarville, PA. The fuel was produced by hydrotreatment of a 1:1 mixture of a coal-derived refined chemical oil (RCO) and a petroleum-derived light cycle oil (LCO). The RCO is produced from a distillate cut from coal tar produced in metallurgical coke plants. The original coal source is a bituminous coal. The LCO was obtained from United Refining Co. of Warren, PA and is heavy product from catalytic cracking.

Numerous properties, characteristics, and behavior of the fuel were evaluated including both standard jet fuel specification tests and evaluations using research equipment and facilities. The fuel was evaluated for its performance in a variety of physical and chemical property tests including high temperature thermal stability, low temperature flowability, and combustion emissions characteristics. In addition, a series of analysis techniques were used to determine the chemical composition of the fuel both before testing and subsequent to many of the test procedures. The testing included evaluation of the fuel as a direct substitute for JP-8, as well as evaluation of performance characteristics desired for advanced applications. With regard to advanced applications, the coal-based fuel was designed to have improved high-temperature thermal stability beyond that of conventional fuels. One goal was production of a fuel with a maximum temperature capability of 480°C (900°F), for which a candidate is referred to as "JP-900" to reflect this temperature goal. Due to these ambitious thermal stability goals, the fuel was evaluated in a number of thermal stability test devices with measurement of both oxidative stability (i.e., the ability of the fuel to resist surface and bulk deposit formation at moderate temperature, 120-300°C, exposure in the presence of oxygen) and pyrolytic stability (i.e., the ability of the fuel to resist pyrolytic degradation and formation of deposits at higher temperatures, >400°C).

The Department of Defense has also been contemplating the use of synthetic jet fuels produced from various sources, e.g. natural gas and/or coal, by the Fischer-Tropsch (FT) process. Where relevant, this report includes comparisons of properties, characteristics, and behavior of sample synthetic, Fischer-Tropsch based jet fuels. When distilled to the properties of petroleum-based JP-8 fuel, the synthetic fuel is referred to here as "S-8" for synthetic JP-8 or "synjet" for synthetic jet fuel. The S-8 fuels used here, which were obtained from the Syntroleum Corporation, were produced from natural gas. The results reported here for these fuels are also representative of FT fuels produced from coal, as the FT process involves converting the fuel source (natural gas or coal) into synthesis gas (i.e., CO and $H_2$) which is subsequently converted to hydrocarbons.

## 3. TESTING AND EVALUATION RESULTS AND DISCUSSION

### 3.1 JP-8 Specification Testing

JP-8 specification testing (MIL-DTL-83133E) was conducted on the coal-based fuel and the results are listed in Table 1 along with the ASTM method used. As shown in the table, the fuel passes nearly all of the JP-8 specification tests except for four tests which yielded results outside of the specification limits (i.e., hydrogen content, API gravity, icing inhibitor concentration, and conductivity). These tests have been marked in the table with a dagger symbol. The fuel did not contain the standard JP-8 additive package (i.e., static dissipater additive, corrosion inhibitor, and icing inhibitor) and thus failed the icing inhibitor and conductivity specifications. The specification failures for hydrogen content (13.2% mass, corresponding to an H/C ratio of 1.81) and API gravity (31.1), as well as the borderline heat of combustion (18,401 BTU/lb), reflect the unusual mixture of hydrocarbon species, when compared to conventional petroleum-derived jet fuels, which constitute the bulk of the fuel (see chemical analysis section below). API gravity is inversely proportional to specific gravity/density, thus the coal-based fuel is denser than petroleum-derived jet fuels. The API gravity of 31.1 corresponds to a specific gravity of 0.87 kg/L, outside of the JP-8 specification range (0.775-0.84 kg/L). The higher density of the coal-based fuel may have payoffs for volume-limited aerospace systems. The role of bulk hydrocarbon species on fuel physical properties is well known (Coordinating Research Council, 2004; Bacha et al., 2000). Based upon the chemical analysis results shown below, the low hydrogen content, low heat of combustion, and low API gravity can be attributed to the high cycloparaffin content of the fuel. In addition to these detrimental effects on fuel properties, the unusual composition of this fuel results in improved values of some properties. For example, the lack of normal alkanes causes the fuel to exhibit a very low freeze point of -65°C. Subsequent sections detail research results which show how the unique composition of the coal-based fuel affects fuel properties.

**Table 1. JP-8 Specification (MIL-DTL-83133E) Test Results for the Coal-based Fuel (POSF-4765)**

| ASTM Method | Test | Limits Min | Limits Max | Lab Results |
|---|---|---|---|---|
| **D3242** | Total Acid Number (mg KOH/g) | | 0.015 | 0.000 |
| **D1319** | Aromatics (%vol) | | 25.0 | 1.9 |
| **D3227** | Mercaptan Sulfur (% mass) | | 0.002 | 0.000 |
| **D4294** | Total Sulfur (% mass) | | 0.30 | 0.00 |
| **D86** | Distillation | | | |
| | IBP (deg C) | | Report | 181 |
| | 10% Recovered (deg C) | | 205 | 192 |
| | 20% Recovered (deg C) | | Report | 194 |
| | 50% Recovered (deg C) | | Report | 204 |
| | 90% Recovered (deg C) | | Report | 243 |
| | EP (deg C) | | 300 | 270 |
| | Residue (% vol) | | 1.5 | 1.1 |
| | Loss (% vol) | | 1.5 | 0.4 |
| **D93** | Flash Point (deg C) | 38 | | 61 |
| **D5972** | Freeze Point (deg C) | | -47 | -65 |
| **D445** | Viscosity @ -20 deg C (cSt) | | 8.0 | 7.5 |
| **D3338** | Heat of Combustion (BTU/lb) | 18400 | | 18401 |
| **D3343** | Hydrogen Content (% mass) | 13.4 | | 13.2† |
| **D1322** | Smoke Point (mm) | 19.0 | | 22.0 |
| **D1840** | Naphthalenes (% vol) | | 3.0 | 0.0 |
| **D130** | Copper Strip Corrosion | | 1 | 1a |
| **D3241** | Thermal Stability @ 260 deg C | | | |
| | Tube Deposit Rating (visual) | | <3 | <1 |
| | Change in Pressure (mmHg) | | 25 | 0 |
| **D381** | Existent Gum (mg/100mL) | | 7.0 | 3.8 |
| **D5452** | Particulate Matter (mg/L) | | 1.0 | 0.3 |
| **D1094** | Water Reaction | | 1B | 1b |
| **D5006** | FSII (DiEGME) (% vol) | 0.10 | 0.15 | 0.00† |
| **D2624** | Conductivity (pS/m) | 150 | 600 | 0† |
| **D4052** | API Gravity @ 60 deg F | 37.0 | 51.0 | 31.1† |

† Lab results out of specification limits.

Specification test results for all the fuels studied in this report are contained in the Appendix.

### 3.2 Chemical Analysis

#### 3.2.1 Gas Chromatography

Chemical analysis of the coal-based fuel was performed using a Agilent 6890 gas chromatograph (GC) with mass spectrometer detection (MS). The GC was outfitted with a DB5-MS column (0.25 mm × 30 m × 0.25 μm) and the following instrument parameters were used: split (40:1), 250°C injector temperature, 40°C initial temperature, 2 minute initial hold, 5°C/min ramp to 210°C, then 30°C/min to 230°C final temperature.

Figure 1 shows the resulting chromatograms of the coal-based fuel (bottom) and a typical JP-8 fuel (top) for comparison. A few components in each chromatogram are depicted to demonstrate the compositional differences between the two fuels. Specifically, components found in the coal-based fuel include: trans- and cis-octahydro-1H-indene (9.2 and 10.2 minutes respectively), trans- and cis-decalin (12.3 and 13.6 minutes respectively), and 1,1'-bicyclohexyl (19.5 minutes). A more complete, semi-quantitative composition of the coal-based fuel is shown in Figure 2. It should be noted that the coal-based fuel is almost completely composed of saturated cycloalkanes, which was also confirmed via hydrocarbon type analysis (see section below). In contrast, the major compounds found in the petroleum-based jet fuels are paraffins (ca. 80 to 85%), i.e., normal, branched and cycloalkanes, and alkyl benzenes (ca. 15 to 20%). Some of the normal alkanes, which create the signature "picket fence" shape on the GC chromatogram, have been labeled in Figure 1 for comparative purposes. The relative distribution of normal alkanes in a JP-8 can vary between fuel samples; however, the distribution shown in the figure is typical.

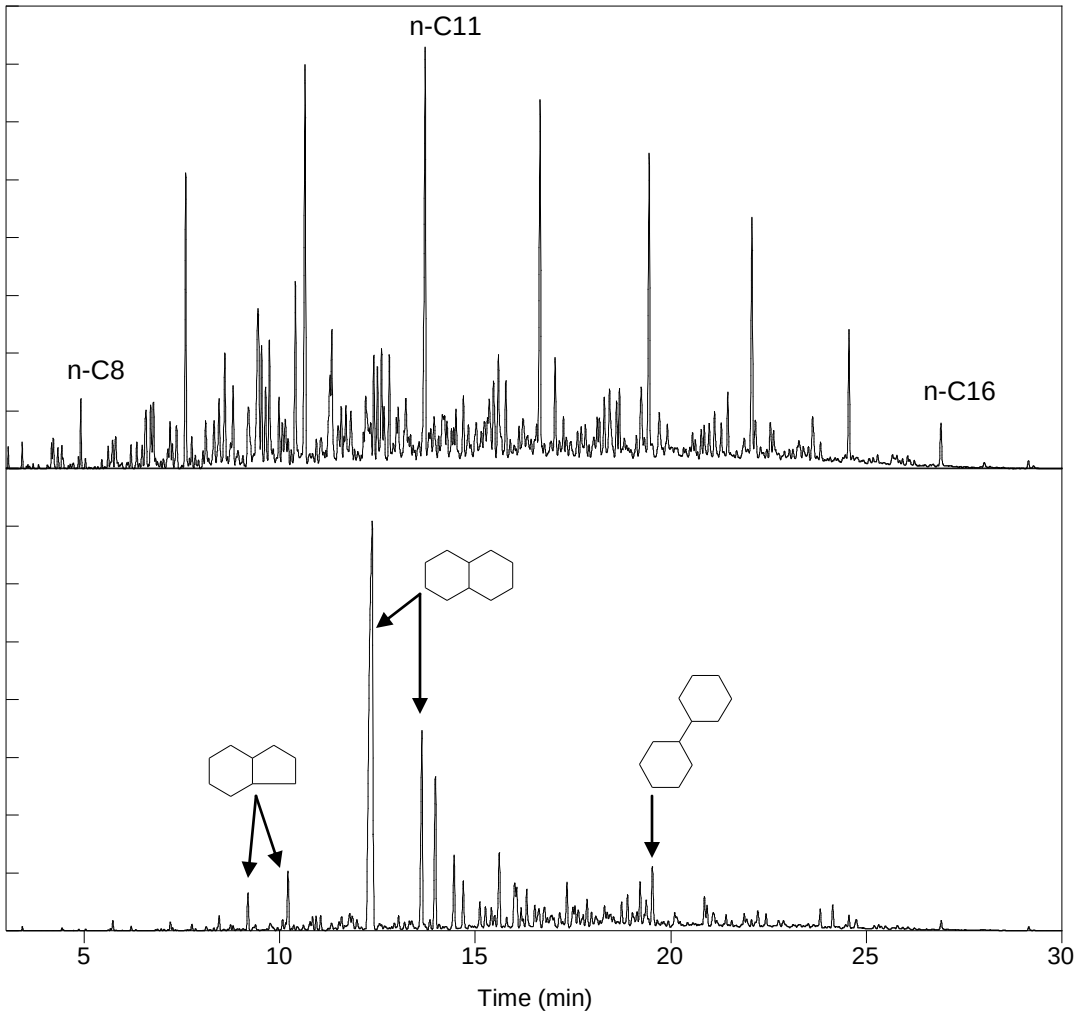


**Figure 1. Gas chromatograms of the coal-based fuel (POSF-4765, bottom) and a typical JP-8 (POSF-3773, top) run under the same conditions.**

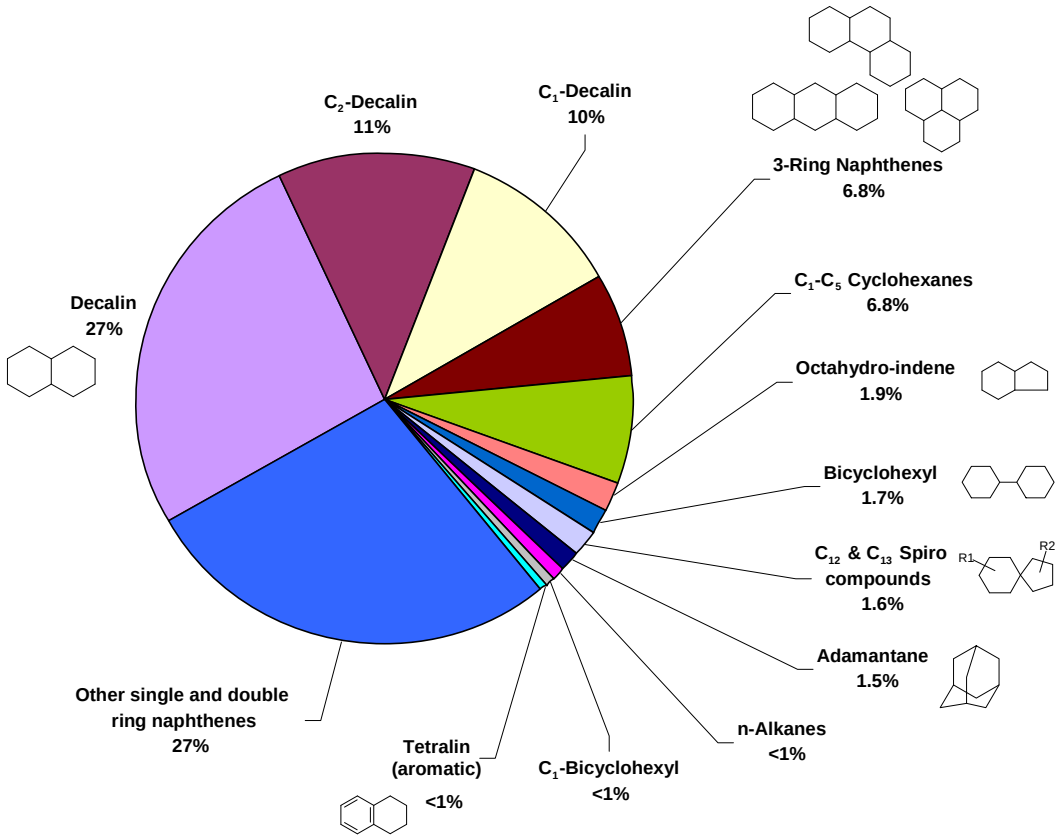


**Figure 2. Semi-quantitative composition of the coal-based fuel**.

### 3.2.2 Hydrocarbon Type Analysis

ASTM method D2425-93, "Hydrocarbon Types in Middle Distillates by Mass Spectrometry," was used to determine the levels of classes of chemical components in the coal-based fuel as well as in a petroleum-based (JP-8) and synthetic (S-8) fuels. The D2425 method involves subjecting a fuel sample to a series of analyses. Initially each fuel sample was analyzed for aromatic hydrocarbon content by ASTM method D6379. In this method normal-phase high performance liquid chromatography (HPLC) with refractive index detection was used. The aromatics were eluted from a cyano column (4.6 x 150 cm) with hexanes as the mobile phase. Standards containing mono-aromatics and diaromatics were used to calibrate the HPLC (Agilent 1100). Both standards and samples were diluted in hexanes before injection into the HPLC. The refractive index peak areas were used to quantify the mono-aromatics and diaromatics concentrations in the fuels in volume percent. The concentrations of the saturated hydrocarbons were then calculated by difference.

In the second part of the D2425 method, the fuel samples diluted in hexanes were separated by normal phase HPLC with the same cyano chromatographic column. Individual fractions of the saturates and aromatics were collected using a diode array detector that served as an indicator of where to separate the fractions. In the third part of the method the two fractions of each of the fuels were analyzed by GC-MS. The column

model used in the Agilent 6890 GC was a 30 m DB-5MS with a 0.25 mm inside diameter (ID) and a 0.25-$\mu$m film. The GC temperature program employed an initial temperature of 40°C (3-min hold) followed by ramping (10°C/min) to 280°C (5-min hold). A constant column flow rate of 1 mL/min, and a splitless 1-µL injection were used. The GC injector temperature was 250°C, and the Agilent 5973 mass spectrometer transfer line was held at a temperature of 280°C.

Extracted ion areas as required by method D2425 were obtained from the mass spectral data through a data analysis macro. The volume percentages of the aromatic and saturate fractions, along with extracted ion areas were then entered into a spreadsheet macro to calculate the percentages of the various classes. The macro was based on the calculations from method D2425, which assigns fragment ion areas to the classes of paraffins, cycloparaffins, alkylbenzenes, alkylnaphthalenes, etc.

The hydrocarbon type analyses results for the coal-based fuel, a JP-8 fuel, and two S-8 fuels are shown in Table 2. Typical JP-8 samples contain approximately 60% paraffins, 20% cycloparaffins, and 20% aromatics (about 2% of which are diaromatics). Both S-8 fuels (synthetic JP-8) are nearly completely composed of paraffins with <1% cycloparaffins and aromatics. The coal-based fuel is almost entirely composed of cycloparaffins with 2% aromatics and <1% paraffins. The breakdown of the cycloparaffins resulting from the D2425 method is nearly an equal mixture of monocycloparaffins and dicycloparaffins, whereas the breakdown from the mass spectral analyses is largely dicycloparaffins with a smaller percentage of monocycloparaffins. This discrepancy may be attributed to the fact that fragment ions from the dicycloparaffins were counted as monocycloparaffins in the hydrocarbon type analysis method.

**Table 2. Hydrocarbon Type Analysis by ASTM D2425**

| | POSF-4765 Coal-based | POSF-3773 JP-8 | POSF-4820 S-8 | POSF-4734 S-8 |
|---|---|---|---|---|
| **Summarized D2425 (vol%)** | | | | |
| Paraffins | 0.6 | 57.2 | 99.3 | 99.7 |
| Cycloparaffins | 46.0 | 17.4 | < 0.2 | <0.2 |
| Dicycloparaffins | 46.7 | 6.1 | 0.7 | 0.3 |
| Tricycloparaffins | 4.6 | 0.6 | < 0.2 | <0.2 |
| Alkylbenzenes | 0.5 | 13.5 | < 0.2 | <0.2 |
| Indan and Tetralins | 1.6 | 3.4 | < 0.2 | <0.2 |
| Indenes CnH2n-10 | <0.2 | <0.2 | < 0.2 | <0.2 |
| Naphthalene | <0.2 | <0.2 | < 0.2 | <0.2 |
| Naphthalenes | <0.2 | 1.7 | < 0.2 | <0.2 |
| Acenaphthenes | <0.2 | <0.2 | < 0.2 | <0.2 |
| Acenaphthylenes | <0.2 | <0.2 | < 0.2 | <0.2 |
| Tricyclic Aromatics | <0.2 | <0.2 | < 0.2 | <0.2 |
| Total | 100.0 | 100.0 | 100.0 | 100.0 |
| | | | | |
| **D6379** | | | | |
| Monoaromatics ( vol%) | 2.1 | 16.6 | < 0.2 | < 0.2 |
| Diaromatics ( vol%) | < 0.1 | 2.1 | < 0.1 | < 0.1 |
| Total Aromatics (vol%) | 2.1 | 18.7 | < 0.2 | < 0.2 |
| Total Saturates (vol%) | 97.9 | 81.3 | 100.0 | 100.0 |

### 3.2.3 Normal Alkanes Analysis

Normal alkane content is an important parameter for understanding the low temperature properties of jet fuels. Thus, the paraffins content of the fuel was further quantified by analyzing for the normal alkanes concentrations. The quantitative analyses of the normal alkanes were performed using a gas chromatograph (Agilent model 6890) combined with a mass spectrometer (GC-MS) and a flame ionization detector (GC-FID). The same column model was used in both detectors (0.25 mm inside diameter (ID) × 30 m DB-5MS with 0.25-$\mu$m film). The GC temperature program consisted of an initial temperature of 40°C (2-min hold) followed by ramping (5°C/min) to 200°C and then an increase (30°C/min) to 280°C. A constant column flow rate of 1 mL/min and a 40:1 split ratio were used. The injector temperature was 250°C. The mass spectrometer (Agilent model 5973) transfer line and FID detector were both held at a temperature of 280°C.

The GC-MS and GC-FID systems were calibrated with standards containing the C7-C19 normal alkanes and an internal standard. Calibration curves were generated by obtaining response factors between the area responses for the compounds of interest and the area response of the internal standard for each level of calibration. The area responses for the GC-MS calibrations were extracted ion areas of the primary characteristic ions for each compound. An average response factor and the relative standard deviation (expressed as a percentage) were calculated for each normal alkane from a minimum of four different concentration levels.

Samples were diluted so that the concentrations of the components were in the linear range of the calibrations. Each sample was diluted to at least two different concentration ranges. The higher concentration components were quantified by GC-MS. The GC-MS quantitation involved the extracted ion areas of the primary characteristic ions, which provided baseline separation of the normal alkanes from other fuel components. The lower concentration normal alkanes were already baseline separated from other fuel compounds and, thus, could be quantified by GC-FID. The concentrations in the fuels were obtained as weight percentages.

The normal alkane concentrations for the four fuels are shown in Table 3. The JP-8 and S-8 fuels have similar concentrations of normal alkanes (15-20% total), while the normal alkanes concentrations in the coal-based fuel are much lower (<1% total). The higher molecular weight normal alkane components tend to have the highest pure component melting points and viscosities of any fuel components and can greatly influence the low-temperature properties. The freezing points, i.e., the temperature at which the last crystal disappears on melting, of the coal-based, JP-8, and two S-8 fuels are -65, -50, -51, and -59°C, respectively. The decreasing order of the freeze points from –50°C to –65°C corresponds to the decreasing order of weight percentages of normal alkanes (18.5 to 0.8) in the fuels.

**Table 3. Normal Alkanes Concentrations**

| | POSF-4765 Coal-based (FP: - 65C) | POSF-3773 JP-8 (FP: - 50C) | POSF-4820 S-8 (FP: - 51C) | POSF-4734 S-8 (FP: - 59C) |
|---|---|---|---|---|
| **COMPOUND** | **Weight %** | **Weight %** | **Weight %** | **Weight %** |
| n-Heptane | 0.001 | 0.12 | 0.14 | 0.009 |
| n-Octane | 0.002 | 0.43 | 1.22 | 1.13 |
| n-Nonane | 0.006 | 2.39 | 2.52 | 2.48 |
| n-Decane | 0.022 | 3.66 | 3.13 | 3.04 |
| n-Undecane | 0.040 | 3.70 | 3.10 | 3.03 |
| n-Dodecane | 0.066 | 3.03 | 2.41 | 2.49 |
| n-Tridecane | 0.075 | 2.36 | 1.83 | 1.62 |
| n-Tetradecane | 0.11 | 1.67 | 1.14 | 0.96 |
| n-Pentadecane | 0.18 | 0.84 | 0.67 | 0.51 |
| n-Hexadecane | 0.15 | 0.25 | 0.33 | 0.17 |
| n-Heptadecane | 0.069 | 0.054 | 0.090 | 0.045 |
| n-Octadecane | 0.024 | 0.008 | 0.010 | 0.010 |
| n-Nonadecane | 0.007 | 0.002 | 0.002 | 0.002 |
| **% n-Alkanes** | **0.8** | **18.5** | **16.6** | **15.5** |

### 3.2.4 Polars Analysis by HPLC

The Agilent 1100 HPLC system described earlier was also used to separate and quantify the polar species in unstressed and stressed samples of the coal-based fuel, JP-8 and S-8 fuels. The cyano column was used in series with a silica column of the same length (4.6 x 150cm). The fuel components were eluted in order of polarity from the columns using a slow gradient of hexanes followed by isopropanol and then methanol. The detector used was a diode array detector at a UV wavelength of 254 nm.

The HPLC was calibrated with standards containing a mixture of phenolic compounds. The polar species of most of the JP-8 fuels previously studied have been found to consist primarily of phenols. The standards used were made to approximate the average phenolic compound composition of the JP-8 fuels. Five standards were made that spanned the linear range of the instrument. 100-uL injections of the standards and samples were analyzed. Some of the stressed fuel samples had to be diluted in hexanes in order to fall within the calibration range.

Fuels were stressed in several different rigs at different temperatures as described elsewhere (Table 4). The coal-based fuel, like the S-8 fuel, contains very few polars. Upon stressing the coal-based fuel forms considerably more polars than the S-8, and even the JP-8 at higher temperatures.

**Table 4. Polars Analysis in Stressed and Unstressed Fuels by HPLC**

| POLARS (mg/L) | | | | | | | |
|---|---|---|---|---|---|---|---|
| Fuel | Unstressed | Stressed in Phoenix Rig @ 1000F | Stressed in Phoenix Rig @ 1075F | Stressed in QCM @ 140C | Stressed in QCM @ 180C | Stressed in ICOT @ 180C | Stressed in ECAT @ 770C & 700PSI |
| Coal -based | <15 | 20 | 30 | 460 | 100 | 7500 | 10000 |
| JP-8 | 420 | N/A | N/A | 910 | N/A | N/A | 2100 |
| JP-8 | 150 | 300 | N/A | N/A | N/A | N/A | N/A |
| S-8 | <15 | N/A | N/A | 140 | 110 | N/A | 15 |

## 3.3 Thermal Stability Evaluation

### 3.3.1 Quartz Crystal Microbalance Testing

A quartz-crystal microbalance (QCM) apparatus has been used previously to study jet fuel thermal stability and help develop jet fuel additives and additive packages (Zabarnick, 1994; Zabarnick and Grinstead, 1994; Zabarnick and Mick, 1999). The QCM system has the capabilities to monitor both oxygen consumption and carbon deposition *in-situ* during fuel thermal stressing. The QCM is a batch test that is normally operated at 140°C for 15 hours and thus is used to study fuel thermal oxidation. Fuel samples are air saturated prior to heating the fuel. The ability to simultaneously monitor oxidation and deposition allow the determination of how both characteristics change with time during thermal exposure.

The resulting mass accumulation and headspace oxygen profiles of the coal-based fuel are plotted in Figure 3, along with those of a synthetic fuel produced using the Fisher-Tropsch process (S-8, POSF-4734) and a typical JP-8 fuel (POSF-4177), run under identical conditions. The figure shows that the coal-based fuel consumes 100% of the available oxygen within the first 2.5 hours. This behavior is commonly exhibited by solvents, such as Exxsol D110 (an aliphatic hydrocarbon blend) and heavily hydrotreated jet fuels, that do not contain synthetic or naturally occurring antioxidants (Zabarnick, 1998). In contrast, the JP-8 fuel still contained about 30% of the oxygen at the end of the 15 hour period, producing an oxygen profile typical of the presence of natural antioxidant species, e.g., alkyl phenols. The figure also shows that the S-8 fuel consumed oxygen very slowly until about 12 hours of thermal stressing where it exhibited a period of very rapid and complete consumption of the available oxygen. This delayed rapid consumption of oxygen is indicative of a fuel containing synthetic antioxidants (e.g., hindered phenols such as BHT). The S-8 fuel was known to contain synthetic antioxidants, thereby verifying these observations. It can be seen in Figure 3 that a level of 0.3 $\mu g/cm^2$ of deposition is produced by thermal stressing of the coal-based fuel after 15 hours. The deposition produced by the coal-based fuel is much less than a typical JP-8, which ranges from ca. 2 to 8 $\mu g/cm^2$ (the JP-8 in Figure 3 gives a value of 2.8 $\mu g/cm^2$), and slightly less than the S-8 fuel, 1.5 $\mu g/cm^2$. Thus, the coal-based fuel exhibits very good oxidative thermal stability producing only very low levels of surface deposits, despite the rapid consumption of oxygen during the run. The rapid oxidation indicates the lack of naturally occurring or synthetic antioxidants in this fuel. The fast oxidation under these conditions indicates that oxidation during long-term storage may be a concern for

this fuel. Addition of a synthetic antioxidant for improved storage stability is recommended for this fuel, as is commonly employed for hydrotreated petroleum-based jet fuels.

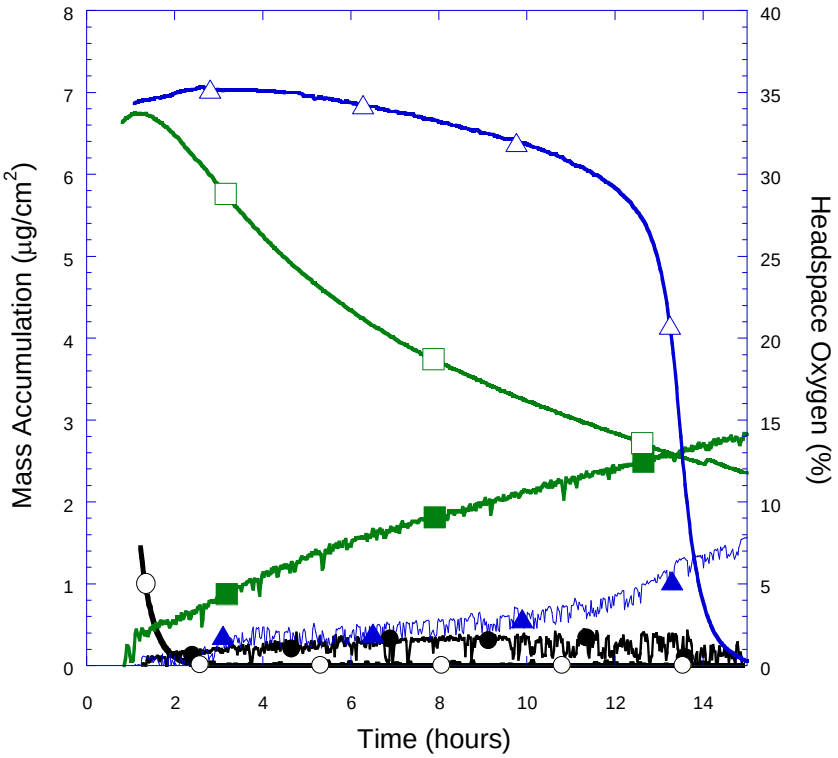


**Figure 3. QCM (140°C) deposition (filled markers) and oxygen profiles (open markers) for the coal-based fuel (POSF-4765, ○), JP-8 fuel (POSF-4177, □), and S-8 fuel (POSF-4734, △).**

Chemical analysis was performed on thermally oxidized samples of the coal-based fuel; however, pretreatment of the samples via solid phase extraction (SPE) was required prior to GC-MS analysis. SPE pretreatment was performed using 1 g basic alumina cartridges, with the following procedure: 1) cartridge preconditioned using 1 aliquot (5 mL) of hexanes (HPLC grade) 2) loaded 5.0 mL of sample onto the cartridge 3) washed the cartridge with 3 aliquots of hexanes and 4) eluted and collected the polar analyte with 1.0 mL of methanol (HPLC grade). The flow rates of solvents and samples were 1-5 mL/min and controlled using a vacuum manifold system. SPE pretreatment of the stressed fuel samples, with subsequent GC-MS analysis, allowed separation and speciation of the polar compounds formed during thermal oxidation of the fuel. Prior to thermal oxidation the unstressed coal-based fuel contained no identifiable polar compounds via the SPE-GC-MS method. The SPE-GC-MS method was then used to analyze samples of the coal-based fuel after thermal oxidative stressing, observed after a variety of stress conditions (i.e., QCM at 140°C & 180°C, ICOT at 185°C, and the ECAT at 310°C bulk outlet temp). Figure 4 shows the SPE-GC-MS chromatogram of the coal-based fuel after thermal stressing in the QCM at 140°C. It can be seen from Figure 4 that the major oxidative species present are: 1-hydroxydecalin, 2-hydroxydecalin, 4a-hydroxydecalin,

1-ketodecalin, 2-ketodecalin, α-tetralol, and α-tetralone. The aforementioned list of major oxidative compounds were found to be common for all of the thermal oxidatively stressed samples examined, and thus are taken to represent the species that are formed upon thermal oxidation of the coal-based fuel. Another observation regarding the major oxidative species was that while they were found to be common in all of the samples examined, the individual product yields varied, which could be expected since temperatures, residence times, and flow conditions were not constant.

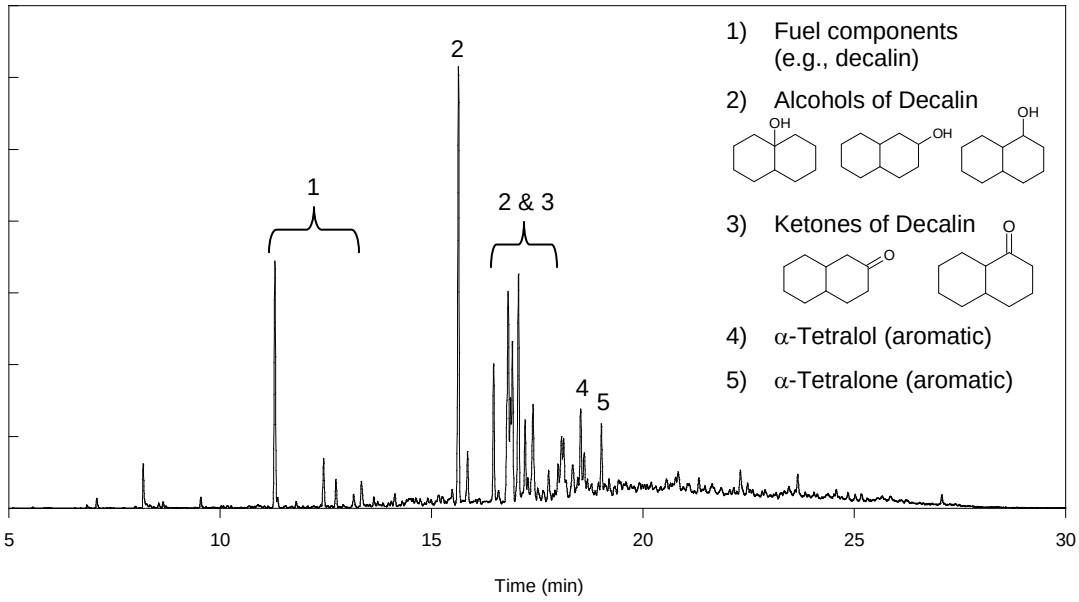


**Figure 4. SPE-GC-MS chromatogram of the coal-based fuel after thermal oxidative stressing in the QCM at 140°C.**

### 3.3.2 Oxidative and Pyrolytic Stability using the ECAT Flow Reactor System

The ECAT Flow Reactor System was used to evaluate the oxidative and pyrolytic stability characteristics of the coal-based fuel in a flowing environment. The system has previously been used to successfully evaluate thermal stability characteristics of fuels under both oxidative and pyrolytic conditions (Edwards and Krieger, 1995; Minus and Corporan, 1998; DeWitt and Zabarnick, 2002). The reaction zone of the ECAT is comprised of a 36-inch actively heated section where the fuel is exposed to sufficient temperature to promote the desired reaction chemistry. The outer wall temperature profile of the reaction tube is monitored using thermocouples (TC) strap-welded at various locations. The bulk fuel outlet temperature is monitored using a TC that is inserted into the outlet fuel flow approximately 7-inches downstream of the actively heated zone. After exiting the reaction zone, the fuel is cooled and passed through a 7 μm sintered filter element to remove any solids that are entrained in the fluid. The stability characteristics are determined by quantifying the total carbon deposition on the internal surface of the reaction tube and on the downstream filter and measuring the volumetric liquid-to-gas conversion.

The oxidative stability experiments in this study were conducted using a 50-inch long, 0.125-inch o.d., 0.085-inch i.d. tube constructed of 316 stainless steel, a reaction pressure of 550 psig and a volumetric flow rate of 10 ml/min. The furnace temperature was set to obtain a target maximum wall temperature of 650°F (bulk ~600°F); the reaction conditions rendered a total residence time of approximately 20 seconds in the actively heated zone. These reaction conditions have previously been shown to be adequate for complete consumption of the dissolved oxygen in the fuel within the reaction zone. Studies were conducted to compare the oxidative stability characteristics of the coal-based fuel with that of a typical JP-8 fuel (designated POSF-4177). A total reaction time of 8 hours was used which was previously shown to be sufficiently adequate to discern differences in deposition between various neat and additized fuels without being time-prohibitive. Each test was conducted twice to provide a measure of the reproducibility. A comparison of the surface deposition profiles for the 8 hour deposition testing with the coal-based fuel and JP-8 are shown in Figure 5. The reaction conditions and total quantities of surface and filter deposits are shown in Table 5. The coal-based fuel demonstrated excellent oxidative stability characteristics during testing resulting in minimal surface deposition on the reaction tube. In addition, the bulk deposits collected on the downstream filter were reduced by an order of magnitude (approximately 270 μg versus 2660 μg for JP-8). The stability characteristics of the coal-based fuel are similar to those observed for a JP-7 fuel, which is a specialty fuel designed to be stable for high-temperature applications (DeWitt and Zabarnick, 2002). Jet fuels produced by the Fischer-Tropsch (F-T) process have been shown to have comparable stability characteristics to the coal-based fuel and JP-7, exhibiting negligible surface deposition, as discussed in a previous publication (Edwards et al., 2004). The improved stability characteristics of the coal-based fuel, F-T fuels and JP-7 relative to a specification JP-8 are most likely due to the absence of heteroatomic containing species in these fuels which have previously been implicated as promoters of undesirable deposit formation in the oxidative regime. The stability of these fuels was better than that obtainable for a JP-8 fuel with the use of the currently qualified JP-8+100 thermal stability additive package (Heneghan et al., 1996). The surface deposition for the JP-8 dosed with the specified treat rate of the JP-8+100 for a reaction time of 6 hours is also shown on Figure 5. Although the deposition for the JP-8+100 additive package is lower than the neat JP-8 test, it is much higher than that observed for the coal-based fuel. This result further demonstrates the improved oxidative stability characteristics of the coal-based fuel relative to a specification JP-8.

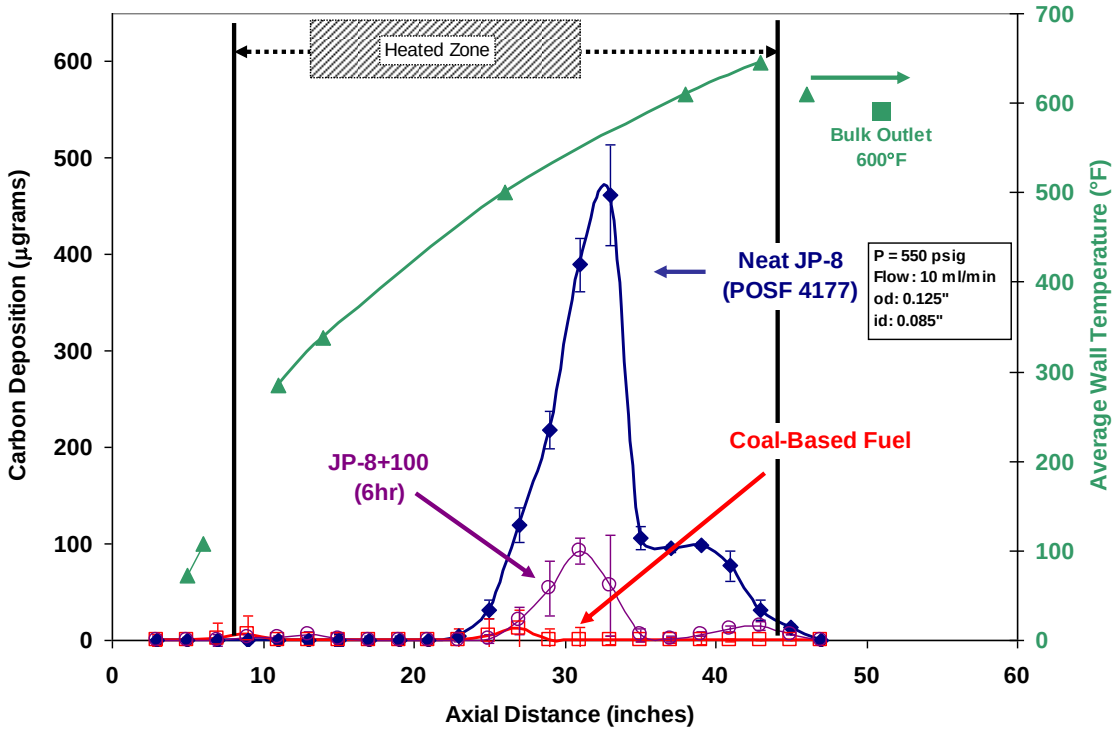


**Figure 5. Comparison of carbon deposition and wall temperature profiles for oxidative stability testing on ECAT flow reactor system with the coal-based fuel (POSF-4765) and a standard JP-8 fuel (POSF-4177) for 8 hours of reaction time. Carbon deposition profile for 6 hour reaction time from testing with JP-8+100 thermal stability additive package is also shown.**

**Table 5. Comparison of Reaction Conditions and Deposition and Liquid-to-Gas Conversion Data for Oxidative and Pyrolytic Stability Testing on ECAT Flow Reactor System with the Coal-Based Fuel (POSF-4765) and a Standard JP-8 Fuel (POSF-4177)**

| | Fuel | Reaction Time (hr) | Pressure (psig) | Furnace Temp (F) | Bulk Outlet Temp (F) | Outlet Wall Temp (F) | Surface Deposits (µg) | Filter Deposits (µg) | Liquid-to-Gas Conversion (volume %) |
|---|---|---|---|---|---|---|---|---|---|
| Oxidative | JP-8 (4177) | 8 | 550 | 908 (486.5C) | 590 (310C) | 645 (340C) | 1634 | 2660 | -- |
| | | | | | | | | | |
| | Coal-Based | 8 | 550 | 908 (486.5C) | 590 (310C) | 645 (340C) | 20 | 266 | -- |
| | | | | | | | | | |
| Pyrolytic | JP-8 (4177) | 6 | 525 | 1364 (740C) | 985 (529C) | 1100 (593C) | 2567 | 6905 | minimal |
| | | | | | | | | | |
| | JP-8 (4177) | 6 | 685 | 1418 (770C) | 1035 (557C) | 1186 (641C) | 3593 | 4970 | 3.9 |
| | | | | | | | | | |
| | Coal-Based | 6 | 685 | 1418 (770C) | 1025 (552C) | 1172 (633C) | -- | 172 | minimal |
| | | | | | | | | | |
| | Coal-Based | 5 | 710 | 1472 (800C) | 1077 (580C) | 1255 (680C) | 200 | 250 | 5.6 |
| | | | | | | | | | |
| | Coal-Based | 4.5 | 710 | 1499 (815C) | 1092 (588C) | 1294 (701C) | 343 | 232 | 8.2 |
| | | | | | | | | | |
| | Coal-Based | 6 | 705 | 1499 (815C) | 1099 (593C) | 1285 (696C) | 460 | 149 | 8.8 |

Pyrolytic testing was conducted to evaluate the higher-temperature stability of the coal-based fuel compared to that for a specification JP-8 and an F-T fuel. A primary goal during these tests was to obtain incipient pyrolytic activity to allow for relative comparisons to be made but to prevent excessive thermal cracking which results in difficulty while interpreting the experimental trends and primary reaction mechanism. The reaction tubing and flow rate used for the pyrolytic studies were identical to the preceding experiments; the reaction pressure was increased to 700 psig to improve control of the system. As stated above, a goal of these studies was to evaluate the pyrolytic stability characteristics of each fuel while preventing excessive thermal cracking. Therefore, the furnace temperature was varied to evaluate the regime where pyrolytic reactions are initiated and studies were conducted near this temperature. During pyrolysis of hydrocarbons, fragmentation and decomposition pathways of parent components in the fuel can result in the formation of lower molecular weight species that partition to the gas-phase at standard conditions. Therefore, an additional indice for comparison during pyrolysis is the relative volumetric liquid-to-gas conversion. In general, lower surface and filter deposition and liquid-to-gas conversion for a given reaction condition indicates enhanced pyrolytic stability. During these tests, the liquid-to-gas conversion was quantified via the difference of the volumetric inlet flow rate and the quantity of stressed fuel collected over an 8 minute period using a 10 ml calibrated graduated cylinder. Change in liquid volume due to density differences between neat and stressed fuel components was assumed to be negligible. All tests were conducted with oxygen dissolved in the fuel allowing for both oxidative and pyrolytic deposition within the reaction tubes; the temperature profile was sufficient to prevent merging of these deposition regimes.

Pyrolytic studies were initiated using a specification JP-8 to determine the onset temperature for testing and verify system operation. For the specified reaction conditions, pyrolytic activity of the fuel was observed to begin with the furnace temperature at 1364°F (740°C). This resulted in a bulk outlet temperature of approximately 985°F (529°C) with a maximum wetted wall temperature of approximately 1100°F (340°C). Gaseous product formation was observed at this temperature, but the volumetric liquid-to-gas conversion was insufficient to quantify. Pyrolytic testing of JP-8 was also conducted with a furnace temperature of 1418°F (770°C). The total reaction time was set to 6 hours for these tests. The carbon deposition profiles and pertinent data are shown in Figure 6 and Table 5. As shown in Figure 6, the surface deposition under the oxidative (lower temperature—left side of plot) and pyrolytic (high temperature—end of reaction zone) regimes can be clearly resolved. The decrease in surface deposition between the regimes is an indication of complete consumption of the dissolved oxygen (DeWitt et al., 2003). With respect to the oxidative deposition, the increase in reaction temperature profile resulted in a peak shift upstream with a slight increase in total deposition. These observations are consistent with those from previous testing on the ECAT investigating the effect of the temperature distribution on the oxidative deposition profile with a constant volumetric flow rate (DeWitt, 2004). As expected, an increase in surface deposition and liquid-to-gas conversion was observed as the reaction temperature was increased. This is expected as the pyrolytic free radical reaction rates are inherently dependent on the reaction temperature via the Arrhenius relationship. Stressed fuel was

collected at the outlet of the reactor system and species quantities were estimated via total area response using a HP 6890 Gas Chromatograph/Mass Spectrometer (GC/MS). Based on comparison with the neat fuel, it was possible to estimate the conversion of parent fuel components and product yields. For the test with the outlet temperature of 985°F, conversions from 25-35% were observed for the long-chain alkanes (tridecane to octadecane) with formation of lower molecular weight alkanes, alkenes and aromatics. These products, along with the formation of gaseous species (not identified but most likely $C_1$-$C_6$ alkanes and alkenes), are consistent with the free radical reaction chemistry observed during pyrolytic decomposition of long-chain hydrocarbons at intermediate temperature/high pressure for short reaction times (Fabuss et al., 1964; Mushrush and Hazlett, 1984; Zhou and Crynes, 1985; Ford, 1986; Song et al., 1994a).

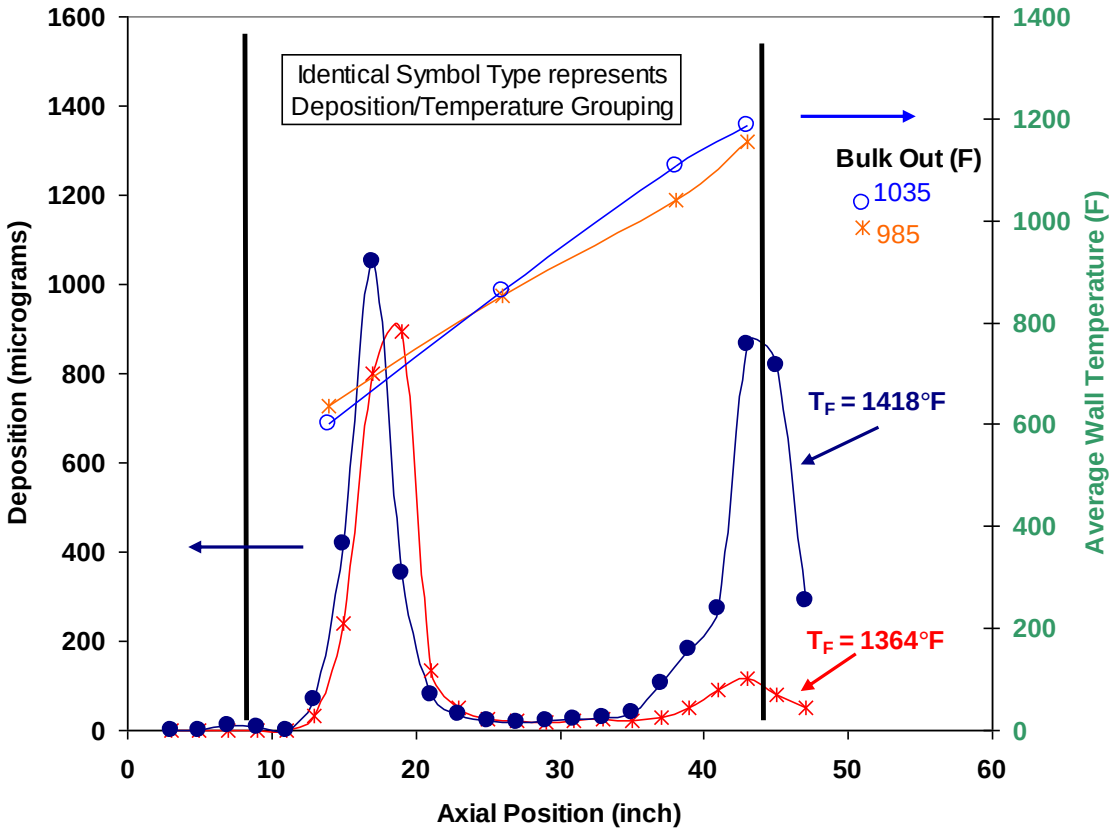


**Figure 6. Comparison of carbon deposition and wall temperature profiles for pyrolytic stability testing on ECAT flow reactor system with a standard JP-8 fuel (POSF-4177) for 6 hours of reaction time.**

Pyrolytic testing with the coal-based fuel was initiated with a furnace temperature of 1418°F (770°C) for comparison to the JP-8 testing. All reaction conditions were identical to the previous testing—the volumetric flow rate was not changed to account for density differences between the coal-based fuel and JP-8 during these tests. The results from this testing are shown in Table 5 and Figure 7. Under this condition there was incipient pyrolytic activity as indicated by gaseous product formation. However, neither oxidative

nor pyrolytic surface deposition was not observed for this testing and the gaseous product formation was insufficient to quantify. Since the overall reaction conditions for this and the second JP-8 test were comparable, this data indicates that the coal-based fuel exhibits enhanced pyrolytic stability characteristics with respect to both surface deposition and gaseous product (i.e., via fragmentation) formation. Additional testing with the coal-based fuel was performed with furnace temperatures of 1472°F (800°C) and 1499°F (815°C) which resulted in bulk outlet temperatures of approximately 1077°F (580°C) and 1092°F (588°C), respectively. The testing at 1472°F was conducted for 5 hours while the testing at 1499°F was conducted at 4.5 and 6 hours total. The results from this testing are also shown in Table 5 and Figure 7. An increase in the pyrolytic activity was observed as the overall reaction temperature was increased; oxidative deposition was not observed. During comparison of the tests at 1499°F, the rate of pyrolytic deposition was linear with reaction time. Specifically, the ratio of the reaction times was 1.33 while the ratio of the surface deposition in the reaction zone was approximately 1.34. For all tests with the coal-based fuel, minimal filter deposits were observed. As the temperature was increased, there was a concurrent increase in the liquid-to-gas conversion (as expected). Via comparison of Figures 6 and 7, it can be readily observed that the coal-based fuel shows enhanced pyrolytic stability relative to the JP-8, as defined by surface deposition and gaseous product formation. An alternate manner to consider the data is to compare the surface deposition characteristics under a similar total liquid-to-gas conversion, as shown in Figure 8. As shown for approximate conversions of 4-5%, the coal-based fuel showed reduced surface deposition with a higher reaction temperature.

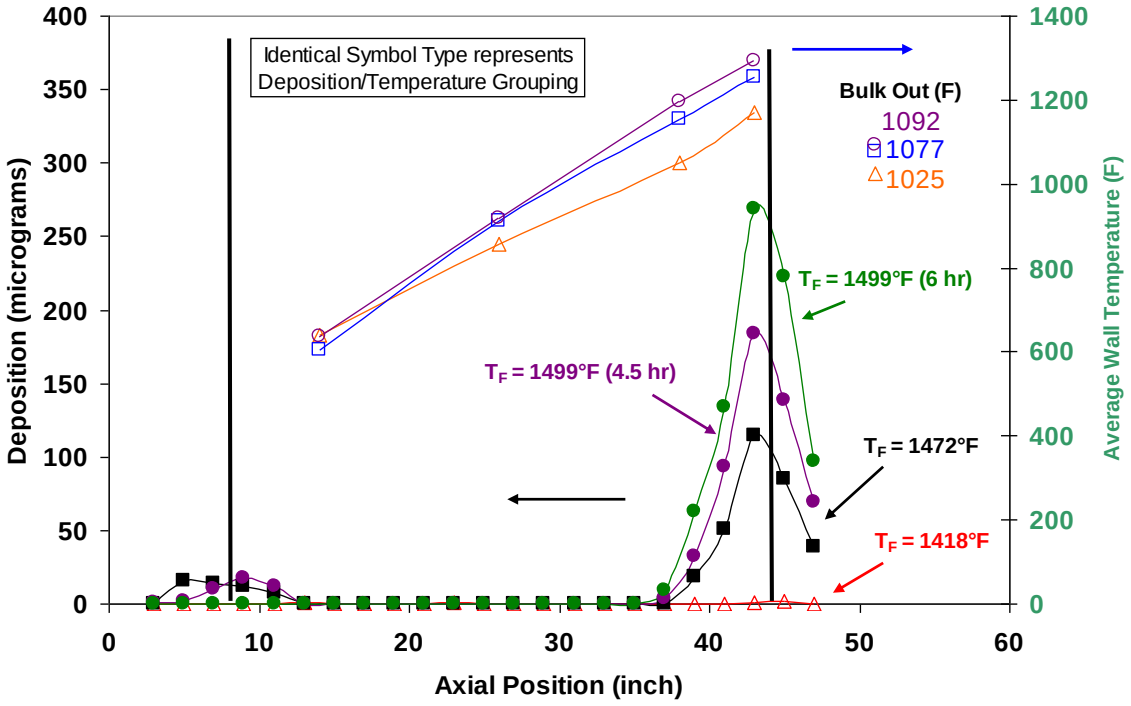


**Figure 7. Comparison of carbon deposition and wall temperature profiles for pyrolytic stability testing on ECAT flow reactor system with the coal-based fuel as a function of reaction temperature and time.**

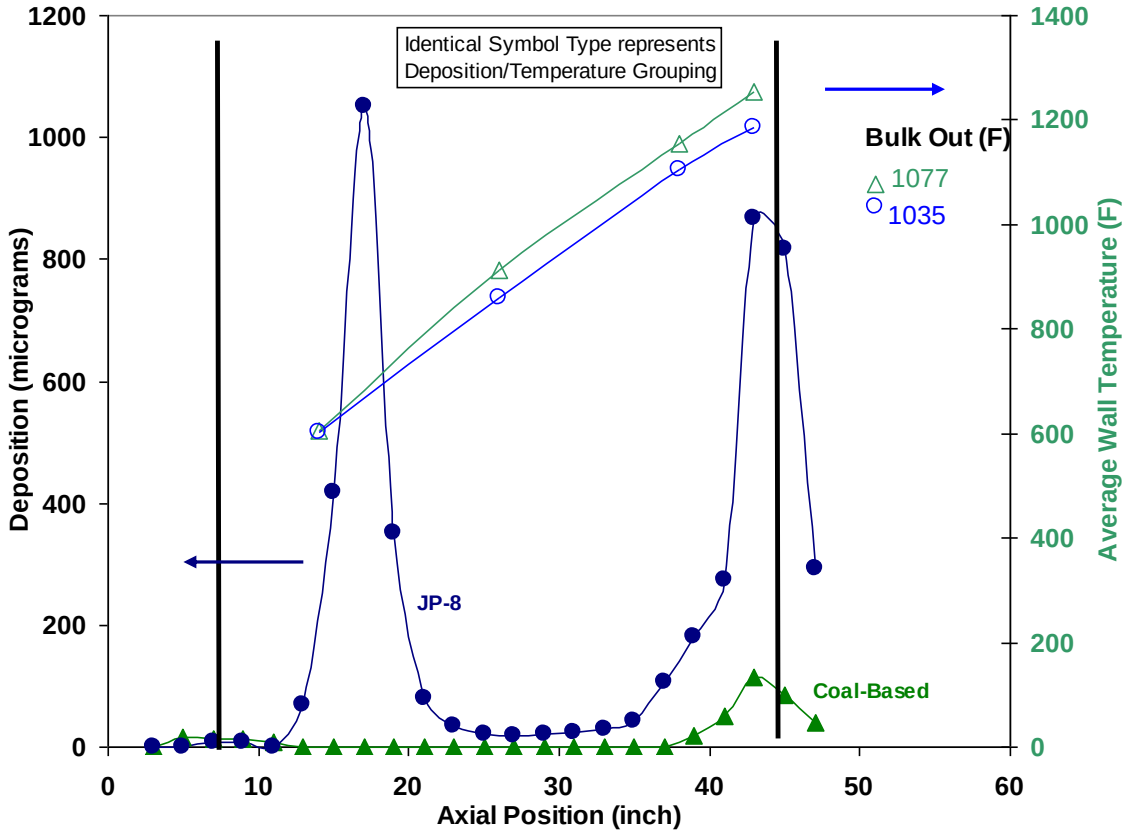


**Figure 8. Comparison of carbon deposition and wall temperature profiles for pyrolytic stability testing on ECAT flow reactor system with the coal-based fuel and JP-8 at similar liquid-to-gas conversions of 4-5%.**

The improvement in the inherent pyrolytic stability of the coal-based fuel can be understood by considering both the composition of the base fuels and the types of products formed during thermal stressing. As previously stated, the coal-based fuel is primarily comprised of cycloparaffins, with decalin being the major constituent. During pyrolysis, cycloparaffins can act as hydrogen donors to terminate the free radicals, reducing the overall propagation rate, ultimately forming unsaturated bonds (i.e., alkene formation) (Song et al., 1994b). The role of the cycloparaffins as hydrogen donors to effectively cap free radicals to reduce subsequent reactions, such as β-scission decomposition and radical recombination reactions, is well known. In particular, decalin and tetralin are frequently used as hydrogen donor solvents for liquefaction and upgrading of heavy hydrocarbon feed streams due to their high selectivity for hydrogen donation and formation of stable products (Probstein and Hicks, 1982). As previously discussed, JP-8 primarily contains normal and branched alkanes and aromatics—these species readily decompose during the propagation of free radical pyrolysis resulting in a long chain length with high yields of lower molecular weight products. The specific product selectivity is affected by the reaction conditions, with pressure having a significant influence on the ratio of saturate/unsaturated formation. Analysis of the neat component conversion and relative product formation for the coal-based fuel supports the

assertions above for the experimental results presented. During testing, stressed samples of the coal-based fuel were collected and analyzed as previously discussed. Reactant conversions were calculated via concentration difference with the neat fuel while accounting for volume change due to gaseous product formation. Since quantitation was performed via area response of the GC/MS rather than use of an internal standard, it was not possible to calculate absolute product concentrations. Therefore, relative product yields for the higher temperature runs were normalized to the formation at the lowest test temperature (1418°F Furnace). Analysis of the product yields in this manner allows for the product selectivity trends to be made. If products were only formed at a higher reaction temperature, the yields were normalized to the lowest production temperature. Comparison of the neat fuel component conversions and primary product yields is shown in Table 6. The area responses qualitatively indicate the representative concentrations of each product formed (e.g., higher area count indicates higher concentration). The primary constituent in the coal-base fuel is trans-decalin; it was not possibly to determine the conversion for this component due to saturation of the MS detector. Therefore, cis-decalin was used as an indicator of the relative reactivity. As shown in Table 6, significant conversions of the components in the coal-based fuel were observed although there was low surface deposition and gaseous product formation. The primary products are consistent with those that would be produced via decomposition and hydrogen abstraction pathways. For example, methyl cyclohexanes, -enes, -dienes and aromatic products have previously been reported for pyrolysis of decalin (Stewart et al., 1998; Yu and Eser, 1998). The deposition and gaseous product trends indicate that the pyrolytic reaction pathways readily terminate following primary product formation due to hydrogen donation, preventing subsequent decomposition (i.e., fragmentation and gaseous product formation). In addition, the high formation yields of the aromatic species (toluene and ethyl benzene) further support the hydrogen-donor propensity of the coal-based fuel and its products. It should be noted that under excessive thermal stressing, the potential exists for significant aromatic product formation to occur. This may result in a detrimental effect on the particulate and gaseous emissions of the fuel during combustion.

## Table 6. Comparison of Normalized Product Yields and Neat Fuel Component Conversions for Pyrolytic Stability Testing on ECAT Flow Reactor System with the Coal-Based Fuel (POSF-4765) as a Function of Reaction Temperature.

| Furnace Temperature (F) | | 1418 | | 1472 | | 1499 | |
|---|---|---|---|---|---|---|---|
| Liquid-to-Gas Formation | | -- | | 5.60% | | 8.20% | |
| Products | Retention Time (min) | Area | Yield | Area | Yield | Area | Yield |
| Benzene | 2.67** | 2.25E+05 | 1.0 | 4.76E+06 | 19.9 | 7.30E+06 | 32.4 |
| Methylene-cyclopentene | 2.76 | 4.49E+05 | 1.0 | 1.24E+06 | 2.6 | 1.59E+06 | 3.5 |
| Ethenyl-cyclobutane | 2.89** | 2.92E+06 | 1.0 | 8.38E+06 | 2.7 | 1.00E+07 | 3.4 |
| Dimethyl-cyclopentane | 2.94 | 2.08E+05 | 1.0 | 4.81E+05 | 2.2 | 5.41E+05 | 2.6 |
| Dimethyl-cyclopentane | 2.98 | | | 1.73E+05 | 1.0 | 1.96E+05 | 1.1 |
| Heptene | 3.01 | 5.27E+05 | 1.0 | 1.15E+06 | 2.1 | 1.24E+06 | 2.4 |
| Heptane | 3.12 | 2.94E+05 | 1.0 | 5.25E+05 | 1.7 | 5.49E+05 | 1.9 |
| Dimethyl cyclopentene | 3.16 | 1.62E+05 | 1.0 | 7.26E+05 | 4.2 | 9.20E+05 | 5.7 |
| Dimethyl cyclopentene | 3.18 | | | 3.38E+05 | 1.0 | 4.46E+05 | 1.3 |
| Heptene | 3.23 | | | 3.93E+05 | 1.0 | 4.78E+05 | 1.2 |
| Dimethyl-cyclopentene | 3.33 | 5.45E+04 | 1.0 | 1.62E+05 | 2.8 | 1.94E+05 | 3.6 |
| Methyl-methylene-cyclopentane | 3.46 | | | 1.49E+04 | 1.0 | 1.53E+05 | 10.3 |
| Methyl cyclohexane | 3.54** | 2.85E+06 | 1.0 | 5.43E+06 | 1.8 | 5.80E+06 | 2.0 |
| Methyl-hexatriene | 3.61 | | | 3.02E+05 | 1.0 | 3.83E+05 | 1.3 |
| Ethyl-cyclopentane | 3.71 | 3.58E+05 | 1.0 | 8.42E+05 | 2.2 | 9.86E+05 | 2.8 |
| Methyl-cyclohexene | 3.8 | | | | | 4.81E+05 | |
| Methyl-cyclohexene | 3.83** | 6.38E+05 | 1.0 | 1.69E+06 | 2.5 | 1.94E+06 | 3.0 |
| Methylene cyclohexane | 3.87** | 9.97E+05 | 1.0 | 2.36E+06 | 2.2 | 2.59E+06 | 2.6 |
| Methyl-hexatriene | 3.96 | 2.58E+05 | 1.0 | 8.65E+05 | 3.2 | 8.89E+05 | 3.4 |
| Heptadiene | 4.02 | 2.42E+05 | 1.0 | 1.03E+06 | 4.0 | 1.31E+06 | 5.4 |
| Ethyl-cyclopentene | 4.09** | 6.30E+05 | 1.0 | 2.18E+06 | 3.3 | 2.71E+06 | 4.3 |
| Heptatriene | 4.23 | 2.63E+05 | 1.0 | 8.63E+05 | 3.1 | 1.12E+06 | 4.3 |
| Toluene | 4.32** | 2.31E+06 | 1.0 | 1.70E+07 | 7.0 | 2.56E+07 | 11.1 |
| Methyl-cyclohexene | 4.39** | 4.98E+06 | 1.0 | 1.39E+07 | 2.6 | 1.58E+07 | 3.2 |
| Dimethyl-cyclopentadiene | 4.49 | 2.07E+05 | 1.0 | 7.79E+05 | 3.5 | 9.74E+05 | 4.7 |
| Ethylidene cyclopentane | 4.55 | | | 8.37E+05 | 1.0 | 1.05E+06 | 1.3 |
| Cycloheptadiene* | 4.63** | 3.13E+06 | 3.4 | 6.64E+06 | 2.0 | 7.44E+06 | 2.4 |
| Dimethyl-cyclohexene | 4.87 | 5.39E+05 | 1.0 | 1.09E+06 | 1.9 | 1.17E+06 | 2.2 |
| Dimethyl-cyclohexene | 5.15 | 4.26E+05 | 1.0 | 9.94E+05 | 2.2 | 1.09E+06 | 2.6 |
| Dimethyl-cyclohexane | 5.25 | 7.05E+05 | 1.2 | 1.01E+06 | 1.4 | 1.02E+06 | 1.4 |
| Dimethyl-hexadiene | 5.67 | 4.57E+05 | 1.0 | 1.10E+06 | 2.3 | 1.47E+06 | 3.2 |
| Dimethyl-cyclohexene | 5.72** | 6.81E+05 | 1.0 | 1.67E+06 | 2.3 | 1.86E+06 | 2.7 |
| Dimethyl-cyclohexene | 5.81** | 8.72E+05 | 1.0 | 2.05E+06 | 2.2 | 2.22E+06 | 2.5 |
| Dimethyl-cyclohexene | 6.22 | | | 2.87E+05 | 1.0 | 3.75E+05 | 1.3 |
| Ethyl-cyclohexene | 6.4 | 7.06E+05 | 1.0 | 1.61E+06 | 2.1 | 1.82E+06 | 2.6 |
| Ethyl benzene | 6.66** | 4.36E+05 | 1.0 | 3.47E+06 | 7.5 | 5.51E+06 | 12.7 |
| Dimethyl-methylenecyclopentene | 6.75 | | | 3.20E+05 | 1.0 | 4.30E+05 | 1.3 |
| Ethyl-cyclohexene & Xylene | 6.91** | 1.77E+06 | 1.0 | 7.95E+06 | 4.2 | 1.05E+07 | 5.9 |
| Xylene | 6.96** | 6.98E+05 | 1.0 | 2.26E+06 | 3.1 | 3.22E+06 | 4.6 |
| Octatriene | 7.1 | 2.72E+05 | 1.0 | 7.22E+05 | 2.5 | 8.19E+05 | 3.0 |
| Styrene & Xylene | 7.57** | 3.13E+05 | 1.0 | 2.17E+06 | 6.6 | 3.59E+06 | 11.5 |
| Ethenyl-cyclohexene | 8.03 | 5.80E+05 | 1.0 | 1.41E+06 | 2.3 | 1.67E+06 | 2.9 |
| Ethylidene-cyclohexene | 8.31** | 3.54E+04 | 1.0 | 1.02E+06 | 27.4 | 1.33E+06 | 37.7 |
| Propyl-benzene* | 9.44** | 1.45E+05 | 1.0 | 1.88E+06 | 12.3 | 2.48E+06 | 17.1 |
| Ethyl-methyl-benzene* | 9.68** | 4.70E+04 | 1.0 | 8.13E+05 | 16.3 | 1.38E+06 | 29.3 |
| Hexahydroindene* | 10.28 | 1.51E+06 | 1.0 | 2.32E+06 | 1.5 | 2.38E+06 | 1.6 |
| Trimethyl-benzene | 10.71 | | | 2.29E+04 | 1.0 | 6.71E+04 | 2.9 |
| Octahro-methyl-indene | 12.25 | 1.06E+07 | 1.2 | 1.17E+07 | 1.0 | 1.18E+07 | 1.1 |
| Octahydronaphthalene | 13.23** | 7.77E+05 | 1.0 | 5.71E+06 | 6.9 | 6.30E+06 | 8.1 |
| Decahydro-naphthalenol | 13.42** | 2.72E+06 | 1.0 | 6.35E+06 | 2.2 | 7.18E+06 | 2.6 |
| Octahydronaphthalene* | 14.07** | 3.79E+05 | 1.0 | 4.53E+06 | 11.3 | 5.24E+06 | 13.8 |
| Naphthalene*** | 16.55 | 8.72E+03 | 7.9 | 7.94E+04 | 8.6 | 1.40E+05 | 16.0 |
| Dimethyl-naphthalene*** | 22.97 | 2.51E+03 | 9.2 | 1.05E+04 | 3.9 | 1.48E+04 | 5.9 |
| Acenaphthylene*** | 23.73 | | | 3.56E+02 | 1.0 | 1.63E+03 | 4.6 |
| Acenaphthene*** | 24.57 | 6.91E+02 | 4.3 | 4.23E+03 | 5.8 | 6.94E+03 | 10.0 |
| Fluorene*** | 27.02 | 5.61E+02 | 1.0 | 2.33E+03 | 3.9 | 4.22E+03 | 7.5 |
| Phenanthrene*** | 31.4 | 2.85E+02 | 2.7 | 1.65E+03 | 5.4 | 3.10E+03 | 10.9 |
| Anthracene*** | 31.66 | | | 4.72E+02 | 1.0 | 1.20E+03 | 2.5 |
| Fluoranthene*** | 36.97 | | | 3.65E+01 | 1.0 | 4.11E+02 | 11.3 |
| Pyrene*** | 37.96 | 4.45E+01 | 1.0 | 6.57E+02 | 13.9 | 1.51E+03 | 34.0 |

*product is different than compound in unstressed fuel
**more abundant products @ high stress
***areas are primary ion areas

| Reactants | Retention Time (min) | | %Conversion | | %Conversion | | %Conversion |
|---|---|---|---|---|---|---|---|
| Octahydro-indene | 10.64 | 2.10E+07 | 14.5 | 1.64E+07 | 36.8 | 9.91E+06 | 59.6 |
| Decahydro-naphthalene | 14.16 | 8.70E+07 | 16.6 | 6.67E+07 | 39.7 | 5.65E+07 | 45.9 |
| Decahydro-naphthalene | 14.53 | 7.37E+07 | 9.5 | 6.36E+07 | 26.3 | 5.62E+07 | 31.0 |
| Decahydro-methyl-naphthalene | 14.99 | 3.41E+07 | 8.7 | 3.04E+07 | 23.1 | 2.73E+07 | 26.7 |
| Decahydro-methyl-naphthalene | 15.22 | 1.59E+07 | 7.9 | 1.51E+07 | 17.6 | 1.35E+07 | 22.1 |
| Decahydro-methyl-naphthalene | 15.66 | 7.25E+06 | 19.8 | 5.25E+06 | 45.2 | 4.52E+06 | 50.0 |
| Decahydro-dimethyl-naphthalene | 16.21 | 2.82E+07 | 12.3 | 2.34E+07 | 31.2 | 2.02E+07 | 37.0 |
| Decahydro-dimethyl-naphthalene | 16.51 | 1.65E+06 | 10.4 | 1.38E+06 | 29.4 | 1.16E+06 | 36.9 |
| Decahydro-dimethyl-naphthalene | 16.56 | 1.13E+06 | 10.6 | 9.97E+05 | 25.5 | 8.89E+05 | 29.6 |
| Decahydro-dimethyl-naphthalene | 16.88 | 1.73E+07 | 9.2 | 1.47E+07 | 26.9 | 1.29E+07 | 32.4 |
| Tricyclo-dodecane | 19.84 | 1.38E+07 | 15.7 | 8.74E+06 | 49.6 | 7.77E+06 | 52.6 |
| Adamantane | 19.98 | 8.98E+06 | 14.1 | 6.45E+06 | 41.8 | 5.32E+06 | 49.2 |
| Bicyclohexyl | 20.11 | 2.29E+07 | 21.6 | 1.63E+07 | 47.3 | 1.36E+07 | 53.4 |

Pyrolytic testing of the F-T derived fuel (POSF-4734) was also performed to compare the relative stability characteristics to those for the coal-based fuel and JP-8. Testing was conducted with furnace temperatures of 1364°F (740°C), 1391°F (755°C) and 1418°F (770°C) with a total reaction time of 6 hours. All other reaction conditions were identical to those for the previous testing. The surface deposition profiles for the F-T fuel testing are shown in Figure 9. As the temperature was increased, there was a corresponding increase in the pyrolytic surface deposition—oxidative deposition was negligible for this fuel. Of significant note is the total quantity of pyrolytic deposition for the F-T fuel, which was substantially higher than that observed for either JP-8 or the coal-based fuel under similar reaction conditions. In addition, the measured liquid-to-gas conversion significantly increased for the F-T derived fuel—2.5%, 6.3% and 12.6% for the three reaction temperatures studied. These results imply that the F-T is significantly more reactive than either the JP-8 or coal-based fuel under pyrolytic conditions. The increased reactivity can be explained by reviewing the base composition of the F-T fuel. As previously discussed, the F-T fuel is primarily comprised of methyl-substituted (~85%) and normal alkanes (~15%). The fuel is deficient of aromatics (including alkyl-substituted) and cycloparaffins. These latter components are known to act as hydrogen donors in the pyrolytic process which reduce the overall propagation rate. Radical initiation is also increased due to the high concentration of energetically weaker tertiary carbons (methyl branch of alkanes) in the F-T fuel. Once a radical is initiated, repeated decomposition of the parent components in the F-T can readily proceed resulting in significant yields of low molecular weight (i.e., gaseous) products. Once formed in appreciable yield, these low molecular weight alkanes and alkenes can undergo condensation and molecular growth reactions to form deposit precursors (i.e., PAHs) and species that ultimately form surface deposits. The net effect for the F-T fuel is that the pyrolytic activity is substantially higher than that for either JP-8 or the coal-based fuel, resulting in higher gaseous product yields and possibly unfavorable surface deposition under similar reaction conditions.

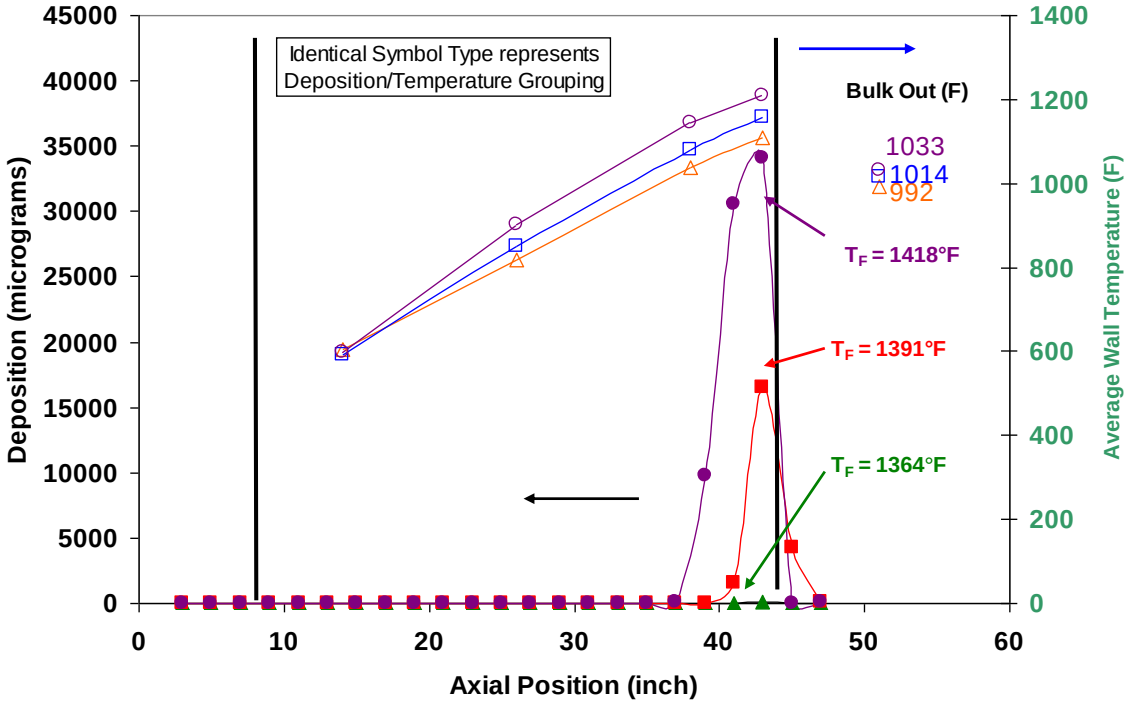


**Figure 9. Comparison of carbon deposition and wall temperature profiles for pyrolytic stability testing on ECAT flow reactor system with a fuel produced via the Fischer-Tropsch process (POSF-4734) as function of temperature for a reaction time of 6 hours.**

Overall, the coal-based fuel demonstrated excellent stability characteristics under a complete oxygen consumption regime. The stability was better than that obtainable for a JP-8 fuel with the use of the currently qualified JP-8+100 thermal stability additive package (Heneghan et al., 1996) and comparable to that for JP-7 and a synthetic fuel produced via the Fischer-Tropsch process. The enhanced stability for the coal-based and F-T fuels relative to JP-8 were attributed to the absence of heteroatomic containing species in these fuels which are known to be oxidative deposit precursors. Under pyrolytic conditions, the coal-based fuel exhibited enhanced stability characteristics (defined by surface deposition and gaseous product formation) compared to both JP-8 and the F-T fuel. The enhanced stability was attributed to the hydrogen-donor capability of the base fuel components which can reduce the overall rate of pyrolysis and stabilize reaction intermediates prior to repeated fragmentation. Conversely, the F-T fuel showed significantly higher surface deposition and gaseous product formation due to the absence of radical-stabilizing species which allows for repeated decomposition of the base components.

### 3.3.3 Phoenix Rig Thermal Stability Studies

The Phoenix Rig (also referred to as the "Advanced Aircraft Fuel System Simulator," or AAFSS) was designed to simulate the thermal loads envisioned for advanced aircraft fuel systems. The AAFSS simulator operates at heat loads, pressures, and temperatures

similar to those expected in advanced fuel/thermal management systems. The simulator can operate for extended periods, while maintaining realistic wall and bulk temperatures. The system can be modified to operate in several different configurations.

For the current studies the system operated as shown in Figure 10. In this configuration the fuel flows vertically upward through two Split Tube Furnaces. The first oven has an active length of 36 inches, comprised of four individually controlled heating zones. The furnace has a 5-inch inside diameter and a maximum output of 11520 watts. The second oven has an active length of 24 inches, divided into three 8-inch individually controllable sections, and a 5-inch inside diameter with a total wattage of 7980 watts. Each oven section has two K type thermocouples per zone with Inconel sheathed spring loaded bayonet type mounts. The maximum operating temperature rating for the split tube furnaces is 1204°C (2200°F). The test tubing is currently assembled for a single pass through the center of the ovens. The tubing is secured, at the bottom end, to the oven base plate and thermally isolated with a ceramic stand off. To compensate for thermal expansion, the top end of the tubing section is held with a constant 5-pound tensile spring load, attached through a ceramic stand off. The section between the furnaces is fully insulated. Bulk dissolved oxygen levels were measured, on-line, at the locations shown in Figure 10, by means of a Hewlett Packard 5890 Series II gas chromatograph. A sample port, for extracting stressed fuel was installed near the input to the waste tank. Thermocouples (20 gage) are welded to the outer surface of the tubing to provide the tube wall temperatures with an uncertainty of (2°C). The bulk fuel temperatures at the exit of the heated sections were also measured (uncertainty of 5°C).

The tubing used is high purity 316 stainless steel, 0.125” ID, 0.085” OD, ASTM grade A269/A213, with a surface roughness of 8-15 microinches. After each test, the tubing was cut into 2 inch sections, rinsed with hexane, dried with low velocity nitrogen gas and then put into a vacuum oven at 150°F for 2 hours. A Leco (RC-412) multiphase carbon analyzer determined the mass of carbon on the segments. The reproducibility in the determination of the carbon deposit profile is on the order of 5%, determined by sequential tests. For all the current deposition experiments, the measurable dissolved oxygen was entirely consumed in the first furnace.

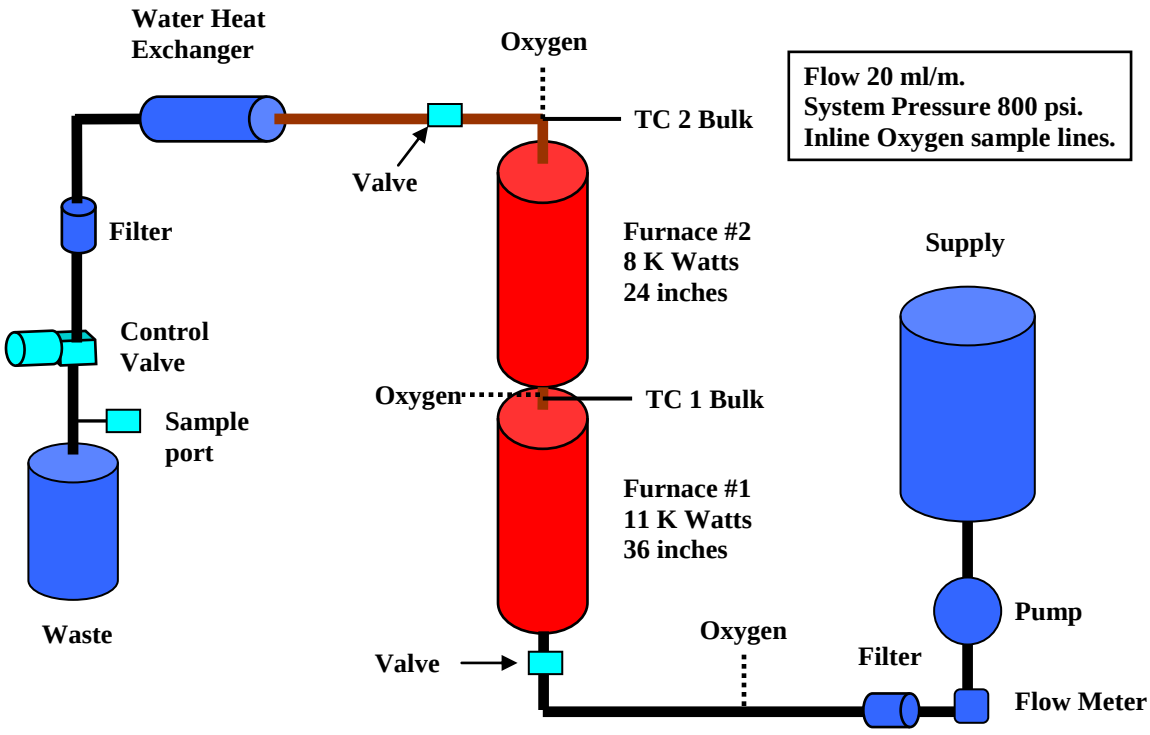


**Figure 10. Phoenix Rig schematic for a two split tube furnaces configuration where fuel flow is vertically upward.**

The coal-based fuel (POSF-4765) was run in comparative tests to a baseline JP-8 fuel (POSF-4751) and a synthetic Fischer-Tropsch fuel (POSF-4734). A summary of the tests results is given in Table 7. The initial test was set to the following conditions: Furnace #1 set to give a bulk output of 550°F and Furnace #2 to give an output bulk fuel temperature of 1075°F. Operationally the system parameters were: fuel flow of 20 ml/min and a pressure of 800 psig for a test duration of six hours. In two attempts at running this test with the baseline JP-8 fuel, deposit formation created within the first hour of operation completely blocked flow in the second furnace. The wall and fuel temperatures in this furnace encompass the regime in which fuel pyrolytic decomposition is likely. Thus the plugging of the second furnace by the JP-8 fuel is thought to be due to pyrolytic deposition. In contrast to the JP-8 fuel, the coal-based fuel did not plug the system under these conditions. The results for the coal based fuel are shown in Figure 11. The figure shows that the coal-based fuel produced minimal deposition in both furnaces under these conditions. The synthetic fuel was not included in these test conditions.

To attempt to provide a direct comparison between the coal-based and JP-8 fuels, the furnace temperatures were reduced and new runs started. Furnace #1 was set to give a bulk output of 500°F and Furnace #2 to an output bulk fuel temperature of 1000°F. These temperature reductions allowed successful completion of the six hour test with all fuels. Figure 12 displays the results of these tests. The JP-8 fuel produced substantial autoxidative deposits in the first furnace. The coal-based fuel did not produce any measurable autoxidative deposits. Neither fuel produced pyrolytic deposits (second

furnace) as the wall temperature was not high enough under these conditions to produce significant pyrolytic decomposition of the fuel. Interestingly, the bulk fuel outlet temperature under these conditions was only 75°F lower than the conditions described above, while the maximum wall temperature was almost 300°F lower. Thus, a significant increase in the wall temperature is required to increase the bulk fuel temperature under these flow conditions.

In a second set of tests, only Furnace#1 was used and the three fuels were thermally stressed to a bulk temperature of 650°F for an extended period of time. For these tests the system parameters were a fuel flow of 20 ml/min and a system pressure of 800 psig for a test duration of twenty hours. The results are shown in Figure 13. In addition to the three fuels being operated in an air saturated condition, an additional test was performed with nitrogen sparged JP-8 fuel. The results show that the JP-8 fuel produces considerable amounts of deposit, while the coal-based fuel, synthetic fuel, and nitrogen-sparged JP-8 fuel do not produce any significant surface deposition.

Figures 14 and 15 show a summary of the summed carbon deposition for the all the Phoenix rig runs. The results indicate that both the coal-based fuel and the synthetic provide substantial high temperature thermal stability improvements relative to the petroleum-derived JP-8 fuel.

**Table 7. Summary of Phoenix Rig Comparative Testing**

| Fuel | Test Time | Furnace #1 Bulk Temp. Set Point (°F) | Furnace #2 Bulk Temp. Set Point (°F) | Total Deposits (mg) | Furnace #1 Temp. (°F) | Furnace #2 Temp. (°F) |
|---|---|---|---|---|---|---|
| JP-8 4751 | ~1 Hours | 550 | 1075 | Plugged | 1275 | 1827 |
| Coal-based 4765 | 6 Hours | 550 | 1075 | 529 | 1275 | 1827 |
| | | | | | | |
| JP-8 4751 | 6 Hours | 500 | 1000 | 2848 | 1227 | 1642 |
| Coal-based 4765 | 6 Hours | 500 | 1000 | 358 | 1257 | 1627 |
| FT 4734 | 6 Hours | 500 | 1000 | 291 | 1270 | 1620 |
| | | | | | | |
| JP-8 4751 | 20 Hours | 650 | NA | 8981 | 1375 | NA |
| JP-8 4751 Nitrogen | 20 Hours | 650 | NA | 366 | 1375 | NA |
| Coal-based 4765 | 20 Hours | 650 | NA | 233 | 1375 | NA |
| FT 4734 | 20 Hours | 650 | NA | 216 | 1375 | NA |

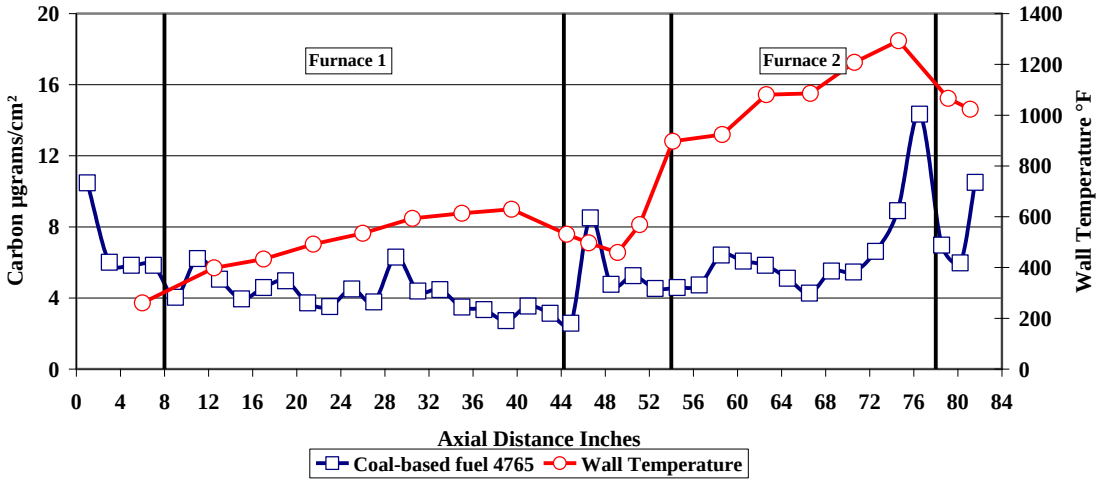


**Figure 11. Six hour Phoenix rig tests with bulk fuel outlet temperatures of 550°F for Furnace #1 and 1075°F for Furnace #2. Very high deposition produced by the petroleum-derived JP-8 fuel plugged the tube under these conditions.**

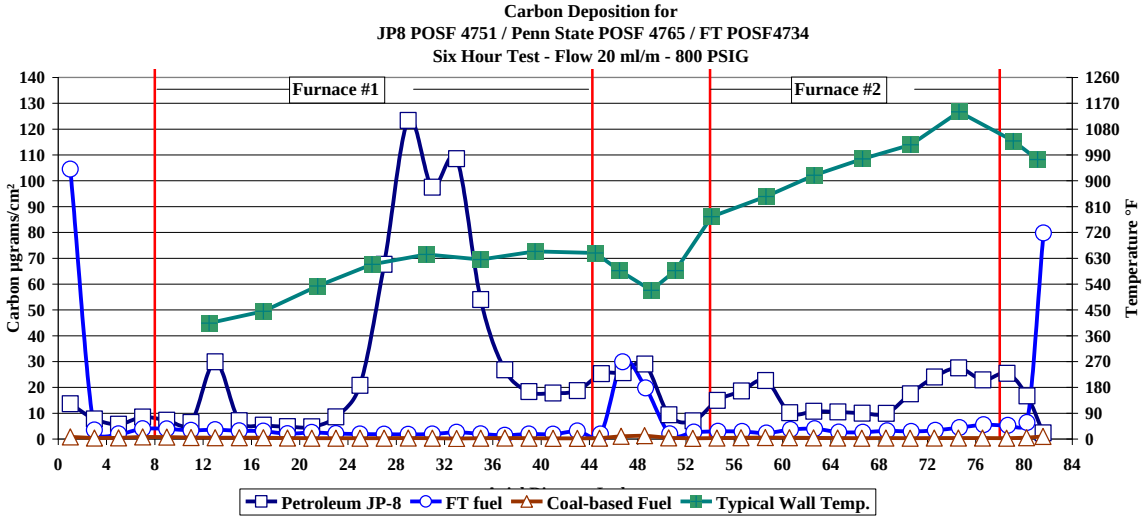


**Figure 12. Six hour Phoenix rig tests with bulk fuel outlet temperatures of 500°F for Furnace#1 and 1000°F for Furnace#2.**

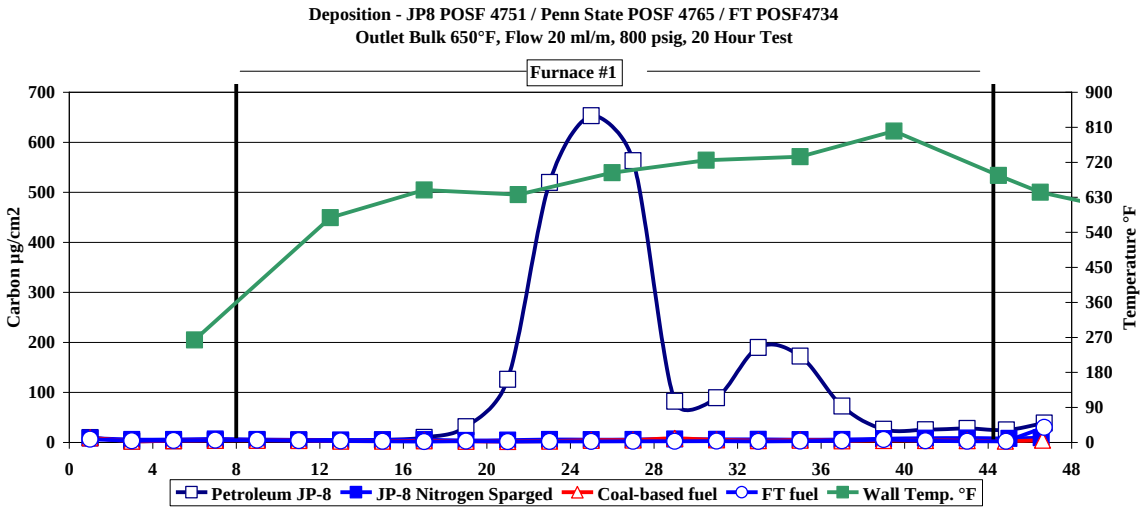


**Figure 13. Phoenix rig results for 20 hour test with a Furnace#1 bulk temperature out of 650°F. The JP-8 nitrogen sparged, coal-based fuel, and FT fuel results overlap and show essentially no deposition.**

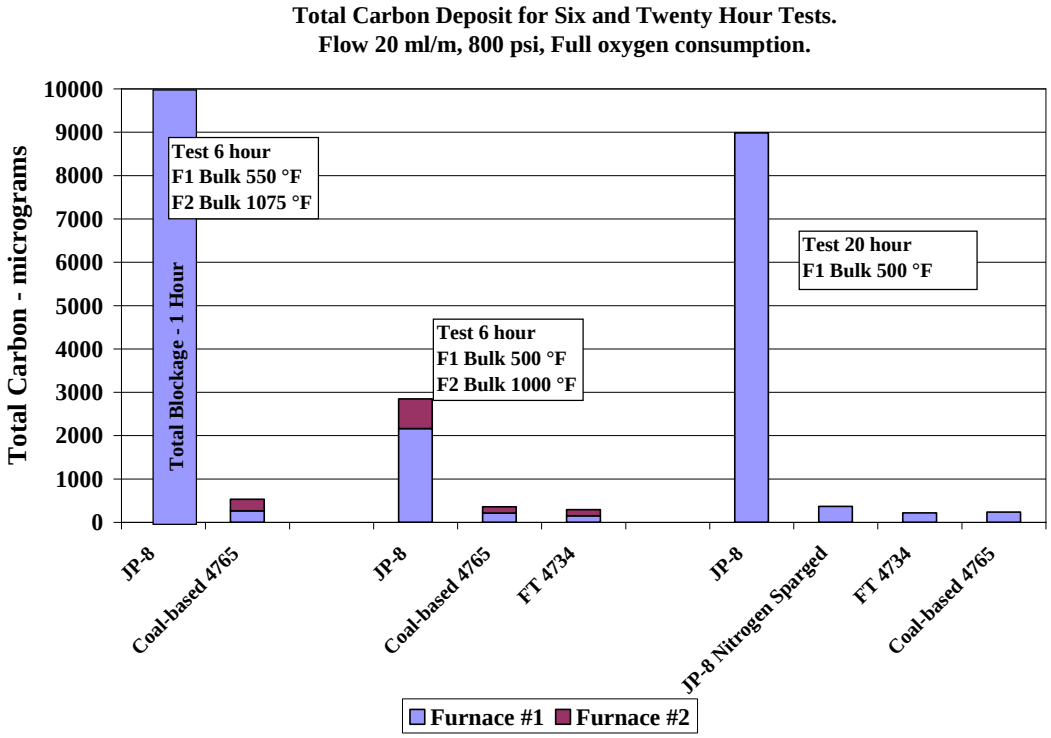


**Figure 14. Total carbon deposits for all Phoenix Rig tests.**

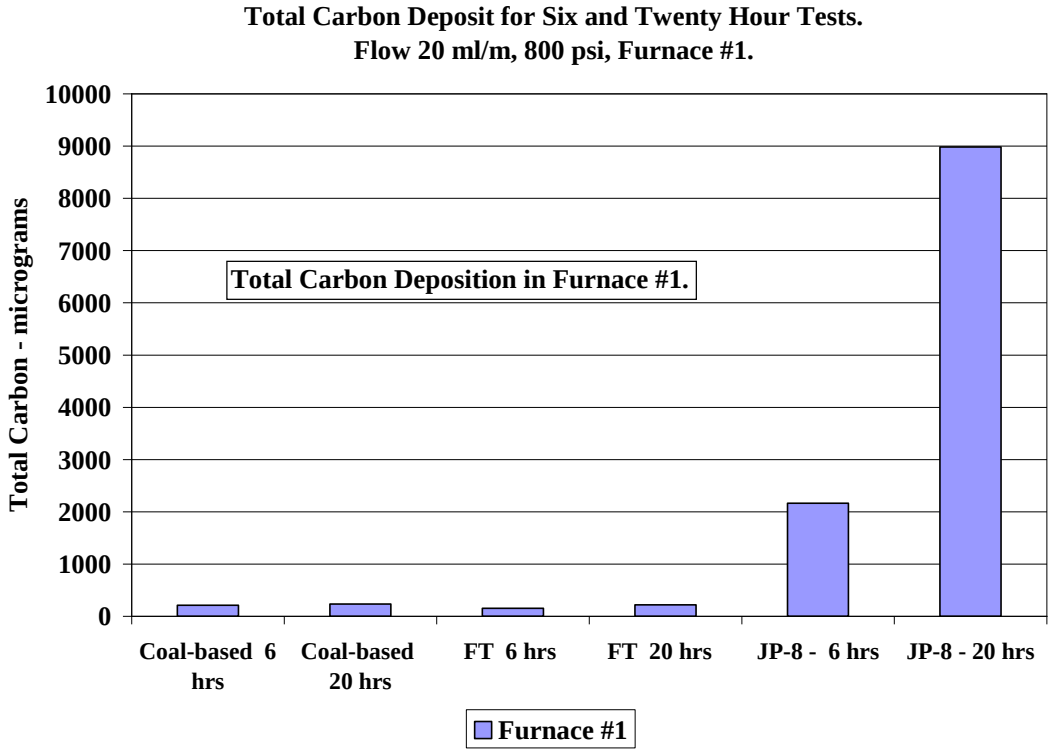


**Figure 15. Total carbon deposits for Phoenix Rig 6 and 20 hour tests of oxidative deposition.**

Samples of the stressed coal-based fuel, JP-8 fuel, and S-8 fuel were collected at the outlet of the Phoenix Rig. The coal-based fuel and the JP-8 fuel were stressed at 500°F and at 1000°F. The coal-based fuel was also stressed at 550° and 1075°F, as was the S-8 fuel. These stressed fuels were analyzed along with unstressed samples of the fuels in an attempt to detect any chemical differences between them.

The samples were diluted in hexanes and analyzed by GC/MS. The column model used in the Agilent 6890 GC was a 30 m DB-5MS with a 0.25 mm inside diameter (ID) and a 0.25-$\mu$m film. The GC temperature program involved an initial temperature of 40°C (2-min hold) followed by ramping (5°C/min) to 280°C. A constant column flow rate of 1 mL/min and a 50:1 split 1-uL injection were used. The GC injector temperature was 250°C, and the Agilent 5973 mass spectrometer transfer line was held at a temperature of 280°C. The resulting chromatograms were compared both qualitatively (for identification of components) and semi-quantitatively (by areas of components) (Tables 8, 9, and 10).

The compounds listed in the tables are those that were either increased (products) or decreased (reactants) from the unstressed to the stressed fuels. The component yields were calculated as ratios of the areas of components in the stressed fuel to the areas in the unstressed fuel. For products formed that were not initially present in the unstressed fuels the yields were calculated as ratios of the areas in the higher-temperature stressed fuels to the areas in the lower-temperature stressed fuels. The conversions are the differences

between the areas of the reactants in the stressed and unstressed fuels expressed as percentages of the areas in the unstressed fuel.

For the JP-8 fuel and the coal-based fuel there were no discernable differences in the major fuel components (alkanes and aromatics) between the unstressed samples and the samples stressed at 500°F and 550°F. However, in the S-8 fuel stressed at 550°F there were increases in several alkanes, along with the formation of a few alkenes not present in the unstressed fuel. At 1075°F there were several more alkenes in the S-8 fuel, as well as increased amounts of the products formed at 550°F. The JP-8 stressed at 1000°F contained small amounts of a few alkenes and cycloalkanes that were beginning to form (less than ten compounds). The coal-based fuel stressed at 1000°F contained approximately ten compounds (alkenes, cycloalkanes, and aromatics), and the fuel stressed at 1075°F contained over a dozen compounds that were not present in the unstressed fuel. There were also some compounds in the unstressed coal-based fuel that were increased in the fuel stressed at 1075°F, and there were fewer of those compounds at 1000°F. The products formed on stressing the coal-based fuel were two to ten times more abundant at 1075ºF than at 1000ºF.

There were no components in the JP-8 fuel or the S-8 fuel that decreased in area more than 5% from the unstressed to the stressed fuel. There were decreases in some of the major components of the coal-based fuel, but these "reactants" exhibited less than 20% conversion even at the highest temperature (1075°F).

**Table 8. GC-MS Analyses of JP-8 Fuel Stressed in Phoenix Rig**

| JP-8 | | Stressed in Phoenix Rig | | |
|---|---|---|---|---|
| **Component** | **Neat Fuel** | **500F** | **1000F** | |
| **Products** | **Area** | **Area** | **Area** | **Yield** |
| Isopropylcyclobutane | | 33735 | 60454 | 1.8 |
| Heptene | | | 4619 | |
| Methyl-cyclohexene | | | 6380 | |
| Methyl-pentanol | | 6674 | 13931 | 2.1 |
| Methyl-heptene | | | 8117 | |
| Cyclooctane | | 26246 | 58967 | 2.2 |

All product areas less than 5000 are left blank

## Table 9. GC-MS Analyses of S-8 Fuel Stressed in Phoenix Rig

| S-8 | | Stressed in Phoenix Rig | | | |
|---|---|---|---|---|---|
| **Component** | **Neat Fuel** | **550F** | | **1075F** | |
| **Products** | **Area** | **Area** | **Yield** | **Area** | **Yield** |
| Methyl-hexene | | 6995 | | 72825 | 10.4 |
| Methyl-hexane | 43624 | 48864 | 1.1 | 128541 | 2.9 |
| Methyl-hexene | | 24116 | | 237215 | 9.8 |
| Heptene | | 14361 | | 399747 | 27.8 |
| Heptane | 89758 | 119463 | 1.3 | 499009 | 5.6 |
| Heptene | | | | 74544 | |
| Heptene | | | | 45171 | |
| Methyl-heptene | | | | 65895 | |
| Dimethyl-hexene | | | | 74256 | |
| Methyl-heptane | 3452135 | 4115363 | 1.2 | 4349719 | 1.3 |
| Methyl-heptane | 4249690 | 5024349 | 1.2 | 5124502 | 1.2 |
| Octane | 14708751 | 16730722 | 1.1 | 17166182 | 1.2 |
| Dimethyl-heptene | | | | 126381 | |
| Methyl-heptene | | | | 152580 | |
| Octene | | | | 8120 | |

All product areas less than 5000 are left blank

## Table 10. GC-MS Analyses of Coal-based Fuel Stressed in Phoenix Rig

| Coal-based fuel | | Stressed in Phoenix Rig | | | | | |
|---|---|---|---|---|---|---|---|
| **Component** | **Neat Fuel** | **500F** | **1000F** | | **550F** | **1075F** | |
| **Products** | **Area** | **Area** | **Area** | **Yield** | **Area** | **Area** | **Yield** |
| Methylene-cyclopentene | | | | | | 20387 | |
| Ethenyl-cyclobutane | | | 16411 | | | 98398 | 6.0 |
| Heptene | | | 3002 | | | 24710 | 8.2 |
| Heptane | 20278 | 21233 | 20338 | 1.0 | 16842 | 33556 | 1.7 |
| Dimethyl-cyclopentene | | | | | | 17940 | |
| Heptene | | | 705 | | | 5116 | 7.3 |
| Dimethyl-cyclopentene | | | | | | 16402 | |
| Methyl-cyclohexane | 130164 | 126951 | 124776 | 1.0 | 130667 | 199304 | 1.5 |
| Ethyl cyclopentane | 13262 | 11860 | 12379 | 0.9 | 13948 | 21438 | 1.6 |
| Methyl-cyclohexene | | | 3250 | | | 24054 | 7.4 |
| Methyl-cyclohexene | | | 7015 | | | 47948 | 6.8 |
| Methylene-cyclohexane | | | 8120 | | | 52647 | 6.5 |
| Ethyl-cyclopentene | | | 2181 | | | 18287 | 8.4 |
| Toluene | 5900 | 6044 | 7121 | 1.2 | 5625 | 42713 | 7.2 |
| Methyl-cyclohexene | | | 18660 | | | 150707 | 8.1 |
| Cycloheptadiene | | | | | | 124742 | |
| Dimethyl-cyclohexene | | | 4010 | | | 22702 | 5.7 |
| Dimethyl-cyclohexene | | | 6947 | | | 30996 | 4.5 |
| Dimethyl-cyclohexene | | | 3180 | | | 29125 | 9.2 |
| Dimethyl-cyclohexene | | | 6004 | | | 31695 | 5.3 |
| Ethyl benzene | 6006 | 5940 | 5775 | 1.0 | 6316 | 14353 | 2.4 |
| Ethyl-cyclohexene & Xylene | 6269 | 5555 | 8651 | 1.4 | 5586 | 41641 | 6.6 |
| Octatriene | | | | | | 15404 | |
| **Reactants** | | | | **% Conversion** | | | **% Conversion** |
| Octahydro-indene | 3097463 | | 2873324 | 7.2 | | 2607099 | 15.8 |
| Decahydro-naphthalene | 13570944 | | 12705285 | 6.4 | | 12148169 | 10.5 |
| Bicyclohexyl | 3692907 | | 3337999 | 9.6 | | 3254042 | 11.9 |

All product areas less than 5000 are left blank

### 3.3.4 Extended Duration Thermal Stability Test (EDTST) Evaluation

Two series of tests were conducted on the coal-based fuel (POSF-4765) and other fuels for comparison purposes in the EDTST system. The first test series was conducted at conditions anticipated for "JP-900" fuel applications. An example of potential aircraft thermal loads that this system represents is shown in Figure 16. A schematic of the EDTST configuration for this series is shown in Figure 17. The bulk fuel temperature out of the preheater represents the engine fuel system temperature resulting from the engine and engine aircraft heat loads. The heater represents the fuel thermal heating associated with air/fuel heat exchangers for cooling of engine compressor discharge air.

The tests were conducted for 24 hours with a bulk fuel temperature out of the preheater of 375°F and 600°F out of the heater. A flow rate of 1 gallon/per hour was used for all of the EDTST evaluations discussed in this report. Tests were conducted on JP-7, Fischer-Tropsch based S-8 (POSF-4734), JPTS (POSF-3775), and JP-8 (POSF-4751) fuels in addition to the coal-based fuel. Some preliminary tests were conducted on the JP-8 and JPTS fuels at lower temperatures due to concerns that the system would have problems at the higher temperatures. A .25 inch OD x .035 inch wall tube was used in the heater instead of the .125 OD tube normally used. The larger tube was used to provide longer residence times associated with future engines with air/fuel heat exchangers. The maximum wetted wall temperature for this tube was approximately 700°F for these tests. A comparison of the carbon deposits in the heater tube for these fuels is shown in Figure 18. The deposit of the coal-based fuel was essentially the same as the S-8 fuel. Both of these fuels had slightly higher deposits than that of the JP-7 fuel. However, the higher fuel deposits are considered to be very acceptable. Witness strips that were located immediately after the heater and further downstream for tests were essentially identical for the two fuels. The strips immediately after the heater had slight deposits for all three fuels. The strips further down from the heater were very clean for all of the fuels. Based on these results the coal-based fuel tested has thermal stability equivalent to the S-8 and JP-7 fuel. The coal-based fuel also exceeded the thermal stability goals (525°F bulk and 625°F WWT) for the JP-8+225 fuel program.

Tests were conducted on a JP-8 fuel to compare its thermal stability characteristics with the coal-based, S-8 and JP-7 fuels as discussed above. The first test at the reduced temperatures was conducted for 24 hours with a bulk fuel temperature out of the preheater of 325°F and 525°F out of the heater. A .25 inch ODx.035 inch wall tube was also used in the heater instead of the.125 OD tube normally used. A comparison of the carbon deposits in the heater tube along with a previous test of JPTS fuel at the same lower temperatures is shown in Figure 19. The maximum deposit of the JP-8 fuel was essentially the same as the JPTS fuel. Witness strips that were located immediately after the heater and further downstream for tests were essentially identical for the two fuels. The strips immediately after the heater had heavy deposits for these fuels. The strips further down from the heater were very clean for both fuels. Based on these results, it was decided to conduct another test of the JP-8 fuel at the higher temperatures.

A second test was conducted on the JP-8 fuel at the same conditions (375°F Bulk in and 600°F out of heater) and test setup that the coal-based, JP-7, and S-8 fuels were tested. A comparison of the carbon deposits of the second test for the heater tube along with a previous test of coal-based, S-8 and JP-7 fuels at the same temperatures is shown in Figure 19. The deposits for the JP-8 fuel were much lower than expected. The deposits were 10 times lower than the deposits experienced at the lower temperatures. The deposits were higher than the other fuels, but the differences were considerably less than expected. The witness strip at the heater exit with the JP-8 fuel had considerably more deposition than the other fuels.

Another series of tests were conducted in the EDTST system on the coal-based, S-8, and JP-7 fuels to evaluate their capability to recirculate at high temperatures. It is anticipated that recirculation of fuel back to the aircraft tanks will be necessary for future aircraft at low fuel flow conditions. These tests were conducted by flowing the fuel (2 drums) through the preheater with a bulk outlet temperature of 600°F. The stressed fuel was collected in drums. A second pass of the fuel was then conducted through the preheater with an outlet temperature of 600°F and the heater with a maximum wetted wall temperature of 725°F. A smaller diameter heater tube (0.125 inch OD x.035 inch wall) was used for these tests to provide a shorter residence time (1.2 seconds) in the heater tube. This shorter time is representative of the short residence time in an engine nozzle. The test duration for stressing the fuels was 96 hours. The duration for the second pass for the JP-8 and S-8 fuels was also 96 hours. However, the second pass with the coal-based fuel was terminated after 84 hours because of a gear pump failure. Comparisons of the carbon deposits in the preheater and heater tubes for these fuels are shown in Figures 20 and 21, respectively. The coal-based fuel had considerably higher deposition in the preheater than the other two fuels. This indicates that recirculation of the coal-based fuel is limited to a lower recirculation temperature. The witness strip at the preheater outlet also had significant more deposition with the coal-based fuel than with the other fuels. The preheater witness strips for the S-8 and the JP-7 fuel had only slight deposition. The S-8 fuel deposition in the heater tube was higher than the other fuels. However, the heater fuel deposits are considered to be very acceptable for all three fuels.

The gear pump that failed during the test with coal-based fuel was new at the start of the test. This indicates that the fuel may not have sufficient lubricity for proper aircraft pump operation. Teardown of the pump revealed considerable wear of the pump's gear teeth. The EDTST has over 40,000 hours of testing and never had a pump fail in this manner. Section 3.7 of this report details lubricity testing of the fuel that was performed to address this issue.

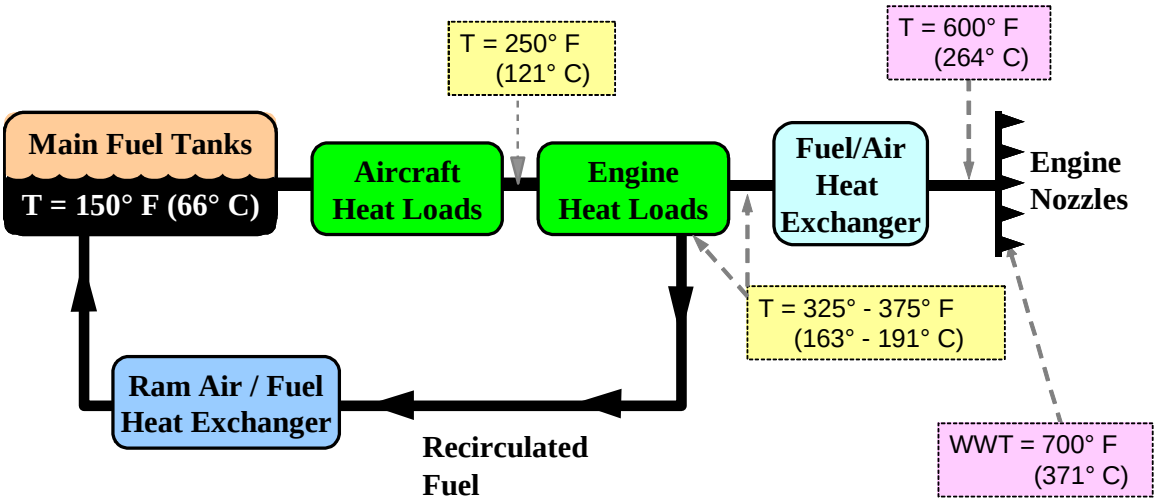


**Figure 16. Potential system thermal load for use of "JP-900" fuels.**

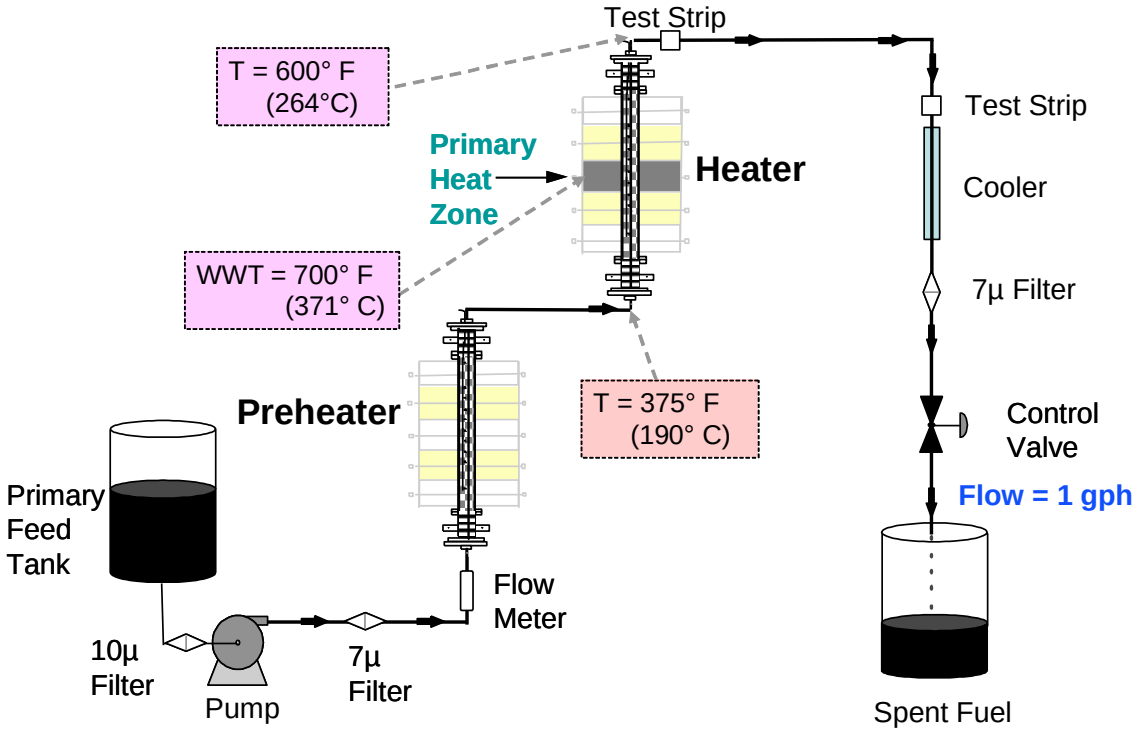


**Figure 17. EDTST schematic for coal-based fuel tests.**

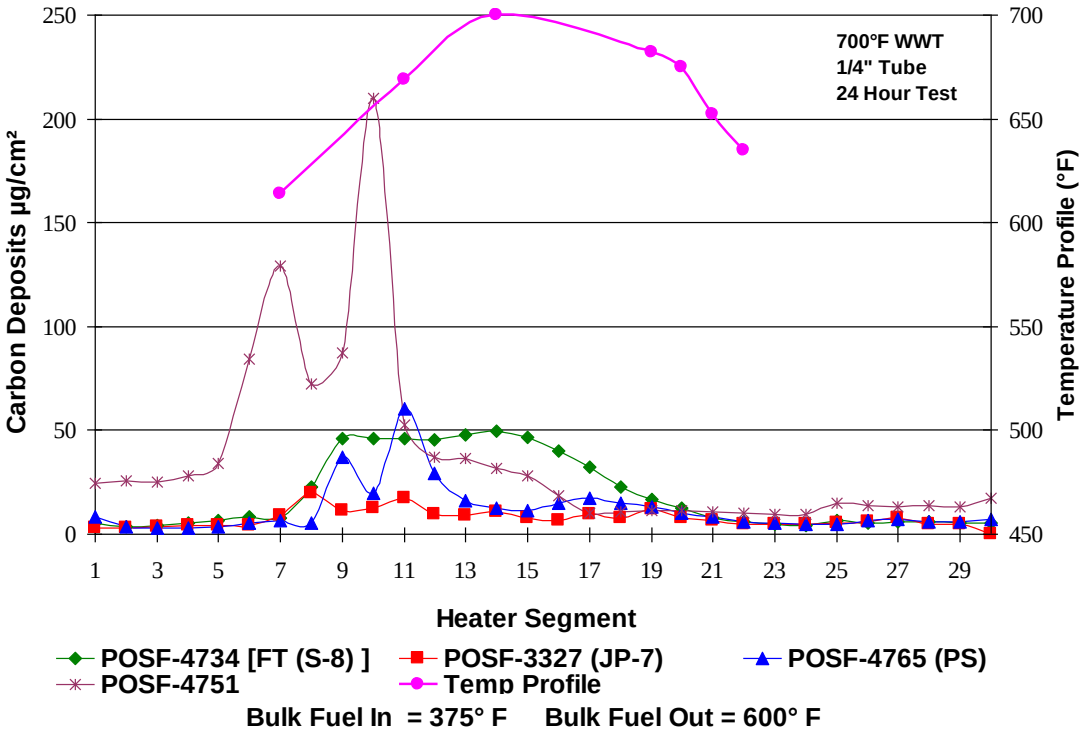


**Figure 18. EDTST heater tube carbon deposits for the various fuels for 600°F bulk fuel out and 24 hour test period.**

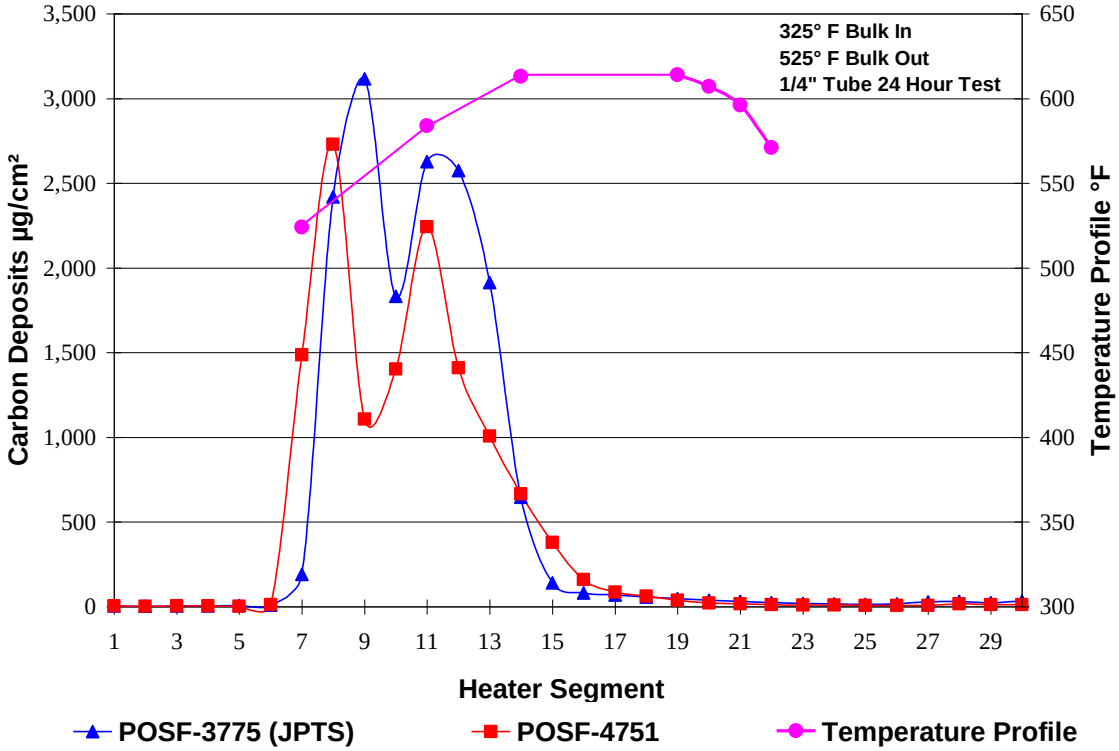


**Figure 19. EDTST heater tube carbon deposits for JP-8 and JPTS fuels for 525°F bulk fuel output tests.**

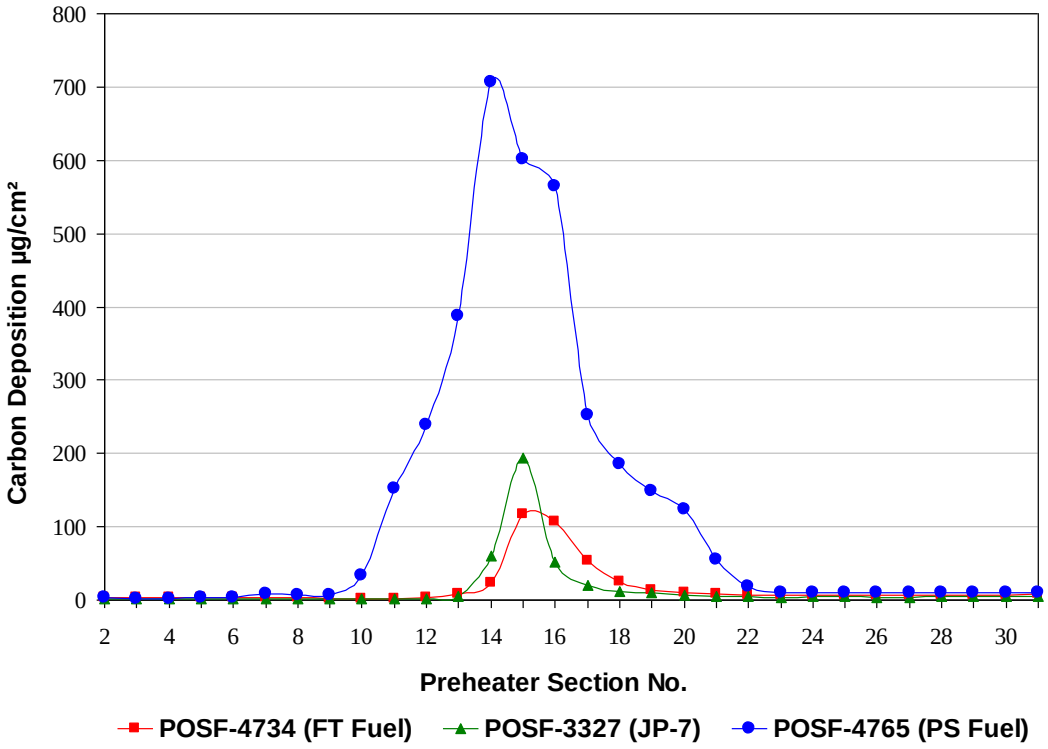


**Figure 20. EDTST preheater tube carbon deposits for recirculating 600°F fuel tests.**

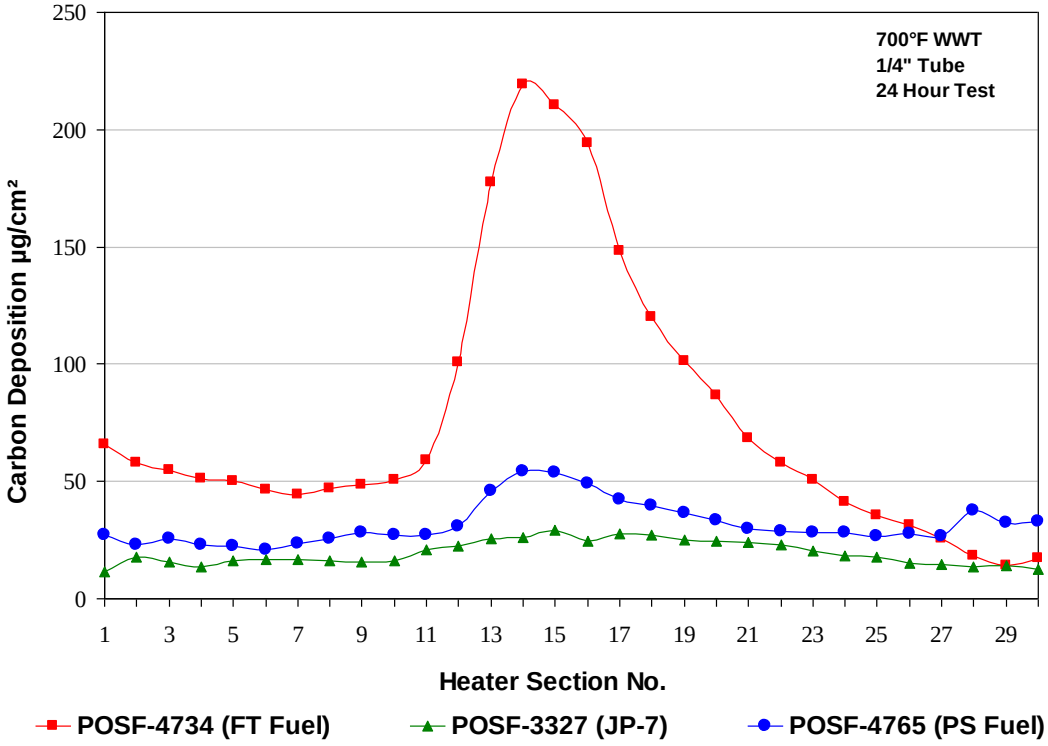


**Figure 21. EDTST heater tube carbon deposits for recirculating 600°F fuel tests.**

### 3.4 Low Temperature Properties Evaluation

#### 3.4.1 Scanning Brookfield Viscosity

The low-temperature viscosity behavior of the coal-based fuel was studied using scanning Brookfield viscometry. In this technique a stationary sample container (stator) containing the fuel sample and a metal rotor suspended in the center of the sample were connected to a viscometer head. The stator and rotor were lowered into a temperature-programmable methanol bath. The head provided the torque to the rotor to maintain it a constant velocity as the temperature in the bath was lowered from –20 to –70°C at a rate of 5°C per hour. The torque was relayed from the head to the computer program, which also recorded the corresponding bath temperature.

The viscometer was calibrated with a mineral oil standard having measured viscosities in centipoise (cP) at five temperatures from –20 to –45°C. The calibration was accomplished by first obtaining the slope and intercept of the relationship between viscosity (η) and temperature (T) in degrees Kelvin (K) from the MacCoull, Walther, Wright equation (Selby et al., 2004).

$$\mathrm{LogLog}(\eta+0.7) = m(\log T) + b$$

Then the torque of the mineral oil was measured at temperatures from -20 to –45°C using the viscometer, and a bath cooling rate of 2°C per hour. The viscosity was calculated at each temperature and a linear relationship between torque and viscosity was generated. The slope and intercept of this linear relationship was used to convert torque measurements to viscosity measurements for fuel samples. Dynamic viscosity curves could then be generated of viscosity (cP) versus temperature (°C).

The dynamic viscosity curves for the coal-based fuel, a JP-8 fuel and two S-8 fuels are shown in Figure 22. For JP-8 fuels the viscosity gradually increases with decreasing temperature until the there is a sudden sharp rise in viscosity. This sharp increase or "knee" in the viscosity curve occurs at the cloud point of the fuel. The cloud point is the temperature at which crystals begin forming on cooling and is usually a few degrees below the freezing point. The S-8 fuels display a more gradual increase in viscosity after the cloud point. The coal-based fuel viscosity rises gradually throughout the temperature decrease and displays no sharp break or "knee." This behavior is consistent with the low amount of normal alkanes present in the coal-based fuel. It also appears from the curves that the coal-based fuel has a higher viscosity than the JP-8 and S-8 fuels from -20°C to their cloud points.

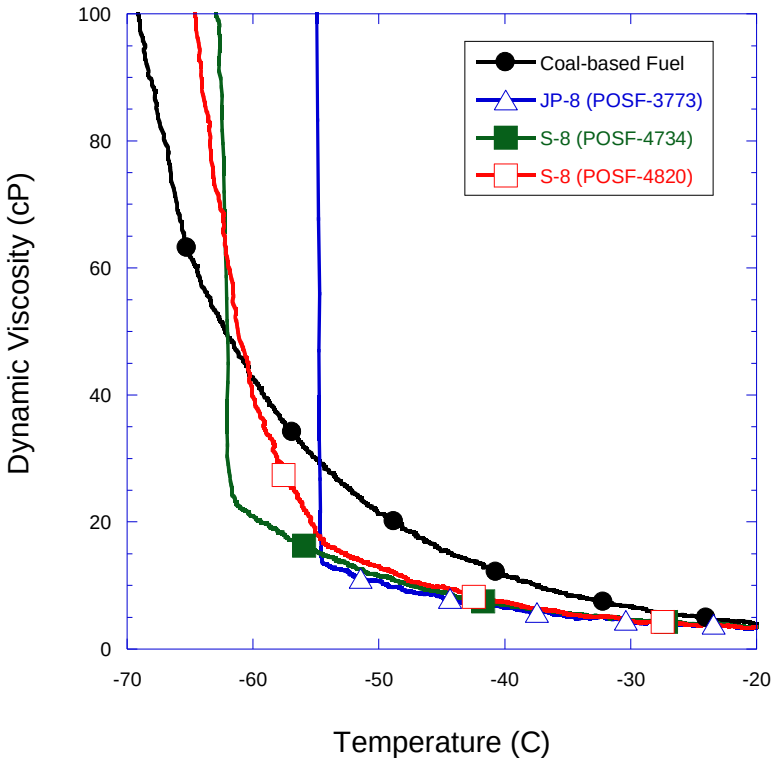


**Figure 22. Dynamic viscosities of the coal-based fuel compared with JP-8 and S-8 fuels.**

### 3.4.2 Kinematic Viscosity

While the dynamic viscosity curves give accurate indications of the relative behaviors of fuels over a range of decreasing temperatures, kinematic viscosity measurements are more accurate measurements of absolute viscosities at particular temperatures. The kinematic viscosities of the coal-based fuel, JP-8 and S-8 fuels were measured at -20°C and -40°C by ASTM method D445 (Table 11). The kinematic viscosities of the coal-based fuel are significantly higher than those of the JP-8 and S-8 fuels. The 7.5 cSt value at -20°C is very close to JP-8 specification maximum viscosity of 8 cSt at -20°C. In addition, the 12.8 cSt value at -40°C exceeds the JP-TS specification maximum viscosity of 12 cSt at -40°C.

Table 11. Measured Kinematic Viscosities (cSt)

| Viscosity (cSt) | Coal-based (FP: - 65C) | JP-8 (FP: - 50C) | S-8 (FP: - 51C) | S-8 (FP: - 59C) |
|---|---|---|---|---|
| @ - 20C | 7.5 | 3.9 | 4.6 | 4.4 |
| @ - 40C | 12.8 | 7.9 | 9.3 | 8.9 |

### 3.4.3 Low Temperature Density Measurements

To convert between the dynamic and kinematic viscosity measurements, it is essential to have accurate measurements of fuel density. Thus, density measurements of each of the fuels were performed over a range of temperatures using a pycnometer. The pycnometer is a specially designed glass sample container of a calibrated volume. The density measurements were made at ambient temperature (23°C) and two additional temperatures that were at least twenty degrees below 0°C. A linear relationship between temperature and density was calculated from the three data points for each of the fuels (Figure 23).

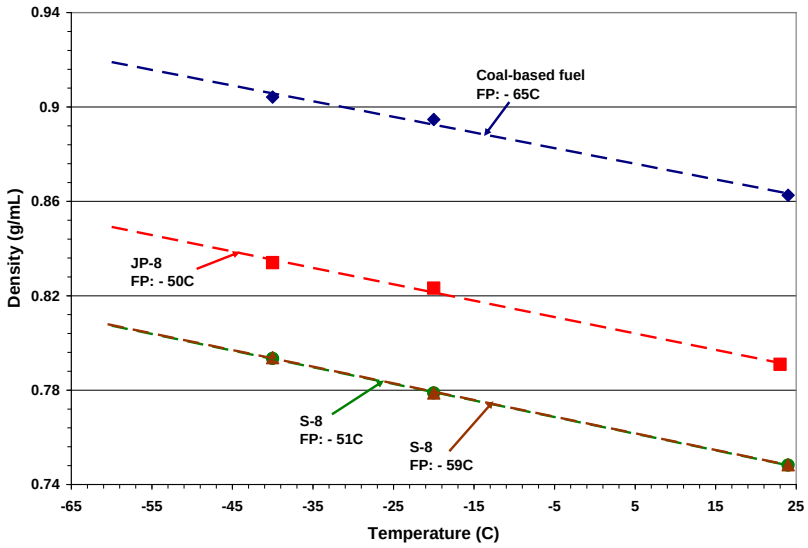


**Figure 23. Density vs. temperature plots for the fuels studied.**

The coal-based fuel exhibits a high density relative to the JP-8 and S-8 fuels. This is due to the fuel being composed primarily of cycloparaffins (especially dicycloparaffins, such as decalin), which have higher densities than the normal and branched chain paraffins which comprise the bulk of the petroleum and synthetic fuels. The densities of the synthetic fuels are lower than the petroleum-derived fuel. This is due primarily to the absence of aromatic compounds, relative to the petroleum-derived fuel. Aromatic components, which are typically at 15-20% levels in the JP-8 fuels, have pure component densities of ~0.87 g/mL, and contribute to increasing the JP-8 densities above the synthetic fuels.

### 3.4.4 Glass Wing Studies of the Freezing of Flowing Fuel

For long missions at relatively high altitudes or within low-temperature regions, the potential exists for the freezing of hydrocarbon fuels. With sufficient crystallization, there is potential for catastrophic fuel system failure due to blocked filters, valves, and other flow passages. Hence, it is desirable to study the freezing of coal-based fuels which may potentially be used in aircraft. Commercial and military jet fuels such as Jet A and JP-8 consist of normal alkanes, branched alkanes, cycloparaffins, olefins, and aromatics. Since

each hydrocarbon has its own solidification temperature, these jet fuels freeze over a range of temperatures, and solidified jet fuel mainly consists of larger normal alkanes. Moreover, these jet fuels form a liquid-solid matrix during solidification. Since the composition (see chemical analysis section) of the coal-based fuel in this study is different from that of conventional commercial and military jet fuels**,** its freezing behavior is expected to be dissimilar from that of current jet fuels. The fuel temperature and interaction between solid particles and the liquid are influenced by the fuel flow rate. Thus, it is important to consider the freezing of jet fuel under flowing conditions. It is also essential to study fuel solidification using a geometry that has some complexities because aircraft fuel tanks include internal structures (e.g., baffle plates, ribs, stringers) that may affect the overall heat transfer during the solidification process. Flow visualization experiments were performed to study the solidification behavior of the coal-based fuel under flowing conditions in a quartz duct which had an internal plate containing flow passages. The duct containing flowing fuel was subjected to temperatures below the freeze point of the fuel sample. For purposes of comparison, flow experiments were also performed using JP-8 and Fischer-Tropsch fuels.

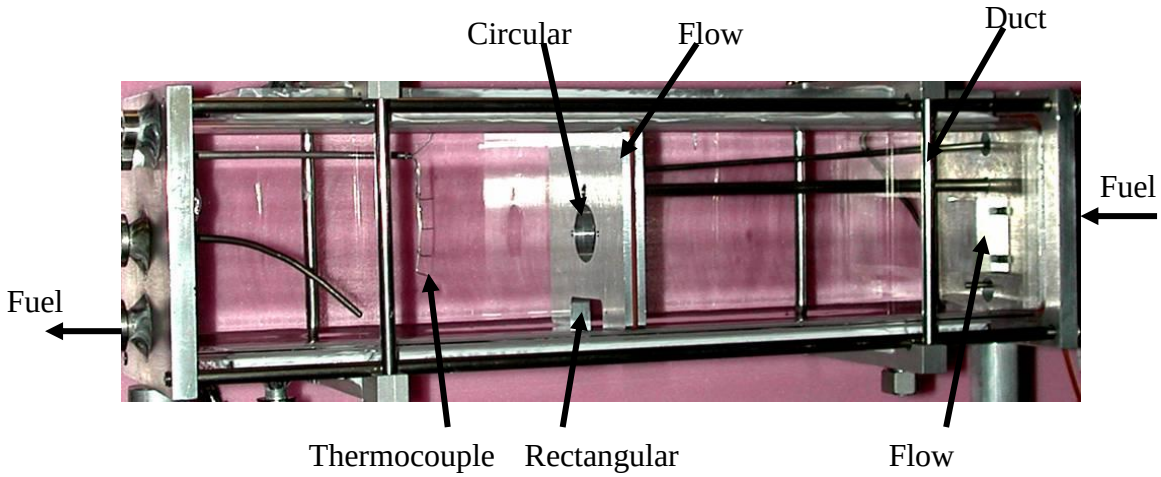


**Figure 24. Photographic image of the quartz duct.**

To study the behavior of flowing jet fuel at low temperatures, a quartz duct (Figures 24 and 25) was fabricated. The rectangular duct (39.4 cm x 8.9 cm x 8.9 cm) was fabricated from quartz because of its high optical quality and strength. Figure 24 shows an image of the duct which demonstrates that it is separated into two compartments by a dividing plate similar to what might be encountered in some flow passages within a fuel tank. The dividing plate has two openings available for flow. One opening is circular (2.5 cm diameter) and located at the dividing plate center, while the other is rectangular (3.8 cm x 1.3 cm) at the plate bottom. The jet fuel flows into the duct through an inlet (1.3 cm diameter) located on one of the sidewalls. A deflector near the inlet redirects the inlet flow. In the absence of the deflector, much of the fuel entering through the inlet would essentially pass straightway through the circular opening on the dividing plate. It is presumed that this would result in inadequate mixing of the fuel. In addition, an outlet (1.3 cm diameter) is located at the opposite end of the chamber. Hollow aluminum plates are attached to the external top and bottom surfaces. The plates are sealed on both the

ends and allowed for threaded pipe fittings and mountings. By passing chilled methanol through these plates, the horizontal surfaces were cooled to the desired temperature range (between –63 and –72$^{o}$C). Thermally conductive grease was applied to enhance thermal contact between the quartz duct and plates.

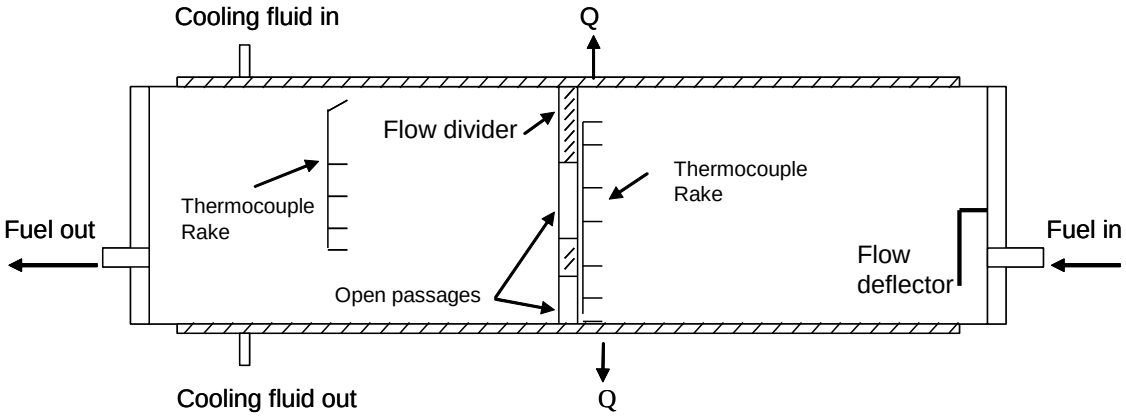


**Figure 25. Schematic of the quartz duct.**

The entire quartz duct was placed in an environmental chamber to simulate the low temperature conditions that exist during high altitude flight. Well-insulated tubing (0.64 cm diameter) was used throughout the fuel system. A positive displacement pump pumped fuel from an insulated reservoir (5 liter capacity) through the duct. A flow meter installed at the pump outlet monitored the fuel flow rate. Flow rates between 60 and 250 ml/min were used in this study. A coil-type heat exchanger was used to cool the fuel before entering the duct. Fuel exited the duct through the outlet and passed through insulated tubing back to the reservoir. Three different jet fuel samples were used in these experiments: F3804 (JP-8), F4734 (FT), and F4765 (coal-based).

Calibrated (Type T) thermocouples were located inside the duct. Figure 25 shows a rake of seven thermocouples near the flow divider and another rake of five thermocouples near the center of the other compartment within the duct. Thus, temperature measurements on both sides of the flow divider were recorded. Thermocouples were installed in the fuel lines entering and exiting the duct, and the temperature of the methanol entering and leaving the chiller plates was also measured. The temperatures of the top and the bottom walls were also recorded. A pressure transducer measured the pressure drop between the inlet and outlet of the duct. The data was digitally acquired (Personal DaqView PlusXL Version 1.9) at a rate of 60 Hz.

Lighting for the quartz duct consisted of an optical fiber panel that uniformly illuminated the cell. Polarizing filters on the front and back of the duct maximized the contrast between the solid and liquid fuel as cross polarization eliminated light transmittance through the liquid fuel. A high-resolution digital camera (Sony DKC- ST5, 4 Mega-Pixel) equipped with a zoom lens (Sony VCL1205B) was used to capture several images every 30 minutes.

Figures 26 to 28 show images of solidifying flow in the quartz duct. As the horizontal walls are actively cooled by the circulating methanol, layers of solidified fuel accumulate at the top and bottom surfaces. The region occupied by solid-liquid fuel matrix on both horizontal surfaces grows in time as the temperature decreases. In these particular images, the upper and lower surfaces were cooled to temperatures near -70°C with flow rates in the range 120-130 mL/min. Figure 26 shows the solidification of flowing JP-8 (F3804) after 2.5 hours of cooling with an inlet fuel temperature of –46°C. In addition, temperatures obtained with the thermocouple rakes are shown near their measurement location. It can be observed that more solidified fuel accumulates near the bottom surface than the top surface. This is due to the flow of relatively warmer fuel on the upper surface that inhibits the growth of solidified fuel on the top surface. In Figure 26, the solidifying fuel layer fills the lower opening in the flow divider (located in the center of the image). Although the duct exit appears to be blocked, fuel still flows from the duct. However at later times, the exit became blocked, and the test was discontinued.

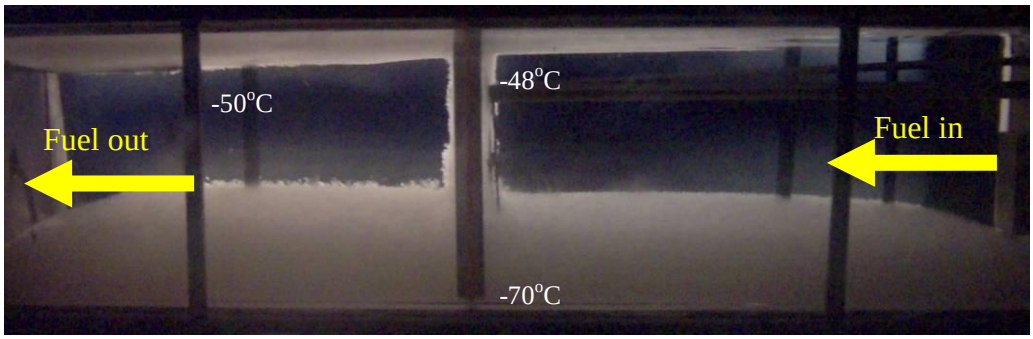


**Figure 26. Image of JP-8 (F3804) after 2.5 hours of cooling and a flow rate of 120 mL/min. Measured temperatures are shown.**

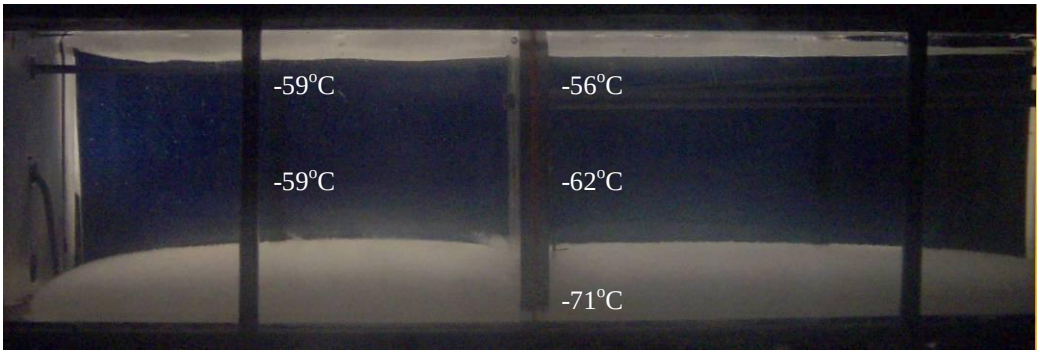


**Figure 27. Image of FT fuel (F4734) after 4 hours of cooling and a flow rate of 120 mL/min. Measured temperatures are shown.**

Figure 27 shows an image of the solidifying FT fuel (F4734) after four hours of cooling at a flow rate of 120 mL/min. Here, the nominal fuel inlet temperature is –46°C. In the case of the FT fuel, there is a lower volume of solidified fuel attached to the upper and lower surfaces. The FT fuel has lower freeze and cloud point temperatures than the corresponding values for the JP-8 fuel sample. Thus after four hours of cooling, the liquid

phase of the FT fuel for a given location in the duct can be cooled to a lower temperature than that of the JP-8 fuel (cloud point of –52°C).

Figure 28 shows the solidification of the coal-based fuel after 6 hours of cooling at a flow rate of 130 mL/min (inlet temperature of –42°C). The solidifying fuel in Figure 28 is different from that of the other fuels in that the solidified fuel does not form a semi-rigid solid-liquid matrix for these temperature and flow conditions. In addition, the crystals formed from the coal-based fuel are much smaller than those which formed from the JP-8 and FT fuel samples and, thus, do not block the lower opening in the flow divider. Figure 28 shows that there is a layer of flowing crystals near the lower wall, and crystal inception occurs between -58°C and -62°C. This temperature corresponds to an increase in the rate of the rise in viscosity with temperature shown in the viscosity measurements section.

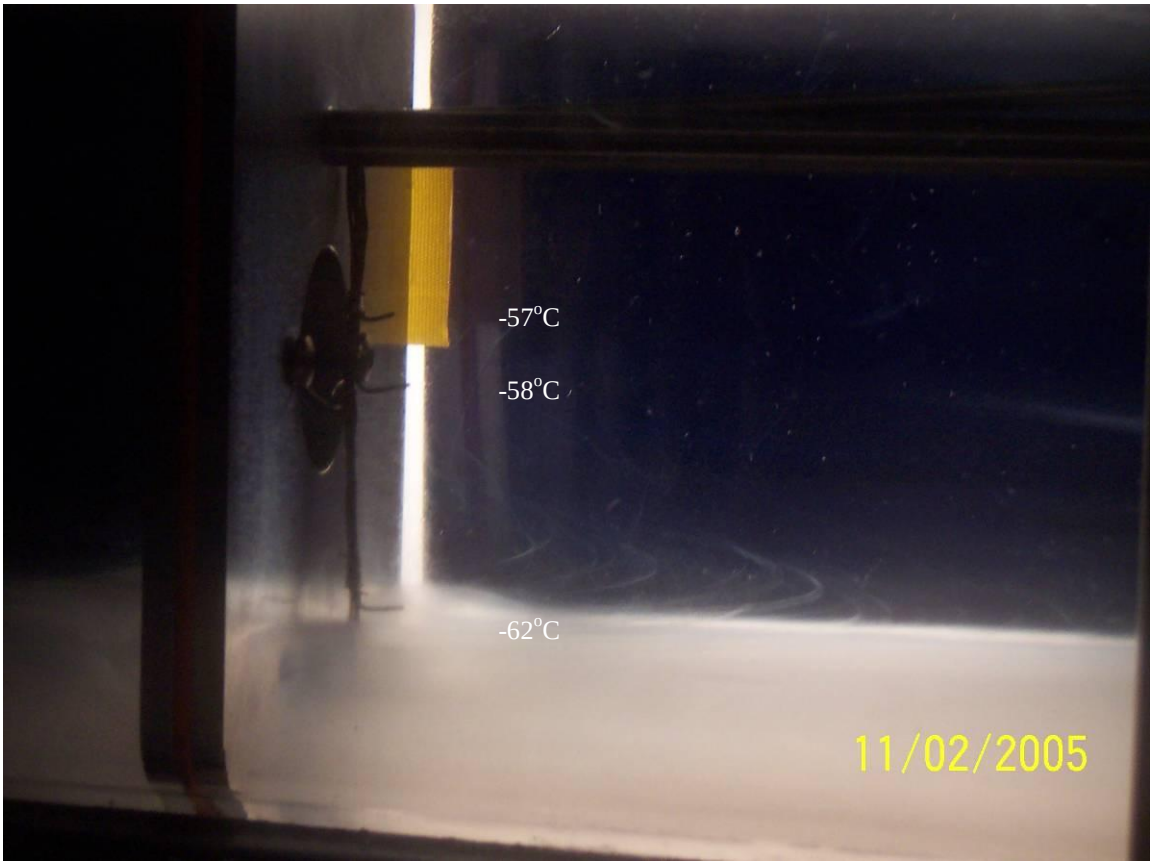


**Figure 28. Image of coal-based fuel after 6 hours of cooling and a flow rate of 130 mL/min. Measured temperatures are shown.**

### 3.4.5 Differential Scanning Calorimetry

Differential Scanning Calorimetry (DSC) was employed to determine the thermal behavior of the coal-based fuel upon exposure to low temperatures where crystallization of fuel components is expected. A Mettler Toledo Model DSC823 equipped with a

sample robot and cryostat cooler was used to measure the thermal behavior upon both cooling and heating of the coal-based fuel (FP= -65°C), a representative JP-8 fuel (POSF-3773, FP= -50°C), and a synthetic fuel produced via Fischer-Tropsch synthesis (POSF-4734, FP= -59°C). Heating and cooling were performed at 1°C/min over the temperature range -40 to -85°C. The results are shown in Figure 29.

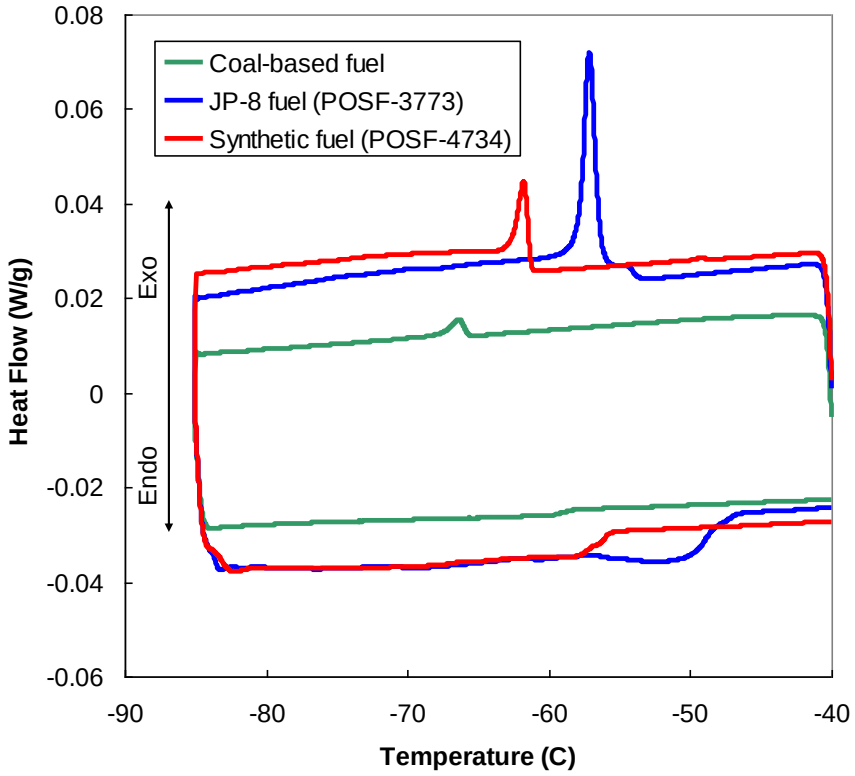


**Figure 29. Differential scanning calorimetry thermal analysis of the freezing of the coal-based fuel during heating and cooling at 1°C/min.**

The coal-based fuel exhibits a very small exotherm near -66°C. This exotherm is significantly smaller than either the JP-8 fuel or the synthetic fuel. For the case of these other fuels, crystallization exotherms result primarily from the heat of fusion of normal alkane components (Zabarnick and Widmor, 2001). Thus, the small exotherm for the coal-based fuel results from the very low concentration of normal alkanes (<1%) in this fuel. As relatively long chain (C15-C18) normal alkanes are the first fuel species to crystallize upon cooling, a lack of these components, along with the presence of large quantities of cycloalkanes, which exhibit very low melting points, contribute to the very low freeze point of the coal-based fuel.

In addition to the cooling exotherm near -66°C, the coal-based fuel exhibits a very small endotherm upon heating near -60°C. For petroleum-based fuels, the temperature of the heating endotherm is ordinarily the same as the freeze point temperature obtained via the ASTM specification techniques. This holds for the JP-8 fuel which exhibits an endotherm near -50°C and the synthetic fuel which exhibits an endotherm near -59C. The -60C

endotherm of the coal-based fuel does not agree with the -65°C freeze point obtained via ASTM D5972. This discrepancy is likely due to the fact that the ASTM technique relies on light scattering from the formation of normal alkane crystals. As the coal-based fuel is nearly devoid of these species, the freeze point measurement is unable to accurately determine the crystallization temperature of the fuel.

Figure 29 also indicates that the coal-based fuel has a lower heat capacity than the JP-8 or synthetic fuels. This results from the high concentration of cycloalkanes, such as decalin, which tend to have lower heat capacities than the major petroleum-based fuel components, such as n-alkanes.

### 3.5 Combustion Properties

#### 3.5.1 Investigation of Emissions from a T63 Turboshaft Engine

A preliminary evaluation of the emission characteristics of the coal-based fuel was performed using a T63-A-700 turboshaft engine. A specification JP-8 (POSF-3773) was also tested to provide a basis of comparison for the particulate and gaseous emissions produced by the coal-based fuel. This engine facility has previously been used to successfully evaluate the effect of fuel chemical composition or chemical additive addition on the overall emissions produced and the combustor operation (Corporan et al., 2004; Corporan et al., 2004b; Corporan et al., 2005a). A detailed description of the engine facility and operation has been provided in an earlier publication (Corporan et al., 2004). During this study, the engine was operated at two power settings, designated as Ground Idle and Normal Rated Power (also referred to as cruise). The fuel flow rate was adjusted during testing to maintain a constant turbine outlet temperature (e.g., power output) for a given setting. This strategy assured the best run-to-run reproducibility and provided a constant basis of comparison for the coal-based fuel and the JP-8. The engine was initially operated using the baseline JP-8 supplied from an underground facility tank. Operation was then transitioned to the coal-based fuel which was supplied from an external tank pressurized with nitrogen. Upon completion of the evaluation of the coal-based fuel, operation was transitioned to the baseline JP-8 to verify the emissions returned to the initial levels.

Gaseous and particulate emissions were collected using oil-cooled probes installed facing the exhaust flow near the exit of the engine. The sampling was performed close to the engine exit to obtain a “representative” sample of the exhaust and minimize dilution or contamination with surrounding air. The particulate samples were immediately diluted at the probe tip with nitrogen to minimize particle loss by diffusion or agglomeration and prevent saturation of the analytical equipment. The sample was drawn to the analytical equipment using a vacuum pump and the dilution and total flows were controlled using high precision flow controllers. The overall dilution ratio was determined via quantitation of the carbon monoxide (CO) concentration in the raw and diluted gas streams; all measurements were corrected for dilution. On-line characterization of the particulate (aerosol) emissions included quantitation of the particle number density (i.e., count of total particles per unit volume) using a TSI Model 3022A Condensation Nuclei Counter

(CNC), the particle size distribution for particles less than 200 nm using a TSI Model 3936 Scanning Mobility Particle Sizer (SMPS), the size distribution for particles greater than 300 nm using a MetOne Model 237B Laser Particle Counter (LPC), and the mass concentration using a Model 1105 Rupprecht & Pataschnick Tapered Element Oscillating Microbalance (TEOM). The SMPS incorporated the use of a Nano-Differential Mobility Analyzer with a Model 3025 CNC during operation. Undiluted particulate samples were collected for off-line analysis using an in-house designed smoke machine. These samples were collected on either paper filters to estimate the engine smoke number via reflectance or on quartz filters to quantify the carbon mass collected via temperature programmed oxidation (TPO). Gaseous emissions were extracted using an undiluted probe and quantified using an MKS MultiGas 2030 Fourier transform Infrared (FTIR) analyzer fitted with a solid-oxide (zirconia-based) oxygen analyzer (Markham et al., 2004) and a Thermo Environmental Instruments, Inc. Model 51 Total Hydrocarbon Analyzer. The FTIR is capable of simultaneously quantifying all major and minor gaseous species other than oxygen without requiring removal of the water produced during combustion.

The coal-based fuel showed slightly higher particulate and gaseous emission production at the lower power condition with less of a difference at the cruise condition. The particle number density (PND) emissions for the coal-based fuel were approximately 14.4% and 3.5% higher than those for the JP-8 (POSF-3773) at the idle and cruise conditions, respectively. Although there was a slight increase in the PND with the coal-based fuel, the particle size distributions quantified with the SMPS were not altered indicating that the basic soot formation mechanism for the two fuels is similar. A comparison of the mass concentration and smoke number emissions is shown in Table 12. These measurements all showed an increase in the particulate matter production for the coal-based fuel. The differences in the absolute percentage increases for the various analytical techniques is most likely due to the various factors that affect the absolute values (e.g., sampling methodology) during measurement. As shown, the smoke number and carbon mass quantified via TPO showed a substantial increase in the mass concentration emissions at the idle condition. This may be the result of an increase in large particle formation (e.g., greater than 300 nm in size), which can contribute significantly to these indices but not affect the PND (particles less than 200 nm) as strongly. Accordingly, the LPC showed an increase in larger particle formation of approximately 9% (idle) and 6% (cruise) for the coal-based fuel. The TPO analysis also revealed that the qualitative volatile and elemental carbon composition of the particulate was similar for the coal-based fuel and JP-8 further supporting the assertion that the soot formation mechanisms are similar. Carbon monoxide was the only gaseous emission which varied by more than 3% during testing; the CO increased by approximately 21% (idle) and 18% (cruise) during testing with the coal-based fuel. The total unburned hydrocarbon concentration showed approximately a 30% increase at idle with negligible difference at cruise. The increase in the CO was most likely related to the reduced combustion efficiency of the coal-based fuel relative to the JP-8, which also rendered the increase in the particulate emissions. It is not straightforward to estimate the overall combustion efficiency since the engine was maintained at a constant power output and there were various chemical/physical differences between the fuels. For example, the volumetric fuel flow rate to the combustor was lower for the coal-based fuel (4.8%-idle and 3.3%-cruise)

during testing. However, when accounting for the density difference of the fuels (0.80 g/cm$^3$ versus 0.87 g/cm$^3$), there was an increase of approximately 3.5% and 5.1% in the required mass flow rates for the coal-based fuel to maintain the identical power output.

**Table 12. Comparison of Smoke Number and Mass Concentration Emissions for the Coal-Based Fuel and a JP-8 (POSF-3773) during Testing on a T63 Turboshaft Engine at Idle and Cruise Power Conditions.**

| Engine Condition | Fuel | Smoke Number | | Quartz Filter | | TEOM | |
|---|---|---|---|---|---|---|---|
| | | Smoke Number | % Increase | Mass Conc. (mg/m$^3$) | % Increase | Mass Conc. (mg/m$^3$) | % Increase |
| Idle | JP-8 (3773) | 7.3 | 23.4 | 5.7 | 41.5 | 3.0 | 9.5 |
| | Coal-Based | 9.6 | | 8.0 | | 3.3 | |
| | | | | | | | |
| Cruise | JP-8 (3773) | 37.0 | 9.5 | 9.2 | 16.7 | 10.5 | 8.5 |
| | Coal-Based | 40.7 | | 10.8 | | 11.4 | |

The overall effect of the coal-based fuel on the emission production of the T-63 engine can be placed in context when compared to results from previous testing evaluating the effect of fuel composition on emission production (Corporan et al., 2004; Corporan et al., 2005a). Although the coal-based fuel showed slight increases relative to the specification JP-8, significantly higher emission production was observed during testing with a fuel high in aromatics (~41%) and naphthenes (designated JP-8X 45), as shown for the PND measurements in Table 13. As shown, the increases with the JP-8X 45 were an order of magnitude higher than that for the coal-based fuel. The significant increase was attributed to the high aromatic content in the JP-8X 45, which can act as seed molecules for molecular growth and polymerization to form larger hydrogen-deficient molecules (polycyclic aromatic hydrocarbons), that produce mature soot (Bockhorn et al., 1983; Richter and Howard, 2000). Though the coal-based fuel contains multi-ring cycloparaffins, such as decalin, these species must first undergo dehydrogenation to produce the aromatic species for the soot formation process. Fuels that were primarily comprised of normal (designated NORPAR-13) or branched paraffins (designated S-8 or synjet), showed significant reductions in emission production. Comparison of the reduction relative to JP-8 for testing with these fuels is also shown in Table 13. The synthetic set fuel, synjet, was produced by Syntroleum Corporation from natural gas via the Fischer-Tropsch process (POSF-4734). Detailed discussion of all emission production characteristics for testing with this fuel has been made previously (Corporan et al., 2005a). As shown, both NORPAR-13 and the synjet showed significant reduction in the PND relative to JP-8, JP-8X 45 and the coal-based fuel. These fuels also showed extremely favorable emission production and combustion characteristics for all other measured indices on the T-63 platform.

**Table 13. Comparison of Percentage Increase in Particle Number Density Emissions Relative to JP-8 (POSF-3773) for Testing of the Coal-Based-Fuel and Fuels Previously Evaluated on a T63 Turboshaft Engine at Idle and Cruise Power Conditions.**

| Engine Condition | Coal-Based Fuel | JP-8X 45 | Synjet | NORPAR-13 |
|---|---|---|---|---|
| Idle | 14.4 | 362 | -96 | -97 |
| Cruise | 3.5 | 854 | -78 | -62 |

** Negative (-) Percentage Indicates Decrease in PND Emissions

Although the emission production increased for the coal-based fuel relative to the JP-8, the magnitude of the differences is much lower than observed for other fuels, such as JP-8X 45. Comparison of the results from the coal-based fuel testing in this context implies that the overall emissions produced are most likely similar or only slightly greater than those for a typical JP-8 fuel. The various studies performed on this platform have demonstrated that there is sufficient sensitivity of the gaseous and particulate emission formation to the fuel composition to allow for quantitative comparisons of data and trends to be made. It should be noted that the current study did not account for chemical changes to the coal-based fuel that could be experienced if it was used for high-heat sink applications (e.g., formation of unsaturated and aromatic compounds). Since it is well accepted that higher aromatic content increases particulate matter formation during combustion (Naegeli and Moses, 1980; Monroig et al., 2005), subsequent emission studies of the coal-based fuel following thermal stressing would be warranted if ultimate use of the fuel is for applications where significant alterations to the chemical structure would be experienced.

### 3.5.2 Emissions from an Atmospheric Pressure Swirl-Stabilized Research Combustor

A preliminary evaluation of the particulate emission characteristics of the coal-based fuel from an atmospheric pressure swirl-stabilized research combustor was performed. Testing on the research combustor was performed to supplement the T-63 study and to assess the emission production of the coal-based fuel relative to a specification JP-8 (POSF-3773) and a synthetic jet fuel (synjet) produced via the Fischer-Tropsch process (POSF-4734). A detailed description of the combustor assembly and results from testing with the synjet has been provided in an earlier publication (Corporan, 2005b). The combustor is located in the Atmospheric-Pressure Research Complex at AFRL's Propulsion Directorate. The combustor consists primarily of a fuel injector, a square cross-sectional flame tube (combustion section), and an exhaust nozzle (Figure 30). The injector configuration, shown in Figure 31, is a generic swirl-cup liquid-fuel injector consisting of a commercial pressure-swirl atomizer (Delavan Model 27710-8) with a nominal flow number of 1.6. The 4-cm exit diameter fuel injector is centrally located in the 15.25 cm x 15.25 cm square cross-sectional dome. Most of the air to the combustor entered through the swirl-cup injector, while a small percentage entered through aspiration holes along the dome wall. The combustion products from the primary flame

zone were allowed to mix thoroughly along the 48 cm long flame tube before entering a 43 cm long, 5.7 cm exit diameter exhaust nozzle designed to generate a uniform exhaust gas temperature and particle concentration profile. The combustor overall equivalence ratio (Φ or phi) was varied from Φ = 0.60 to 1.10 (primary-zone equivalence ratio from Φ = 0.65 to 1.30) by changing the pressure drop across the fuel injector from approximately 1.5 to 10 atm, resulting in fuel mass flow rates of 1.0 to 2.2 g/s, respectively. The fuel flow rate was measured using a Max Machinery positive-displacement flow meter and the air flow with a sonic nozzle. The inlet air was heated to 177°C with an electric heater and the flow rate was kept constant at approximately 0.028 kg/s throughout the study. The air pressure drop across the combustor dome was approximately 5.0% of the main supply. The stoichiometric fuel/air ratio was calculated for each fuel using the density and approximate molecular formula, allowing for the calculation of phi during testing.

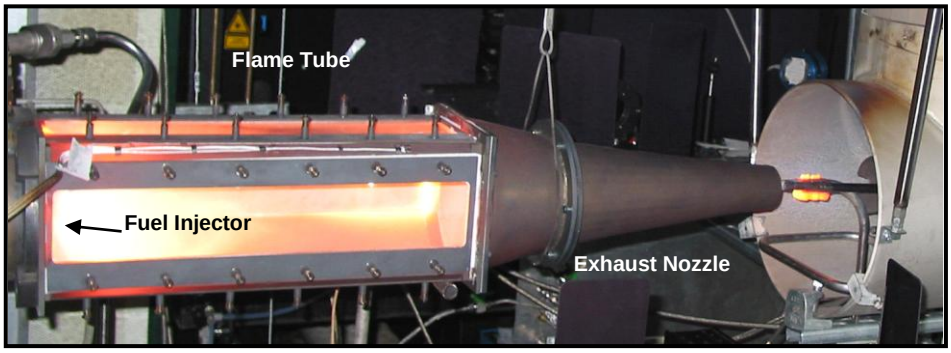


**Figure 30. Swirl-stabilized atmospheric pressure research combustor**

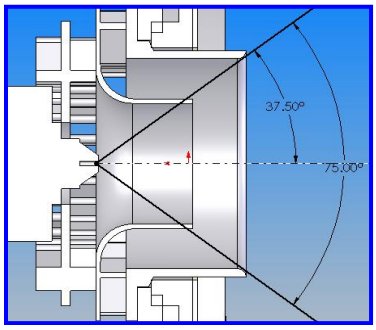


**Figure 31. Fuel injector geometry**

Particulate matter (PM) emissions from the research combustor were captured and transported to the analytical instruments via an oil-cooled probe installed facing the flow in the center and at the exit of the combustor. The exhaust sample was immediately diluted at the probe tip, and the sample line was maintained at 75°C to minimize water condensation and particulate loss to agglomeration. Sample dilution also prevented saturation of the analytical equipment at the high equivalence ratios. Dilution ratios of 16:1 were used in these studies. The diluted sample was drawn into the instruments via a

vacuum pump, and the dilution air and sample flows were controlled and measured with high precision flow controllers. All particulate measurements were corrected for dilution flow. For this testing, on-line analysis was performed using a TSI Model 3022A Condensation Nuclei Counter (CNC) to provide a count of the total particles per unit volume (particle number density) and a TSI Model 3936 Scanning Mobility Particle Sizer (SMPS) to obtain a particle size distribution. These indices were previously measured for testing on the T-63 engine. Sampling of the emissions for off-line analysis (via smoke number or temperature programmed oxidation) was not performed during this testing due to the very low particulate yields for lean operation. The low yields are most likely due to the oxidation of the particulate via excess oxygen downstream of the primary zone.

The particle number density (PND) emissions data for testing with the coal-based fuel, a specification JP-8 (POSF-3773) and the synjet fuel (POSF-4734) are shown in Figure 32 as a function of the equivalence ratio. Under fuel-lean conditions, there is relatively low net production of particulate with the coal-based fuel emissions similar to those for JP-8. As the fuel/air ratio approaches stoichiometric, there is a continued decrease in the PND for all fuels. This decrease is most likely a result of the increasing flame temperatures, which results in enhanced oxidation rates and improved combustion efficiency. The synjet fuel showed slight reductions in the PND under all fuel-lean conditions compared to both the coal-based fuel and JP-8. As the fuel/area ratio exceeds stoichiometric, the particulate production rate is significantly enhanced, resulting in significantly higher PND values. The increase is due to insufficient oxygen for the complete oxidation of the fuel; accordingly, the unburned and partially oxidized combustion products proceed to form particulate matter. Under fuel-rich conditions, the coal-based fuel produced higher PND emissions compared to the JP-8 (155% increase at phi = 1.10) while the synjet showed a significant reduction (99% decrease at phi = 1.10). Consistent with the discussion of the T-63 results, the trends in the PND data under fuel-rich conditions are due to the inherent differences in the base fuel compositions. Specifically, the oxidation of normal and branched paraffins proceeds more readily than that for cycloparaffins and aromatics resulting in inherently lower particulate production. In addition, the multi-ring cycloparaffins in the coal-based fuel can readily undergo dehydrogenation to produce the aromatic species which can act as seed molecules for the soot formation process. The primary products formed during the oxidation of the normal and branched paraffins (composition of synjet) do not produce particulate matter at the rates similar to those for the coal-based fuel. It should be noted that the magnitude of the increase for the coal-based fuel may be reduced with the introduction of dilution air downstream of the primary zone and mixing (i.e., expansion through turbine section), similar to that experienced on the T-63 engine. This may be the primary reason that the magnitude of the PND increase is much higher for this platform than for the previous combustion testing. Particle size distribution data could only be obtained under fuel-rich conditions due to the inherently low particulate production observed for all fuels under fuel-lean operation. Specifically, the signal-to-noise at phi less than one was too low to discern quantitative trends in the size distribution data. Under fuel-rich conditions, the relative size distributions were similar for all fuels tested, indicating that the basic soot formation mechanism is similar and that the overall production is strongly influenced by the types of components within the fuel.

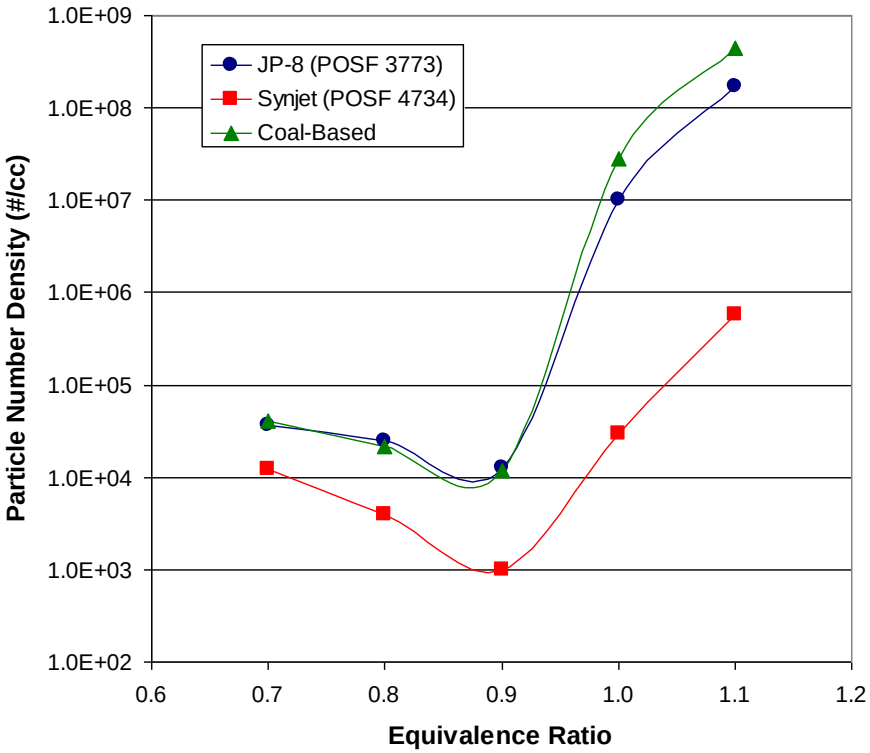


**Figure 32. Comparison of particle number density emissions as a function of equivalence ratio for the coal-based fuel, a specification JP-8 (POSF-3773), and a fuel synthesized via Fischer-Tropsch process (Synjet POSF-4734) for testing on an atmospheric research combustor.**

Overall, the trends for particulate production for the coal-based fuel relative to a specification JP-8 were similar during testing on the atmospheric combustor and the T-63 engine. The coal-based fuel showed slight to moderate increases in the particulate production relative to JP-8, with the synjet fuel showing significantly lower particulate production. The primary cause of this is most likely related to the high cycloparaffinic content of the coal-based fuel, which can form aromatic species upon pyrolytic dehydrogenation and fragmentation reactions which can promote particulate production. The cycloparaffinic nature of the fuel also leads to a lower overall fuel H/C ratio for the coal-based fuel (1.81), versus JP-8 (1.91 wt avg mean in 2004) and S-8 (2.15). Soot emissions (as characterized by smoke number) from gas turbine engines have been correlated to fuel H/C ratio (Lefebvre, 1983).

### 3.6 Elastomer Swell

The materials interaction properties of the coal-based fuel were tested. In particular, the ability of the coal-based fuel to swell elastomer materials was studied. Recent studies of fuels produced by the Fischer-Tropsch (FT) process, which do not contain significant levels of aromatic or polar species, show that these materials lack the ability to swell o-rings and elastomers to the same extent as conventional petroleum distillate fuels (Graham et al., 2004). Elastomer swell is required for proper operation of most aircraft

fuel system seals and studies show that aromatic and polar species, particularly phenols and the glycol-based fuel system icing inhibitor, are primarily responsible for the swelling properties of fuels (Graham et al., 2005). The coal-based fuel also has only very low levels of these aromatic and polar species, and therefore, may be unable to swell elastomers in a fuel system. Optical dilatometry was employed to monitor the physical swelling of o-rings as a function of time at ambient temperature. In Figure 33, is shown a plot of volume swell vs. time for a typical petroleum-based JP-8 fuel (POSF-4177) in comparison to an FT fuel (S-8) and the coal-based fuel. Very little swelling of the o-ring occurs while soaking in the FT fuel. The JP-8 fuel, which contains 17% aromatics and diaromatics and significant levels of polar compounds (~440 mg/L), swells the nitrile o-ring by approximately 16%. In comparison, the highly naphthenic coal-based fuel, while containing neither polar compounds nor aromatics, has the same swelling characteristics for this o-ring as does JP-8.

The observation that the coal-based fuel provides significant elastomer swell may be a noteworthy positive attribute of such fuels. The results suggest that cycloalkanes, such as decalin and related compounds, may have excellent seal swell characteristics compared to acyclic hydrocarbons. Additional work needs to be performed to confirm this observation, for example using ASTM methods, and to determine the mechanism by which naphthenic coal-based fuels swell elastomeric seal materials. Studies also need to be performed to determine if these naphthenic species provide improved swell characteristics, not only as major fuel components, but also as percent level additives for improving the elastomer swell characteristics of FT fuels.

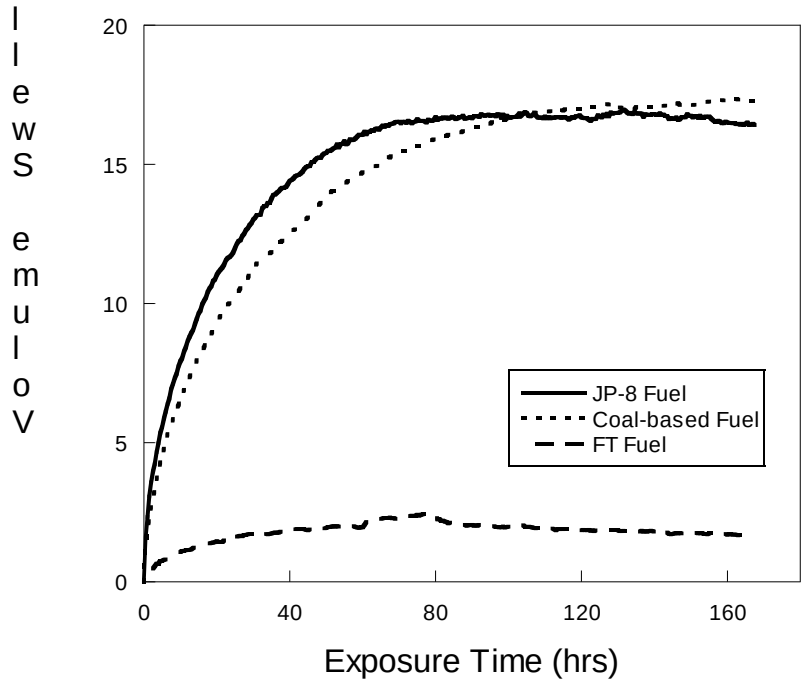


**Figure 33. Volume swell versus time for nitrile rubber o-ring samples (Parker N-602-214) aged in selected fuels at room temperature as measured by optical dilatometry.**

### 3.7 Fuel Lubricity

Jet fuel needs to have sufficient lubricity to permit trouble-free operation of fuel system components, including pumps and flow control components. While the JP-8 specification does not include a lubricity performance requirement, addition of a corrosion inhibitor additive, which also has the property of improving fuel lubricity, is required by the specification. Pump failures due to a lack of sufficient lubricity have been attributed to the use highly hydrotreated and/or hydrocracked fuels. These processes remove the heteroatomic species that are thought to impart improved lubricity properties to the fuel. To address these issues, the British Ministry of Defence has included a lubricity requirement in recent versions of the DEF STAN 91-91 Jet A-1 specification. This requirement is evaluated using ASTM D 5001, the Ball-on-Cylinder Lubricity Evaluator (BOCLE), with a maximum wear scar of 0.85 mm. The British specification requires BOCLE testing of fuels with hydroprocessed or synthetic components.

Here we evaluated the lubricity of the coal-based fuel via BOCLE testing of the fuel and the fuel with lubricity additive UNICOR J at a concentration of 16 mg/L. The results show wear scars of 0.79 and 0.62 mm for the fuel and the fuel with additive, respectively. These results indicate that the coal-based fuel exhibits satisfactory lubricity, using the <0.85 mm DEF STAN 91-91 requirement, without the lubricity additive. The results also show that the lubricity additive is effective in the coal-based fuel in further improving the lubricity.

## 4. SUMMARY AND CONCLUSIONS

A candidate coal-based fuel was evaluated both for use as substitute for conventional petroleum-derived JP-8 fuel and as a candidate for advanced applications which require improved high temperature properties (e.g, thermal stability). Numerous properties and performance behavior were monitored through a combination of specification tests and research-type evaluations. This testing included a variety of physical and chemical property tests in the areas of high temperature thermal stability, low temperature flowability, and combustion emissions characteristics, as well as a thorough series of chemical analysis evaluations. The fuel was found to meet the vast bulk of the testing, but had some off-specification test results (e.g., hydrogen content and API gravity) due to the unusual hydrocarbon constituents present in the fuel. In general, the fuel performed extremely well in thermal stability testing, producing minimal surface and bulk deposition at both moderate temperatures (oxidative deposits relevant to current aircraft) and high temperature (pyrolytic deposits relevant to future aircraft) conditions. Fuel recirculation during oxidative thermal stability testing, as would occur in advanced applications, appeared to significantly increase deposition relative to the petroleum-derived fuel. Also, a pump failure during thermal stability testing indicated that the fuel may require addition of lubricity improving additives, but subsequent lubricity testing indicated satisfactory lubricity performance. At low temperature conditions, while the fuel passed the JP-8 specification freeze point and viscosity tests, it displayed a significantly higher viscosity than typical petroleum-derived fuels at liquid-phase temperatures. At even lower temperatures, where solid crystals begin to form, the coal-based fuel remained flowable with production of very small crystals which is desirable behavior relative to conventional fuels. In combustion emission testing, the fuel displayed a slightly increased production of particulates relative to petroleum-derived fuels. These increased emissions indicate that liquid-phase pyrolytic thermal stressing of the fuel may exacerbate the increased combustion emissions, and that this effect should be further studied. In studies of elastomer swell, the fuel was found to provide significant swelling of seal material, equivalent to conventional fuels. In addition to comparison with petroleum-derived fuels, the coal-based fuel was also compared to a synthetic JP-8 produced via the Fischer-Tropsch process from natural gas. The coal-based fuel was found to be superior to the synthetic fuel in limiting pyrolytic deposition, while the synthetic fuel had slightly better low temperature liquid-phase viscosity characteristics and was superior in lowering combustion emissions.

The coal-based fuel tested here is not suitable as received for use in current military aircraft as a substitute for JP-8 fuel, as a number of properties do not meet specification. These include hydrogen content and API gravity, which need to be increased to meet the JP-8 specification. The fuel would also need to be additized with fuel system icing inhibitor, static dissipater, and corrosion inhibitor additives. In addition, the heat of combustion, which is very near the specification minimum, should be increased so that sample to sample variations do not result in failures of this property. The significant oxidative and pyrolytic thermal stability benefits of the coal-based fuel could be used in the future to greatly improve the fuel heat sink and enable engine and aircraft technologies that are currently limited by thermal concerns.

## 5. REFERENCES


Bacha, J., Barnes, F., Franklin, M., Gibbs, L., Hemighaus, G., Hoge, N., Lesnini, D., Lind, J., Maybury, J., Morris, J., 2000. Aviation Fuels Technical Review. Chevron Products Company, San Ramon, CA.

Bockhorn, H., F. Fetting and H. Wenz, 1983. Investigation of the Formation of High Molecular Weight Hydrocarbons and Soot in Premixed Hydrocarbon-Oxygen Flames. Berichte der Bunsen-Gesellschaft 87, 1067-1073.

Coordinating Research Council, 2004. CRC Report No. 635: Handbook of Aviation Fuel Properties, Third Edition, Coordinating Research Council, Inc., Alpharetta, GA.

Corporan, E., DeWitt, M.J., Wagner, M., 2004a. Evaluation of Soot Particulate Mitigation Additives in a T63 Engine. Fuel Processing Technology 85, 727-742.

Corporan, E., Monroig, O., Wagner, M., DeWitt, M.J., 2004b. Influence of Fuel Chemical Composition on Particulate Matter Emissions of a Turbine Engine. ASME Turbo Expo 2004, Vienna, Austria.

Corporan, E., DeWitt, M.J., Monroig, O., Ostdiek, D., Mortimer, B., Wagner, M., 2005a. Reduction of Turbine Engine Particulate Emissions Using Synthetic Jet Fuel. Preprints of Symposia - American Chemical Society, Division of Fuel Chemistry 50, 338-341.

Corporan, E., Belovich, V., DeWitt, M.J., Pawlik, R., Lynch, A.C., Gord, J.R., and Meyer, T.R., 2005b. Impacts of Synthetic Jet Fuel on the Emissions of a Turbine Engine Combustor. Proceeding of the 9th International Conference on Stability and Handling of Liquid Fuels, Sitges, Spain.

DeWitt, M. J., 2004. Unpublished results.

DeWitt, M. J., Zabarnick, S., 2002. Development and Evaluation of Additives to Inhibit Oxidative Deposition of Jet Fuels. Prepr.-Am. Chem. Soc., Div. Pet. Chem. 47, 183-186.

DeWitt, M. J., Zabarnick, S., Ervin, J.S., and Williams, T.F., 2003. Inhibition of Jet Fuel Deposition Within a Complete Oxygen Consumption Regime. Proceedings of the 8th International Conference on Stability and Handling of Liquid Fuels, Steamboat Springs, CO.

Edwards, T., Minus, D., Harrison, W., Corporan, E., DeWitt, M., Zabarnick, S., and Balster, L., 2004. Fischer-Tropsch Jet Fuels – Characterization for Advanced Aerospace Applications. AIAA-2004-3885.

Edwards, T., Krieger, J., 1995. The Thermal Stability of Fuels at 480C (900F). Effect of Test Time, Flow Rate, and Additives. ASME IGTI Paper No. 95-GT-68.

Fabuss, B. M., Smith, J.O., and Satterfield, C.N., 1964. Thermal Cracking of Pure Saturated Hydrocarbons. Chapter 4 of Advances in Petroleum Chemistry Refining -Vol. IX, Interscience, New York.

Ford, T. J., 1986. Liquid-Phase Thermal Decomposition of Hexadecane: Reaction Mechanisms. Ind. Eng. Chem. Fundam. 25, 240-243.

Graham, J.L., Striebich, R.C., Minus, D.K., Harrison, W.E., III, 2004. Prepr.-Am. Chem. Soc., Div Pet. Chem. 49, 435-439.

Graham, J.L., Striebich, R.C., Myers, K.J., Minus, D.K., Harrison, W.E., 2005. The Swelling of Nitrile Rubber by Selected Aromatics Blended in a Synthetic Jet Fuel. Energy & Fuels, submitted for publication.

Grinstead, B., Zabarnick, S., 1999. Studies of Jet Fuel Thermal Stability, Oxidation, and Additives Using an Isothermal Oxidation Apparatus Equipped with an Oxygen Sensor. Energy & Fuels 13, 756-760.

Heneghan, S. P., Zabarnick, S., Ballal, D.R., Harrison, W.E., 1996. JP-8+100: Development of a Thermally Stable Jet Fuel. Journal of Energy Resource Technology 118, 170-179.

Lefebvre, A., 1983. Gas Turbine Combustion, Hemisphere Publishing Corporation, New York.

Markham, J. R., Bush, P.M, Bonzani, P.J. Jr., Scire, J.J. Jr., Zaccardi, V.A., Jalbert, P.A., Bryant, M.D., and Gardner, D.G. 2004. Integrated Gas Analyzer for Complete Monitoring of Turbine Engine Test Cells. Applied Spectroscopy 58, 130-136.

Minus, D. K., Corporan, E., 1998. Deposition Effects of Radical Stabilizing Additives in JP-8 Fuel. Prepr.-Am. Chem. Soc., Div. Pet. Chem. 43, 360-363.

Monroig, O., Corporan E., DeWitt, M.J., Mortimer, B., Ostdiek, D., Wagner, M., 2005. Effects of Jet Fuel Aromatic Concentration on the Emission of a T63 Engine. Preprints of Symposia - American Chemical Society, Division of Fuel Chemistry 50, 335-337.

Mushrush, G. W. and Hazlett, R.N., 1984. Pyrolysis of Organic Compounds Containing Long Unbranched Alkyl Groups. Ind. Eng. Chem. Fundam. 23, 288-294.

Naegeli, D. W., Moses, C.A., 1980. Effects of Fuel Molecular Structure on Soot Formation in Gas Turbine Engines. ASME Gas Turbine Conference, New Orleans.

Probstein, R. F. and Hicks, R.E., 1982. Synthetic Fuels. pH Press, Cambridge, MA.

Richter, H. and Howard, J.B. 2000. Formation of Polycyclic Aromatic Hydrocarbons and their Growth to Soot – A Review of Chemical Reaction Pathways. Progress in Energy and Combustion Science 26, 565-608.

Selby, T.W., Vangsness, M., Shafer, L., 2004. Studies of the Flow and Gelation Response of Jet Fuels at Critical Low Temperatures. Presented at International Condition Monitoring Conference 2004 – Joint Oil Analysis Program, Pensacola, FL.

Song, C., Lai, W. C. and Schobert, H.H., 1994a. Condensed-Phase Pyrolysis of *n*-Tetradecane at Elevated Pressures for Long Duration. Product Distribution and Reaction Mechanisms. Ind. Eng. Chem. Res. 33, 534-547.

Song, C., Lai, W. C. and Schobert, H.H., 1994b. Hydrogen-Transferring Pyrolysis of Long-Chain Alkanes and Thermal Stability Improvement of Jet Fuels by Hydrogen Donors. Ind. Eng. Chem. Res. 33, 548-557.

Stewart, J., Brezinsky, K., and Glassman, I., 1998. Supercritical Pyrolysis of Decalin, Tetralin, and *n*-Decane at 700-800K. Product Distribution and Reaction Mechanism. Comb. Sci. Tech. 136, 373-390.

Yu, J., Eser, S., 1998. Thermal Decomposition of Jet Fuel Model Compounds under Near-Critical and Supercritical Conditions. 2. Decalin and Tetralin. Ind. Eng. Chem. Res. 37, 4601-4608.

Zabarnick, S., 1994. Studies of Jet Fuel Thermal Stability and Oxidation Using a Quartz Crystal Microbalance and Pressure Measurements. Ind. Eng. Chem. Res. 33, 1348-1354.

Zabarnick, S., 1998. Chemical Kinetic Modeling of Antioxidant Chemistry for Jet Fuel Applications. Energy and Fuels 12, 547-553.

Zabarnick, S., Grinstead, R.R., 1994. Studies of Jet Fuel Additives using the Quartz Crystal Microbalance and Pressure Monitoring at 140 C. Ind. Eng. Chem. Res. 33, 2771-2777.

Zabarnick, S. and Mick, M.S., 1999. Inhibition of Jet Fuel Oxidation by Hydroperoxide-Decomposing Additives. Ind. Eng. Chem. Res. 38, 3557-3563.

Zabarnick, S. and Widmor, N., 2001. Studies of Jet Fuel Freezing by Differential Scanning Calorimetry. Energy and Fuels 15, 1447-1453.

Zhou, P. and Crynes, B.L., 1985. Thermolytic Reactions of Dodecane. Ind. Eng. Chem. Process. Res. Dev. 25, 508-514.

## APPENDIX. FUEL SPECIFICATION TEST RESULTS

JP-8 Fuel POSF-3773

DEPARTMENT OF THE AIR FORCE
Det 13 SA-ALC/AFTLA
2430 C Street, Room 125, Bldg 70
Wright-Patterson AFB, OH 45433-7632

LABORATORY TEST REPORT

Submitter's Sample No: POSF-3773
Date Sampled: / /

Lab Report No: F-2000LA02221
Date Reported: 08/17/2000
Date Received: 08/07/2000
Product/Manufacturer/Contractor:

Sample Submitter:
AFRL/PRSF
BLDG 490
1790 LOOP RD N
WRIGHT-PATTERSON AFB, OH 45433-

Reason for Submission: Refinery Correlation (DLAM 4155.1)
Product: Aviation Turbine Fuel, Kerosene
Specification: MIL-T-83133 JP-8
Sample Origin:
Quantity Represented:

NSN:
Contract No:
Batch/Lot:
Date Manufactured:

| METHOD | TEST | LIMITS MIN | LIMITS MAX | LAB RESULTS |
|---|---|---|---|---|
| SPEC\W | Workmanship | | Pass | Pass |
| D3242 | Total Acid Number, mg KOH/g | | 0.015 | 0.000 |
| D1319 | Aromatics, %vol | | 25.0 | 15.9 |
| D1319 | Olefins, %vol | | 5.0 | 0.7 |
| D3227 | Mercaptan Sulfur, % mass | | 0.002 | 0.001 |
| D4294 | Total Sulfur, % mass | | 0.30 | 0.07 |
| D86 | Distillation | | | |
| | IBP, deg C | | Report | 150 |
| | 10% Recovered, deg C | | 205 | 170 |
| | 20% Recovered, deg C | | Report | 176 |
| | 50% Recovered, deg C | | Report | 196 |
| | 90% Recovered, deg C | | Report | 237 |
| | EP, deg C | | 300 | 256 |
| | Residue, %vol | | 1.5 | 0.7 |
| | Loss, %vol | | 1.5 | 1.1 |
| D93 | Flash Point, deg C | 38 | | 47 |
| D1298 | API Gravity | 37.0 | 51.0 | 45.8 |
| D5972 | Freezing Point, deg C (Automatic) | | -47 | -50 |
| D445 | Viscosity @ -20 deg C, cSt | | 8.0 | 4.4 |
| D3338 | Heat of Combustion, BTU/lb | 18400 | | 18625 |
| D3701 | Hydrogen Content, % mass | 13.4 | | 13.9 |
| D1322 | Smoke Point, mm | 19.0 | | 25.0 |
| D1840 | Naphthalenes, % vol | | 3.0 | Not Req. |
| D130 | Copper Strip Corrosion | | 1 | 1a |
| D3241 | Thermal Stability @ 260 deg C | | | |
| | Tube Deposit Rating, Visual | | <3 | 1 |
| | Change in Pressure, mm Hg | | 25 | 3 |
| D381 | Existent Gum, mg/100mL | | 7.0 | 1.0 |
| D5452 | Particulate Matter, mg/L | | 1.0 | 0.2 |
| SPEC\F | Filtration Time, minutes | | 15 | 9 |
| D1094 | Water Reaction | | 1B | 1b |
| D3948 | WSIM | 70 | | 61## |
| D5006 | FSII (DiEGME), % vol | 0.10 | 0.15 | 0.07## |
| D2624 | Conductivity, pS/m | 150 | 600 | 176 |

DEPARTMENT OF THE AIR FORCE
Det 13 SA-ALC/AFTLA
2430 C Street, Room 125, Bldg 70
Wright-Patterson AFB, OH 45433-7632

LABORATORY TEST REPORT

Submitter's Sample No: POSF-3775
Date Sampled: / /

Lab Report No: S-2000LA02219
Date Reported: 08/10/2000
Date Received: 08/07/2000
Product/Manufacturer/Contractor:

Sample Submitter:
AFRL/PRSF
BLDG 490
1790 LOOP RD N
WRIGHT-PATTERSON AFB, OH 45433-

Reason for Submission: Acceptance Testing
Product: Turbine Fuel, A/C, Thermally Stable
Specification: MIL-DTL-25524 JPTS
Sample Origin:
Quantity Represented:

NSN:
Contract No:
Batch/Lot:
Date Manufactured:

| METHOD | TEST | LIMITS MIN | LIMITS MAX | LAB RESULTS |
|---|---|---|---|---|
| SPEC\W | Workmanship | | Pass | Pass |
| D3242 | Total Acid Number, mg KOH/g | | 0.015 | 0.002 |
| D1319 | Aromatics, % vol | 5.0 | 20.0 | 13.5 |
| D4294 | Total Sulfur, % mass | | 0.3 | 0.0 |
| D3227 | Mercaptan Sulfur, % mass | | 0.001 | 0.000 |
| D86 | Distillation | | | |
| | IBP, deg C | 157 | | 164 |
| | 10% Recovered, deg C | | 193 | 171 |
| | 50% Recovered, deg C | | 204 | 185 |
| | 90% Recovered, deg C | | 238 | 213 |
| | EP, deg C | | 260 | 231 |
| | Residue, %vol | | 1.5 | 1.0 |
| | Loss, %vol | | 1.5 | 0.8 |
| D93 | Flash Point, deg C | 43 | | 52 |
| D1298 | API Gravity | 46.0 | 53.0 | 47.7 |
| D5972 | Freezing Point, deg C (Automatic) | | -53 | -56 |
| D445 | Viscosity @ -40 deg C, cSt | | 12.0 | 7.9 |
| D3338 | Net Heat of Combustion, MJ/kg | 42.8 | | 43.4 |
| D3701 | Hydrogen Content, % mass | 14.00 | | 14.08 |
| D1322 | Smoke Point, mm | 25.0 | | 27.0 |
| D130 | Copper Strip Corrosion | | 1b | 1a |
| D3241 | Thermal Stability @ 335 deg C | | | |
| | JFTOT TDR, max | | 12 | 11 |
| | Change in Pressure, mm Hg | | 25 | 0 |
| D381 | Existent Gum, mg/100mL | | 5.0 | 0.2 |
| D5452 | Particulate Matter, mg/L (Destin.) | | 0.5 | 0.4 |
| D3948 | WSIM | | Report | 44 |
| D5006 | FSII, % vol | 0.10 | 0.15 | 0.11 |
| D1094 | Water Reaction | | 1b | 2## |

DEPARTMENT OF THE AIR FORCE
OL Det3 WR-ALC/AFTLA
2430 C St, Rm 125, Bldg 70 Area B
Wright-Patterson AFB, OH 45433-7632

LABORATORY TEST REPORT

Submitter's Sample No: 02-POSF-4177
Date Sampled: / /

Lab Report No: F-2002LA02056
Date Reported: 07/11/2002
Date Received: 06/27/2002

Sample Submitter:
AFRL/PRSF
BLDG 490
1790 LOOP RD N
WRIGHT-PATTERSON AFB, OH 45433-

Product/Manufacturer/Contractor:

Reason for Submission: Refinery Correlation (DLAM 4155.1)
Product: Aviation Turbine Fuel, Kerosene
Specification: MIL-T-83133 JP-8
Sample Origin:
Quantity Represented:

NSN:
Contract No:
Batch/Lot:
Date Manufactured:

| METHOD | TEST | LIMITS MIN | LIMITS MAX | LAB RESULTS |
|---|---|---|---|---|
| SPEC\W | Workmanship | | Pass | Pass |
| D3242 | Total Acid Number, mg KOH/g | | 0.015 | 0.004 |
| D1319 | Aromatics, %vol | | 25.0 | 16.3 |
| D1319 | Olefins, %vol | | 5.0 | 0.9 |
| D3227 | Mercaptan Sulfur, % mass | | 0.002 | 0.001 |
| D4294 | Total Sulfur, % mass | | 0.30 | 0.14 |
| D86 | Distillation | | | |
| | IBP, deg C | | Report | 129 |
| | 10% Recovered, deg C | | 205 | 179 |
| | 20% Recovered, deg C | | Report | 187 |
| | 50% Recovered, deg C | | Report | 205 |
| | 90% Recovered, deg C | | Report | 235 |
| | EP, deg C | | 300 | 261 |
| | Residue, %vol | | 1.5 | 1.3 |
| | Loss, %vol | | 1.5 | 0.9 |
| D93 | Flash Point, deg C | 38 | | 52 |
| D1298 | API Gravity | 37.0 | 51.0 | 42.4 |
| D5972 | Freezing Point, deg C (Automatic) | | -47 | -57 |
| D445 | Viscosity @ -20 deg C, cSt | | 8.0 | 2.7 |
| D3338 | Heat of Combustion, BTU/lb | 18400 | | 18539 |
| D3343 | Hydrogen Content, % mass | 13.4 | | 13.7 |
| D1322 | Smoke Point, mm | 19.0 | | 22.0 |
| D1840 | Naphthalenes, % vol | | 3.0 | 1.0 |
| D130 | Copper Strip Corrosion | | 1 | 1a |
| D3241 | Thermal Stability @ 260 deg C | | | |
| | Tube Deposit Rating, Visual | | <3 | 2 |
| | Change in Pressure, mm Hg | | 25 | 4 |
| D381 | Existent Gum, mg/100mL | | 7.0 | 1.8 |
| D5452 | Particulate Matter, mg/L | | 1.0 | 0.9 |
| SPEC\F | Filtration Time, minutes | | 15 | 5 |
| D1094 | Water Reaction | | 1B | 1b |
| D3948 | WSIM | 70 | | 57## |
| D5006 | FSII (DiEGME), % vol | 0.10 | 0.15 | 0.11 |
| D2624 | Conductivity, pS/m | 150 | 600 | 197 |

DEPARTMENT OF THE AIR FORCE
DET 3, WR-ALC/AFTLA
2430 C St, Bldg 70 Area B
Wright-Patterson AFB, OH 45433-7632

LABORATORY TEST REPORT

Submitter's Sample No: POSF-4734
Date Sampled: / /

Lab Report No: F-2005LA00013
Date Reported: 10/08/2004
Date Received: 10/01/2004

Sample Submitter:
AFRL/PRTG
BLDG 490
1790 LOOP ROAD N
WRIGHT-PATTERSON AFB, OH 45433-

Product/Manufacturer/Contractor:

Reason for Submission: Specification Conformance Testing
Product: Aviation Turbine Fuel, Kerosene
Specification: MIL-T-83133 JP-8
Sample Origin:
Quantity Represented:

NSN:
Contract No:
Batch/Lot:
Date Manufactured:

| METHOD | TEST | LIMITS MIN | LIMITS MAX | LAB RESULTS |
|---|---|---|---|---|
| SPEC\W | Workmanship | | Pass | Pass |
| D3242 | Total Acid Number, mg KOH/g | | 0.015 | 0.001 |
| D1319 | Aromatics, %vol | | 25.0 | 0.0 |
| D3227 | Mercaptan Sulfur, % mass | | 0.002 | 0.000 |
| D4294 | Total Sulfur, % mass | | 0.30 | 0.00 |
| D86 | Distillation | | | |
| | IBP, deg C | | Report | 153 |
| | 10% Recovered, deg C | | 205 | 169 |
| | 20% Recovered, deg C | | Report | 176 |
| | 50% Recovered, deg C | | Report | 201 |
| | 90% Recovered, deg C | | Report | 249 |
| | EP, deg C | | 300 | 271 |
| | Residue, %vol | | 1.5 | 1.4 |
| | Loss, %vol | | 1.5 | 0.8 |
| D93 | Flash Point, deg C | 38 | | 49 |
| D5972 | Freezing Point, deg C (Automatic) | | -47 | -59 |
| D445 | Viscosity @ -20 deg C, cSt | | 8.0 | 4.6 |
| D3338 | Heat of Combustion, BTU/lb | 18400 | | 18965 |
| D3343 | Hydrogen Content, % mass | 13.4 | | 15.3 |
| D1322 | Smoke Point, mm | 19.0 | | >40.0 |
| D1840 | Naphthalenes, % vol | | 3.0 | Not Req. |
| D130 | Copper Strip Corrosion | | 1 | 1a |
| D3241 | Thermal Stability @ 260 deg C | | | |
| | Tube Deposit Rating, Visual | | <3 | <1 |
| | Change in Pressure, mm Hg | | 25 | 1 |
| D381 | Existent Gum, mg/100mL | | 7.0 | 0.2 |
| D5452 | Particulate Matter, mg/L | | 1.0 | 0.1 |
| SPEC\F | Filtration Time, minutes | | 15 | 11 |
| D1094 | Water Reaction | | 1B | 1 |
| D3948 | WSIM | 70 | | 98 |
| D5006 | FSII (DiEGME), % vol | 0.10 | 0.15 | 0.00## |
| D2624 | Conductivity, pS/m | 150 | 600 | 0## |
| D4052 | API Gravity @ 60°F | 37.0 | 51.0 | 55.3## |
| D5001 | Lubricity Test(BOCLE), wear scar mm | | REPORT | 0.85 |

DEPARTMENT OF THE AIR FORCE
DET 3, WR-ALC/AFTLA
2430 C St, Bldg 70 Area B
Wright-Patterson AFB, OH 45433-7632

LABORATORY TEST REPORT

Submitter's Sample No: POSF-4751
Date Sampled: / /

Lab Report No: F-2005LA02282
Date Reported: 03/01/2005
Date Received: 02/24/2005

Sample Submitter:
AFRL/PRTG
BLDG 490
1790 LOOP ROAD N
WRIGHT-PATTERSON AFB, OH 45433-

Product/Manufacturer/Contractor:

Reason for Submission: Specification Conformance Testing
Product: Aviation Turbine Fuel, Kerosene
Specification: MIL-T-83133 JP-8
Sample Origin:
Quantity Represented:

NSN:
Contract No:
Batch/Lot:
Date Manufactured:

| METHOD | TEST | LIMITS MIN | LIMITS MAX | LAB RESULTS |
|---|---|---|---|---|
| SPEC\W | Workmanship | | Pass | Fails## |
| D3242 | Total Acid Number, mg KOH/g | | 0.015 | 0.003 |
| D1319 | Aromatics, %vol | | 25.0 | 21.0 |
| D3227 | Mercaptan Sulfur, % mass | | 0.002 | 0.000 |
| D4294 | Total Sulfur, % mass | | 0.30 | 0.04 |
| D86 | Distillation | | | |
| | IBP, deg C | | Report | 157 |
| | 10% Recovered, deg C | | 205 | 181 |
| | 20% Recovered, deg C | | Report | 188 |
| | 50% Recovered, deg C | | Report | 208 |
| | 90% Recovered, deg C | | Report | 244 |
| | EP, deg C | | 300 | 267 |
| | Residue, %vol | | 1.5 | 1.2 |
| | Loss, %vol | | 1.5 | 0.4 |
| D93 | Flash Point, deg C | 38 | | 50 |
| D5972 | Freezing Point, deg C (Automatic) | | -47 | -50 |
| D445 | Viscosity @ -20 deg C, cSt | | 8.0 | 5.2 |
| D3338 | Heat of Combustion, BTU/lb | 18400 | | 18584 |
| D3343 | Hydrogen Content, % mass | 13.4 | | 13.7 |
| D1322 | Smoke Point, mm | 19.0 | | 25.0 |
| D1840 | Naphthalenes, % vol | | 3.0 | Not Req. |
| D130 | Copper Strip Corrosion | | 1 | 1a |
| D3241 | Thermal Stability @ 260 deg C | | | |
| | Tube Deposit Rating, Visual | | <3 | <1 |
| | Change in Pressure, mm Hg | | 25 | 0 |
| D381 | Existent Gum, mg/100mL | | 7.0 | 0.6 |
| D5452 | Particulate Matter, mg/L | | 1.0 | 0.4 |
| SPEC\F | Filtration Time, minutes | | 15 | 5 |
| D1094 | Water Reaction | | 1B | 1 |
| D5006 | FSII (DiEGME), % vol | 0.10 | 0.15 | 0.11 |
| D2624 | Conductivity, pS/m | 150 | 600 | 140## |
| D4052 | API Gravity @ 60°F | 37.0 | 51.0 | 44.5 |

DEPARTMENT OF THE AIR FORCE
DET 3, WR-ALC/AFTLA
2430 C St, Bldg 70 Area B
Wright-Patterson AFB, OH 45433-7632

LABORATORY TEST REPORT

Submitter's Sample No: POSF-4765
Date Sampled: / /

Lab Report No: F-2005LA01705
Date Reported: 01/31/2005
Date Received: 01/21/2005

Sample Submitter:
AFRL/PRTG
BLDG 490
1790 LOOP ROAD N
WRIGHT-PATTERSON AFB, OH 45433-

Product/Manufacturer/Contractor:

Reason for Submission: Specification Conformance Testing
Product: Aviation Turbine Fuel, Kerosene
Specification: MIL-T-83133 JP-8
Sample Origin:
Quantity Represented:

NSN:
Contract No:
Batch/Lot:
Date Manufactured:

| METHOD | TEST | LIMITS MIN | LIMITS MAX | LAB RESULTS |
|---|---|---|---|---|
| SPEC\W | Workmanship | | Pass | Pass |
| D3242 | Total Acid Number, mg KOH/g | | 0.015 | 0.000 |
| D1319 | Aromatics, %vol | | 25.0 | 1.9 |
| D3227 | Mercaptan Sulfur, % mass | | 0.002 | 0.000 |
| D4294 | Total Sulfur, % mass | | 0.30 | 0.00 |
| D86 | Distillation | | | |
| | IBP, deg C | | Report | 181 |
| | 10% Recovered, deg C | | 205 | 192 |
| | 20% Recovered, deg C | | Report | 194 |
| | 50% Recovered, deg C | | Report | 204 |
| | 90% Recovered, deg C | | Report | 243 |
| | EP, deg C | | 300 | 270 |
| | Residue, %vol | | 1.5 | 1.1 |
| | Loss, %vol | | 1.5 | 0.4 |
| D93 | Flash Point, deg C | 38 | | 61 |
| D5972 | Freezing Point, deg C (Automatic) | | -47 | -65 |
| D445 | Viscosity @ -20 deg C, cSt | | 8.0 | 7.5 |
| D3338 | Heat of Combustion, BTU/lb | 18400 | | 18401 |
| D3343 | Hydrogen Content, % mass | 13.4 | | 13.2## |
| D1322 | Smoke Point, mm | 19.0 | | 22.0 |
| D1840 | Naphthalenes, % vol | | 3.0 | 0.0 |
| D130 | Copper Strip Corrosion | | 1 | 1a |
| D3241 | Thermal Stability @ 260 deg C | | | |
| | Tube Deposit Rating, Visual | | <3 | <1 |
| | Change in Pressure, mm Hg | | 25 | 0 |
| D381 | Existent Gum, mg/100mL | | 7.0 | 3.8 |
| D5452 | Particulate Matter, mg/L | | 1.0 | 0.3 |
| SPEC\F | Filtration Time, minutes | | 15 | 7 |
| D1094 | Water Reaction | | 1B | 1b |
| D5006 | FSII (DiEGME), % vol | 0.10 | 0.15 | 0.00## |
| D2624 | Conductivity, pS/m | 150 | 600 | 0## |
| D4052 | API Gravity @ 60°F | 37.0 | 51.0 | 31.1## |